

Sample and Computationally Efficient Simulation Metamodeling in High Dimensions

Liang Ding

Department of Industrial and Systems Engineering, Texas A&M University, College Station, TX 77843, USA,
ldingaa@tamu.edu

Xiaowei Zhang

Faculty of Business and Economics, The University of Hong Kong, Pokfulam Road, Hong Kong SAR, xiaoweiz@hku.hk

Stochastic kriging has been widely employed for simulation metamodeling to predict the response surface of a complex simulation model. However, its use is limited to cases where the design space is low-dimensional, because the number of design points required for stochastic kriging to produce accurate prediction, in general, grows exponentially in the dimension of the design space. The large sample size results in both a prohibitive sample cost for running the simulation model and a severe computational challenge due to the need of inverting large covariance matrices. Based on tensor Markov kernels and sparse grid experimental designs, we develop a novel methodology that dramatically alleviates the curse of dimensionality. We show that the sample complexity of the proposed methodology grows very mildly in the dimension, even under model misspecification. We also develop fast algorithms that compute stochastic kriging in its exact form without any approximation schemes. We demonstrate via extensive numerical experiments that our methodology can handle problems with a design space of more than 10,000 dimensions, improving both prediction accuracy and computational efficiency by orders of magnitude relative to typical alternative methods in practice.

Key words: simulation metamodeling; stochastic kriging; Gaussian process; tensor Markov kernel; sparse grid; experimental design; matrix inversion; high-dimensional inputs

1. Introduction

Simulation is a general-purpose decision-making tool that has been widely used in operations research and management science. It allows one to model dynamics of a complex system and assess arbitrary performance measure of interest. However, simulation models are often computationally intensive to execute. It takes a sizable cost to collect sufficient simulation samples to facilitate informed decisions. Simulation metamodeling is a methodology developed to address the issue and it has drawn substantial research interest from the simulation community; see Barton (2015) and Kleijnen (2017) for recent reviews. The basic idea is to postulate a statistical model for the response surface, that is, the performance measure as a function of the design variables. This statistical

model is fast to run, and it is referred to as the metamodel. Then, the simulation model is executed at a set of judiciously selected design points. Upon calibrated using the simulation samples, the metamodel is used subsequently to predict the value of the response surface so that no further simulation will be needed.

Linear regression metamodels, which are linear in the unknown coefficients of possibly nonlinear transformations (e.g., polynomials) of the design variables, have been studied extensively. They tend to capture the local structure of the response surface, but do not fit well globally in general. Kriging metamodels, In contrast, impose fewer structural assumptions and can provide robust maps over the entire design space. Originated in geostatistics (Matheron 1963), the kriging methodology was introduced by Sacks et al. (1989) into the design and analysis of computer experiments to model the response surface of a deterministic simulation model and has been highly effective in this area. In the present paper, we focus on stochastic kriging (Ankenman et al. 2010) which generalizes kriging to stochastic simulation that usually involves heteroscedastic simulation noise.

Stochastic kriging assumes that the response surface is a sample path of a Gaussian process (GP). Given a sampling budget, its prediction accuracy depends critically on concrete specification of two aspects: (i) the kernel function (i.e., the covariance function) of the GP, and (ii) the experimental design (i.e., the choice of the design points). Upon collecting samples following the experimental design, predicting the response surface with the chosen kernel function is reduced to numerical linear algebra. Particularly, it involves inverting the covariance matrix of the samples. Thanks its nonparametric nature and analytical tractability, stochastic kriging has been widely used in recent years in the simulation field, including output analysis (Barton et al. 2014, Xie et al. 2014) and simulation optimization (Sun et al. 2014, Jalali et al. 2017, Salemi et al. 2019b); see Gramacy (2020) for a general exposition.

Despite its popularity, the use of stochastic kriging has been mostly limited to problems with a low-dimensional design space. This is mainly due to two issues: one is related to sample complexity, while the other computational complexity. The former issue is prominent for high-dimensional problems, because simulation samples are expensive to acquire but the sample size required for stochastic kriging to achieve a prescribed level of prediction accuracy, in general, grows exponentially in the dimension; see detailed discussion in Section 2.3. It is known that the curse of dimensionality on the sample complexity can be mitigated if the response surface is “highly smooth” (Stone 1980). Examples include sample paths of GPs with a Matérn kernel having a large smoothness parameter. Intuitively, this is because a space of smoother functions is smaller, thereby easier to identify the true function in the space. In the limit, if the response surface is infinitely differentiable, which is the case for sample paths of GPs with a Gaussian kernel, then the sample complexity can be independent of the dimension of the design space (van der Vaart and van Zanten 2011). However,

response surfaces of interest in practice may not possess such a high level of smoothness; see, e.g., Salemi et al. (2019a). Using a kernel with a high degree of smoothness in stochastic kriging when the response surface is in fact less smooth leads to model misspecification. It may further exacerbate the curse of dimensionality on sample complexity—at least from the perspective of the rate of convergence—if the misspecification is significant; see Tuo and Wang (2020).

We develop in the present paper a novel methodology that does not rely on strong assumptions on the smoothness of the response surface to solve the issue of excessive sample complexity in high dimensions. Instead, we impose certain tensor structure on the response surface with the use of tensor Markov (TM) kernels, which in fact induce non-differentiable sample paths (see Section 3.3). TM kernels are of product form, constructed by multiplying the kernel functions of Gauss-Markov processes, which are one-dimensional and include Brownian motion and the Ornstein-Uhlenbeck process. Salemi et al. (2019a) proposes a new class of GPs, termed generalized integrated Brownian fields (GIBFs), that exhibit excellent prediction capability. A simple example of GIBF is the Brownian field whose kernel is the product of Brownian kernels, and it is indeed a TM kernel.

The function space that consists of sample paths associated with a TM kernel is not small. The convergence rate of stochastic kriging with TM kernels may still suffer from the curse of dimensionality, if the experimental design is not properly chosen; see Section 5.1. Based on sparse grid (SG) experimental designs (Bungartz and Griebel 2004), we propose a new experimental design termed *truncated sparse grids* (TSGs). The joint use of TM kernels and TSGs allows the convergence rate of stochastic kriging to be “almost” independent of the dimension of the design space.

A second manifestation of the curse of dimensionality is the prohibitive computational complexity. The matrix inversion in stochastic kriging normally incurs a computational cost that is cubic in the sample size, which quickly surpasses the processing capability of typical modern computers as the sample size increases. There is a vast and fast-growing literature on approximations for reducing computational complexity of stochastic kriging and Gaussian process regression (GPR), a closely related method in machine learning. A basic idea is to identify a suitable subset of the samples, and then use them to construct a low rank approximation of the covariance matrix, which is substantially easier to invert. These approximations are usually developed for general kernel functions and general experimental designs. We refer to Rasmussen and Williams (2006, Chapter 8) and Gramacy (2020, Chapter 9) for overviews of the approach, and to Gramacy and Apley (2015), Lu et al. (2020), Burt et al. (2020), and references therein for recent advances in this regard.

We refrain from approximation strategies in the present paper. Instead, we take advantage of properties that are specific to TM kernels and TSG designs to develop fast algorithms for *exact* computation of stochastic kriging.

Another important issue related to matrix inversion is the numerical instability due to limitations of floating point arithmetic and the fact that large covariance matrices tend to be ill-conditioned (Haaland and Qian 2011). The issue is particularly serious when Gaussian kernels are used (Ababou et al. 1994). One may apply the framework in Haaland et al. (2018) and Wang and Haaland (2019) to analyze such numerical errors. We do not pursue in this direction here, although numerical experiments show that covariance matrices induced by TM kernels and TSG designs do not appear to suffer from this issue.

1.1. Main Contributions

Our foremost contribution is to provide a novel solution to two fundamental issues that preclude stochastic kriging from being used for high-dimensional simulation metamodeling, that is, excessive sample complexity and prohibitive computational cost. The solution is based on two key concepts—TM kernel and TSG design. The former appeared in the study of multidimensional Markov properties of random fields (Carnal and Walsh 1991), but as far as we know, no prior theoretical analysis exists on its use in stochastic kriging. The TSG design is indeed new and it allows us to derive error bounds on predictions of stochastic kriging with TM kernels, as well as devise fast algorithms that leverage properties that are specific to TM kernels.

First, we establish an asymptotic upper bound on the mean squared prediction error of stochastic kriging with TM kernels and TSG designs, under the premise that the underlying model is correctly specified. That is, the kernel used in stochastic kriging is identical to the kernel that drives the GP, from which the response surface is realized. The upper bound is uniform in the design variable, and it deteriorates mildly in the dimension d , with d appearing in the exponent of $\log n$ as opposed to the usual case of appearing in the exponent of n , where n is the number of design points. Hence, the curse of dimensionality on sample complexity is mitigated substantially.

Second, in light of the fact that the GP sample paths induced by a TM kernel are non-differentiable everywhere, whereas response surfaces in practice are generally smoother, we extend the theoretical analysis to cope with the model misspecification. That is, one uses a TM kernel in stochastic kriging, but the response surface is actually realized from a GP induced by a tensor product kernel with a higher degree of smoothness. Surprisingly, the upper rate of convergence under model misspecification is substantially faster than that under correct specification. Intuitively, this may be attributed to the fact that the function space induced by a smoother tensor product kernel is “smaller” than one induced by a TM kernel. This theoretical result provides the kind of robustness that is reassuring and encouraging to potential users of our methodology.

Third, typical SG designs are not flexible to use, because they are not defined directly via the number of design points, but via the so-called level parameter. The existing algorithms in the

literature for the computation of kriging with SG designs are very rigid, requiring that the number of design points fit exactly into an SG of some level. The computational efficiency would break down otherwise. We lift such restriction by proposing the TSG design, and develop algorithms that allow any arbitrary number of design points. The key driving force is an explicit characterization of the sparse structure of the inverse kernel matrix, permitting the algorithms to perform fast, exact computation of stochastic kriging with TM kernels, without any approximation strategies.

Fourth, the combination of the upper rates of convergence and the fast algorithms implies that our methodology is a viable option for high-dimensional metamodeling. Through extensive numerical experiments with problems having a design space of dimension as high as 16675, we demonstrate that our methodology significantly outperforms competing approaches in both prediction accuracy and computational efficiency.

At last, since earlier studies predominantly focused on Matérn kernels and Gaussian kernels, the existing approaches to theoretical analysis used there may not apply to our setting. We thus develop a variety of new technical results, particularly an orthogonal expansion of TM kernels and related properties; see the e-companion. They are of independent interest and may be used to facilitate future research that involves TM kernels and TSG designs.

1.2. Related Work

There is a vast literature on convergence rates of kriging and similar methods such as GPR in machine learning and kernel ridge regression (KRR) in nonparametric statistics. The assumptions in the three areas are distinctive owing to the differences in application context. In general, kriging focuses on noiseless samples and fixed designs, whereas both GPR and KRR focus on homoscedastic noise and random designs; meanwhile, both kriging and GPR assume that the function to estimate is a GP sample path, whereas KRR assumes that it lies in the reproducing kernel Hilbert space induced by the kernel. Despite the differences in assumptions and mathematical tools, the theoretical results in the three areas are comparable. An incomplete list of recent papers include Wang et al. (2020) and Tuo and Wang (2020) for kriging; van der Vaart and van Zanten (2011) and Pati et al. (2015) for GPR; and Caponnetto and De Vito (2007) and Tuo et al. (2020) for KRR. Convergence rate analysis for stochastic kriging, which assumes heteroscedastic noise, is scarce, although the results for GPR may conceivably be generalized to this setting. However, most of the existing work in the literature is derived for Matérn kernels or Gaussian kernels. To our knowledge, the present paper is the first work that establishes error bounds for stochastic kriging with TM kernels.

Another related strand of research is SG methods. SG experimental designs were introduced in Zenger (1991) to address the curse of dimensionality in standard grid-based numerical methods for partial differential equations: a d -dimensional grid consists of M^d points if the discretization

scheme in each dimension employs M points. SGs can reduce the number of points from $\mathcal{O}(M^d)$ to $\mathcal{O}(M(\log M)^{d-1})$ with a minor sacrifice of accuracy, thereby greatly alleviating the curse of dimensionality. We refer to Bungartz and Griebel (2004) for a survey of the fundamentals of SGs. Since its inception, SG methods have been applied to a great variety of research fields, including statistics, economics, and financial engineering; see, e.g., Garcke and Griebel (2013). Recently, Plumlee (2014) adopts SGs to enhance the computational efficiency of kriging with tensor product kernels. However, the algorithms developed there do not apply to stochastic kriging.

The remainder of the paper is organized as follows. Section 2 reviews stochastic kriging, including typical choices of kernels and experimental designs in practice, and discusses the curse of dimensionality that comes with such choices. Section 3 and Section 4 introduce TM kernels and TSG designs, respectively, both of which are the key ingredients of our methodology. Section 5 analyzes the convergence rate of stochastic kriging with TM kernels and TSG designs. The issue of model misspecification is also discussed there. Section 6 develops fast algorithms for implementing stochastic kriging with TM kernels and TSG designs. Section 7 presents extensive numerical experiments that focus on high-dimensional problems. Section 8 concludes with a brief discussion on possible extensions. All the proofs are collected in the e-companion to this paper.

2. Stochastic Kriging

We denote the d -dimensional design variable by $\mathbf{x} = (x_1, \dots, x_d)^\top$ and the design space by $\mathcal{X} \subseteq \mathbb{R}^d$. In (deterministic) kriging, the unknown response surface $y : \mathcal{X} \mapsto \mathbb{R}$ is modeled as a realized sample path of the GP

$$Y(\cdot) = \text{GP}(\mu(\cdot), k(\cdot, \cdot)),$$

where $\mu(\cdot)$ is the mean function and $k(\cdot, \cdot)$ is the covariance function, which is also called the *kernel* of Y . In particular, $\mu(\mathbf{x}) = \mathbb{E}[Y(\mathbf{x})]$ and $k(\mathbf{x}, \mathbf{x}') = \text{Cov}[Y(\mathbf{x}), Y(\mathbf{x}')] for all $\mathbf{x}, \mathbf{x}' \in \mathcal{X}$.$

The mean function $\mu(\cdot)$ characterizes the “trend” of the response surface. It is often modeled as $\mu(\mathbf{x}) = \mathbf{f}^\top(\mathbf{x})\boldsymbol{\beta}$, where $\mathbf{f}(\cdot)$ is a vector of known functions, which may encode the modeler’s prior knowledge regarding the shape of the response surface, and $\boldsymbol{\beta}$ is a vector of unknown parameters of compatible dimensions that need to be estimated. Throughout the paper, however, we assume that $\mu(\cdot) \equiv 0$ for simplicity. Our theoretical results can be generalized to the nonzero trend case.

Suppose that the response surface $y(\cdot)$ is sampled at design points $\{\mathbf{x}_1, \dots, \mathbf{x}_n\}$. For deterministic simulation models, $y(\mathbf{x}_i)$ is observed without noise for each i . Kriging then serves as an interpolation method; that is, the prediction at each design point equals exactly the simulation output there.

For stochastic simulation models, on the other hand, the response surface is observed with random noise. Suppose that the simulation model is executed for m_i replications at each \mathbf{x}_i , resulting in

random outputs $Y_r(\mathbf{x}_i) = y(\mathbf{x}_i) + \epsilon_r(\mathbf{x}_i)$, $r = 1, \dots, m_i$, where $\epsilon_r(\mathbf{x}_i)$'s are the simulation noise at \mathbf{x}_i that are independent Gaussian random variables with mean zero and variance $\sigma^2(\mathbf{x}_i)$. Assume that $\sup_{\mathbf{x} \in \mathcal{X}} \sigma^2(\mathbf{x}) < \infty$. In stochastic kriging, the simulation output $Y_r(\mathbf{x}_i)$ is modeled as a realization of the random variable $Y(\mathbf{x}_i) + \epsilon_r(\mathbf{x}_i)$. Throughout the present paper, we assume that the simulation model is executed independently at different design points, that is, $\epsilon_r(\mathbf{x}_i)$ and $\epsilon_s(\mathbf{x}_j)$ are independent for all r, s , and $i \neq j$. For stochastic kriging with the use of common random numbers, which would introduce dependence between $\epsilon_r(\mathbf{x}_i)$ and $\epsilon_s(\mathbf{x}_j)$, we refer to Chen et al. (2012) and Pearce et al. (2019) for details.

We denote the sample mean at \mathbf{x}_i by $\bar{Y}(\mathbf{x}_i) := m_i^{-1} \sum_{r=1}^{m_i} Y_r(\mathbf{x}_i)$ and the sample variance there by $\hat{\sigma}^2(\mathbf{x}_i) := (m_i - 1)^{-1} \sum_{r=1}^{m_i} (Y_r(\mathbf{x}_i) - \bar{Y}(\mathbf{x}_i))^2$. Let $\bar{\mathbf{Y}} := (\bar{Y}(\mathbf{x}_1), \dots, \bar{Y}(\mathbf{x}_n))^\top$ and $\mathbf{k}(\mathbf{x}) := (k(\mathbf{x}, \mathbf{x}_1), \dots, k(\mathbf{x}, \mathbf{x}_n))^\top$. Let $\mathbf{K} \in \mathbb{R}^{n \times n}$ be the covariance matrix, also referred to as the *kernel matrix*, with the (i, j) -th entry $\text{Cov}[Y(\mathbf{x}_i), Y(\mathbf{x}_j)] = k(\mathbf{x}_i, \mathbf{x}_j)$, $1 \leq i, j \leq n$. Let Σ be the covariance matrix with the (i, j) -th entry $\text{Cov}[m_i^{-1} \sum_{r=1}^{m_i} \epsilon_r(\mathbf{x}_i), m_j^{-1} \sum_{s=1}^{m_j} \epsilon_s(\mathbf{x}_j)] = \sigma^2(\mathbf{x}_i)/m_i$ for $i = j$ and 0 otherwise. Stochastic kriging is concerned with predicting the response surface at an arbitrary $\mathbf{x} \in \mathcal{X}$. Specifically, the prediction is given by

$$\hat{Y}(\mathbf{x}) = \mathbf{k}^\top(\mathbf{x})(\mathbf{K} + \Sigma)^{-1} \bar{\mathbf{Y}}. \quad (1)$$

The mean squared error (MSE) of the prediction is

$$\text{MSE}[\hat{Y}(\mathbf{x})] = \mathbb{E}[(\hat{Y}(\mathbf{x}) - Y(\mathbf{x}))^2] = k(\mathbf{x}, \mathbf{x}) - \mathbf{k}^\top(\mathbf{x})(\mathbf{K} + \Sigma)^{-1} \mathbf{k}(\mathbf{x}). \quad (2)$$

Without loss of generality, in the sequel we assume for simplicity that $m_i \equiv 1$ for all $i = 1, \dots, n$, unless specified otherwise explicitly. Hence, the terms “sample size” and “number of design points” will be used interchangeably, both referring to n .

Despite a flexible metamodeling approach that ensures global convergence in general, predication capability of stochastic kriging may vary substantially depending on the choices of the kernel and the experimental design. To a large extent, they collectively determine both the sample complexity and the computational complexity of stochastic kriging. Before introducing the new methodology, we briefly overview typical examples of kernels and experimental designs that are adopted in practice.

2.1. Typical Examples of Kernels

We introduce typical examples of kernels and refer to Rasmussen and Williams (2006, Chapter 4) for more discussion.

EXAMPLE 1 (GAUSSIAN KERNEL). Let $\boldsymbol{\theta} \in \mathbb{R}^d$. The Gaussian kernel is defined by

$$k_{\text{Gauss}}(\mathbf{x}, \mathbf{x}'; \boldsymbol{\theta}) := \exp\left(-\|\boldsymbol{\theta}^\top(\mathbf{x} - \mathbf{x}')\|^2\right), \quad \mathbf{x}, \mathbf{x}' \in \mathbb{R}^d,$$

where $\|\cdot\|$ denotes the Euclidean norm.

EXAMPLE 2 (MATÉRN KERNEL). Let $\boldsymbol{\theta} \in \mathbb{R}^d$ and $\nu > 0$. The Matérn(ν) kernel is defined by

$$k_{\text{Matérn}(\nu)}(\mathbf{x}, \mathbf{x}'; \boldsymbol{\theta}) := \frac{1}{2^{\nu-1}\Gamma(\nu)} \left(\sqrt{2\nu} \|\boldsymbol{\theta}^\top(\mathbf{x} - \mathbf{x}')\| \right)^\nu K_\nu \left(\sqrt{2\nu} \|\boldsymbol{\theta}^\top(\mathbf{x} - \mathbf{x}')\| \right), \quad \mathbf{x}, \mathbf{x}' \in \mathbb{R}^d,$$

where $\Gamma(\cdot)$ is the gamma function and $K_\nu(\cdot)$ is the modified Bessel function of the second kind of order ν . The Matérn kernel has a simplified form if ν is half-integer: $\nu = p + 1/2$ for some non-negative integer p . For instance,

$$\begin{aligned} k_{\text{Matérn}(1/2)}(\mathbf{x}, \mathbf{x}'; \boldsymbol{\theta}) &:= \exp(-\|\boldsymbol{\theta}^\top(\mathbf{x} - \mathbf{x}')\|), \\ k_{\text{Matérn}(3/2)}(\mathbf{x}, \mathbf{x}'; \boldsymbol{\theta}) &:= \left(1 + \sqrt{3}\|\boldsymbol{\theta}^\top(\mathbf{x} - \mathbf{x}')\|\right) \exp(-\sqrt{3}\|\boldsymbol{\theta}^\top(\mathbf{x} - \mathbf{x}')\|). \end{aligned}$$

The parameter ν in the Matérn kernel determines the smoothness of the GP sample paths: a larger ν leads to sample paths having a higher degree of differentiability. Thus, the Matérn kernel is often used for modeling response surfaces with a finite degree of differentiability. This is in contrast to the Gaussian kernel that induces infinitely differentiable GP sample paths. In fact, the Gaussian kernel can be obtained as a limit of the Matérn kernel as $\nu \rightarrow \infty$ (Gramacy 2020, Page 192).

Another approach to constructing multidimensional kernels is via tensor products. If $k_j(\cdot, \cdot)$ is a kernel defined on $\mathcal{X}_j \subseteq \mathbb{R}$ for each $j = 1, \dots, d$, then

$$k(\mathbf{x}, \mathbf{x}') = \prod_{j=1}^d k_j(x_j, x'_j), \quad (3)$$

is a kernel defined on the product space $\mathcal{X} = \times_{j=1}^d \mathcal{X}_j$. Tensor product kernels imply that the dependence structure of the associated GP across each dimension is separable. (But it does not mean that the sample paths are separable functions.) A particular advantage of the tensor product form is that it may induce substantial computational savings (Section 2.2).

Note that the Gaussian kernel has a product form, whereas the Matérn kernel does not. Recently, Salemi et al. (2019a) proposes a new class of tensor product kernels and demonstrate numerically that the corresponding GPs, called GIBFs, have excellent prediction capability.

EXAMPLE 3 (GIBF KERNEL). Let $\ell_j \geq 0$ be an integer and $\boldsymbol{\theta}_j = (\theta_{j,0}, \theta_{j,1}, \dots, \theta_{j,\ell_j+1}) \in \mathbb{R}_{>0}^{\ell_j+2}$, for each $j = 1, \dots, d$. The GIBF kernel is defined by the form (3), where

$$k_j(x_j, x'_j; \boldsymbol{\theta}_j) = \sum_{i=0}^{\ell_j} \theta_{j,i} \frac{(x_j x'_j)^i}{(i!)^2} + \theta_{j,\ell_j+1} \int_0^\infty \frac{(x_j - u)_+^{\ell_j} (x'_j - u)_+^{\ell_j}}{(\ell_j!)^2} du, \quad \mathbf{x}, \mathbf{x}' \in \mathbb{R}_{\geq 0}^d.$$

2.2. Typical Examples of Experimental Designs

There are two typical choices of the experimental design—*space-filling* designs and *lattice* designs. We discuss them briefly here and refer to Santner et al. (2003) for extensive exposition on the subject.

Space-filling designs are widely used for computer experiments. They are developed following the principle that design points should be spread evenly to provide information about all portions of the design space, since the response surface is unknown *a priori* and its interesting features may be just likely to appear in one part of the design space as another.

Standard examples of space-filling designs are Latin hypercube designs (LHDs) developed in McKay et al. (1979) and their variations. The popularity of LHDs stems from their ease of use and the fact that their projections onto one-dimensional subspaces are evenly dispersed. They have been shown to perform well for predicting response surfaces. However, the superiority of LHDs relative to, say, random designs which are formed by generating design points independently from some distribution, usually holds only for large sample sizes, especially when the design space is high-dimensional. The large sample size makes it difficult to compute the stochastic kriging predictor (1), as it involves inverting a large matrix; see Section 2.3 for more discussion.

Lattice designs are formed by the Cartesian product of one-dimensional designs, that is, $\mathcal{X} = \times_{j=1}^d \mathcal{X}_j = \{(x_1, \dots, x_d) : x_j \in \mathcal{X}_j, j = 1, \dots, d\}$, where \mathcal{X}_j is a one-dimensional design of size n_j on the j -th dimension of the design space. Lattice designs can lead to significant computational savings in kriging when used in conjunction with kernels of the product form (3). Specifically, the inverse kernel matrix can be expressed as a Kronecker product of smaller matrices, that is, $\mathbf{K}^{-1} = \bigotimes_{j=1}^d \mathbf{K}_j^{-1}$. Here, \mathbf{K}_j denotes the kernel matrix corresponding to the kernel k_j on the j -th dimension and its associated one-dimensional design \mathcal{X}_j , i.e., entries of \mathbf{K}_j are of the form $k_j(x, x')$ for $x, x' \in \mathcal{X}_j$. \mathbf{K}^{-1} , which can now be computed via $\mathbf{K}^{-1} = \bigotimes_{j=1}^d \mathbf{K}_j^{-1}$. This is massively faster than direct inversion of \mathbf{K} because it reduces inverting one large matrix of size $\prod_{j=1}^d n_j \times \prod_{j=1}^d n_j$ to inverting multiple small matrices, each of size $n_j \times n_j$.

Despite the considerable computational advantage, lattice designs are not practical for high-dimensional problems because they would result in an enormous sample size. For example, when $d = 20$ a lattice design has at least $2^d > 10^6$ design points, implying an excessive sample cost.

2.3. Curse of Dimensionality

The curse of dimensionality affects both sample complexity and computational complexity.

2.3.1. Sample Complexity Under homoscedasticity, the convergence rate of stochastic kriging with the Matérn kernel has been well studied. It is shown in van der Vaart and van Zanten (2011) that under mild conditions, if (i) the response surface is a GP sample path induced by the Matérn(α) kernel, and (ii) the Matérn(ν) kernel and a random design are used in stochastic kriging, then the predictor (1) converges at the rate $n^{-\min(\alpha, \nu)/(2\nu+d)}$, assuming a single observation at each design point. It is easy to see that the fastest rate $n^{-\alpha/(2\alpha+d)}$ is attained at $\nu = \alpha$, that is, the model

is correctly specified. In practice, the convergence rate of stochastic kriging is likely to be worse, since α is usually unknown, thereby prone to misspecification.

Note that the rate $n^{-\alpha/(2\alpha+d)}$ coincides with the *minimax-optimal* rate for estimating with noisy samples an unknown function in a given space of “smooth” functions having a parameter α that measures the degree of smoothness (Stone 1980). The minimax-optimal rate basically specifies a fundamental lower bound on the error of any estimator of an unknown function in such a space (Tsybakov 2009). Hence, if the response surface is a GP sample path induced by the Matérn(α) kernel, then regardless of the experimental design, the sample complexity for the predictor (1) to achieve a small error δ is at least of the order of magnitude $(1/\delta)^{2+d/\alpha}$, which grows exponentially in d , manifesting the curse of dimensionality.

We introduce TM kernels in Section 3 and TSG designs in Section 4. We will show in Section 5 that their joint use can to some extent circumvent the curse of dimensionality on the convergence rate of stochastic kriging.

2.3.2. Computational Complexity The main computational burden of stochastic kriging is to invert the matrix $(\mathbf{K} + \mathbf{\Sigma})$ of size $n \times n$, which requires $\mathcal{O}(n^3)$ arithmetic operations in general. The matrix inversion is involved in the computation of the predictor (1) and its MSE (2). As discussed before, the sample size n is usually large for high-dimensional problems, and it in turn makes the matrix inversion computationally difficult. For example, when $n > 10^5$ both storing $(\mathbf{K} + \mathbf{\Sigma})$ and computing its inverse are costly or even prohibitive on typical modern computers, although the limitation can be somewhat lifted by using high-performance computing infrastructures. Existing research has focused on approximation methods that replace the matrix of interest with one that is easier to invert while preserving the prediction accuracy as much as possible; see Section 2.3.3 for a brief overview. However, for an approximation method to perform well it often requires fine tuning of certain parameters involved to determine the proper trade-off between the approximation accuracy and the computational requirement. Moreover, using approximations in lieu of the exact inverse matrix may yield spurious estimates of the MSE of the prediction (Shahriari et al. 2016).

We do not pursue approximation methods in the present paper. We will show in Section 6 that the joint use of TSG designs and TM kernels permits us to do exact computation of stochastic kriging with dramatically less computational cost.

2.3.3. Approximation Methods Stochastic kriging is closely related to kernel methods in machine learning literature (Schölkopf and Smola 2002). A plethora of approximation methods for computing $(\mathbf{K} + \mathbf{\Sigma})^{-1}$ on a large dataset have been developed; see Liu et al. (2020) for a recent survey. Among the most popular are the Nyström method and the random features method. Both methods seek to construct another kernel function, say \tilde{k} , whose kernel matrix $\tilde{\mathbf{K}}$ is of rank $\ell < n$.

By applying the Woodbury matrix identity (Horn and Johnson 2012, Page 19), the approximation $(\tilde{\mathbf{K}} + \mathbf{\Sigma})^{-1}$ can normally be computed with complexity $\mathcal{O}(\ell^2 n)$.

The Nyström method approximates the first ℓ eigenvectors of \mathbf{K} by selecting a subset of size ℓ of the n design points (Smola and Schölkopf 2000, Williams and Seeger 2001). Let $\tilde{\mathbf{x}}_1, \dots, \tilde{\mathbf{x}}_\ell$ denote the selected points. Then, an approximate kernel function is constructed by $\tilde{k}(\mathbf{x}, \mathbf{x}') = \mathbf{k}_\ell^\top(\mathbf{x}) \mathbf{K}_{\ell, \ell}^{-1} \mathbf{k}_\ell(\mathbf{x}')$, where $\mathbf{k}_\ell(\mathbf{x}) = (k(\tilde{\mathbf{x}}_1, \mathbf{x}), \dots, k(\tilde{\mathbf{x}}_\ell, \mathbf{x}))^\top$ and $\mathbf{K}_{\ell, \ell} = (k(\tilde{\mathbf{x}}_i, \tilde{\mathbf{x}}_j))_{i, j=1}^\ell$. See Rudi and Rosasco (2017) and Lu et al. (2020) for recent developments of this method.

The random features method originates from the seminal work Rahimi and Recht (2007), and has drawn substantial interest in recent years (Liu et al. 2021). In contrast to the Nyström method, for which the approximate kernels are dependent on the given design points, the random features method constructs *data-independent* approximations using Fourier transforms. In particular, this method uses $\tilde{k}(\mathbf{x}, \mathbf{x}') = \sum_{i=1}^\ell \psi_i(\mathbf{x}) \psi_i(\mathbf{x}')$ to approximate $k(\mathbf{x}, \mathbf{x}')$, where $\psi_1(\mathbf{x}), \dots, \psi_\ell(\mathbf{x})$ are basis functions—also known as features in machine learning literature—that are constructed based on random samples drawn from the spectral density (i.e., the Fourier transform) of the kernel function k . (For instance, the spectral density of a Gaussian kernel is the probability density of a multivariate normal distribution.)

These approximation methods can be implemented for general kernel functions. (One exception is that the random features method may not be suitable for nonstationary kernels.) However, we stress that they focus on fast computations. The statistical properties, such as the rate of convergence of the predictor to the true response surface, also depend mainly on the choice of the kernel and need to be analyzed separately. In Section 7, we numerically compare both the Nyström method and the random features method with the approach developed in the present paper.

3. Tensor Markov Kernels

Let us begin with one-dimensional Gauss-Markov processes. Their kernels share a common functional form, characterized in the following lemma. This is a well known result; see Lemma 5.1.8 and Lemma 5.1.9 in Marcus and Rosen (2006) for the proof.

LEMMA 1. *Let $\mathcal{J} \subseteq \mathbb{R}$ be an interval (open or closed). Let $\mathbf{Y} = \{\mathbf{Y}(x) : x \in \mathcal{J}\}$ be a zero mean GP with continuous positive definite kernel $k(\cdot, \cdot)$. Then, \mathbf{Y} is a Gauss-Markov process if and only if there exist positive functions p and q on \mathcal{J} with p/q strictly increasing such that*

$$k(x, x') = p(x \wedge x') q(x \vee x'), \quad x, x' \in \mathcal{J}, \quad (4)$$

where $x \wedge x' = \min(x, x')$ and $x \vee x' = \max(x, x')$.

Here are some typical examples of Gauss-Markov processes and their kernels; see Karatzas and Shreve (1991, Chapter 5.6) for more discussion on their properties.

EXAMPLE 4 (BROWNIAN MOTION KERNEL). Brownian motion is a prominent example of Gauss-Markov processes. The kernel of the standard Brownian motion is

$$k_{\text{BM}}(x, x') = x \wedge x', \quad x, x' \in \mathbb{R}_{\geq 0}.$$

Then, k_{BM} satisfies the form (4) with $p(x) = x$ and $q(x) = 1$ for $x \in \mathbb{R}_{\geq 0}$.

EXAMPLE 5 (BROWNIAN BRIDGE KERNEL). The kernel of a Brownian bridge on $[0, T]$ is given by

$$k_{\text{BB}}(x, x') = (x \wedge x') \left(1 - \frac{x \vee x'}{T} \right), \quad x, x' \in [0, T].$$

Then, k_{BB} has the form (4) with $p(x) = x$ and $q(x) = 1 - x/T$ for $x \in [0, T]$.

EXAMPLE 6 (LAPLACE KERNEL). Let $\theta \in \mathbb{R}_{>0}$. The Laplace kernel is defined by

$$k_{\text{Laplace}}(x, x'; \theta) = \exp(-\theta|x - x'|), \quad x, x' \in \mathbb{R}.$$

It is the same as the Matérn($1/2$) kernel. Then, k_{Laplace} has the form (4) with $p(x) = e^{\theta x}$ and $q(x) = e^{-\theta x}$ for $x \in \mathbb{R}$. The corresponding Gauss-Markov process is the stationary Ornstein-Uhlenbeck process.

We now introduce TM kernels for d -dimensional GPs, based on the characterization on the kernels of one-dimensional Gauss-Markov processes in Lemma 1.

DEFINITION 1 (TENSOR MARKOV KERNEL). For each $j = 1, \dots, d$, let $\mathcal{X}_j \subseteq \mathbb{R}$ be an interval (open or closed), and let p_j and q_j be positive functions on \mathcal{J}_j with p_j/q_j strictly increasing. Then,

$$k(\mathbf{x}, \mathbf{x}') = \prod_{j=1}^d p_j(x_j \wedge x'_j) q_j(x_j \vee x'_j), \quad \mathbf{x}, \mathbf{x}' \in \mathcal{X}, \quad (5)$$

is called a *tensor Markov (TM) kernel* on $\mathcal{X} = \times_{j=1}^d \mathcal{X}_j$. We also call the corresponding GP a *tensor Markov Gaussian process (TMGP)*.

Note that each component kernel k_j may be different in general, and the theory is developed with such generality. However, for simplicity, we focus on the case where the component kernels are identical in the numerical experiments in Section 7.

The GIBF kernel (Example 3) developed in Salemi et al. (2019a) is a TM kernel if its order is $(\ell_1, \dots, \ell_j) = \mathbf{0}$. In this case, the GIBF kernel is reduced to

$$k_{\text{GIBF}(\mathbf{0})}(\mathbf{x}, \mathbf{x}') = \prod_{j=1}^d [\theta_{j,0} + \theta_{j,1}(x_j \wedge x'_j)], \quad \mathbf{x}, \mathbf{x}' \in \mathbb{R}_{\geq 0}^d.$$

The form (5) is verified by setting $p_j(x) = \theta_{j,0} + \theta_{j,1}(x)$ and $q_j(x) = 1$ for $x \in \mathbb{R}$. The corresponding GP is a Brownian field.

3.1. A Connection to Ordinary Differential Equations

The theory we develop in the present paper relies on a connection between Gauss-Markov processes and linear ordinary differential equations (ODE). This connection is well known in probability and statistics literature. We provide a heuristic, exemplary introduction below and refer interested readers to Dolph and Woodbury (1952), Ylvisaker (1987), and Moura and Goswami (1997) for a rigorous treatment, which is beyond the scope of the present paper.

Suppose that $\{Y(x) : x \in \mathbb{R}\}$ is the stationary Ornstein-Uhlenbeck process and $k(x, x')$ is the Laplace kernel with parameter $\theta = 1$ (Example 6) that is associated with it. For each $i \in \mathbb{N}$, let $x_i = ih$ for some constant $h > 0$. Then, the discretized process $\{Y(x_i) : i \in \mathbb{N}\}$ forms a Markov chain and its transition dynamics can be written as

$$Y(x_{i+1}) = e^{-h}Y(x_i) + \varepsilon_i \sqrt{1 - e^{-2h}},$$

where ε_i 's are independent and identically distributed (i.i.d.) standard normal random variables.

We can show via a straightforward calculation that the joint distribution of $\{Y(x_i) : i \in \mathbb{N}\}$ satisfies

$$\begin{aligned} \mathbb{P}(\{Y(x_i) : i \in \mathbb{N}\}) &\propto \exp\left(-\frac{1}{1 - e^{-2h}} \sum_{i \in \mathbb{N}} (Y(x_i) - e^{-h}Y(x_{i-1}))^2\right) \\ &= \exp\left(-\frac{1}{1 - e^{-2h}} \sum_{i \in \mathbb{N}} (1 + e^{-2h})Y^2(x_i) - e^{-h}Y(x_i)Y(x_{i+1}) - e^{-h}Y(x_i)Y(x_{i-1}))\right) \\ &= \exp\left(-\sum_{i,j \in \mathbb{N}} L_{i,j} Y(x_i)Y(x_j)\right), \end{aligned}$$

where $L_{i,i} = \frac{1+e^{-2h}}{1-e^{-2h}}$, $L_{i-1,i} = L_{i,i+1} = \frac{-e^{-h}}{1-e^{-2h}}$, and $L_{i,j} = 0$ for all $i, j \in \mathbb{N}$ such that $|i - j| \geq 2$. Hence, the joint distribution of $\{Y(x_i) : i \in \mathbb{N}\}$ is determined by $\{L_{i,j} : i, j \in \mathbb{N}\}$. Further, note that

$$\begin{aligned} \sum_{i,j \in \mathbb{N}} L_{i,j} Y(x_i)Y(x_j) &= \frac{h}{2} \sum_{i \in \mathbb{N}} Y(x_i) \left(-\frac{Y(x_{i+1}) - 2Y(x_i) + Y(x_{i-1}))}{h^2} + Y(x_i) \right) + \mathcal{O}(h) \\ &\rightarrow \frac{1}{2} \int Y(x)(\mathcal{L}Y)(x) dx, \end{aligned}$$

as $h \rightarrow 0$, where \mathcal{L} is a differential operator defined as $(\mathcal{L}f)(x) := -\frac{d^2 f}{dx^2}(x) + f(x)$. Hence, the joint distribution of $\{Y(x) : x \in \mathbb{R}\}$ is determined by the operator \mathcal{L} , which can be interpreted as a continuous analog of $\{L_{i,j} : i, j \in \mathbb{N}\}$. Moreover, let $p(x) = e^x$ and $q(x) = e^{-x}$ so that $k(x, x') = p(x \wedge x')q(x \vee x')$ as in Example 6. One can easily verify that $(\mathcal{L}p)(x) = (\mathcal{L}q)(x) = 0$.

In general, the distribution of a Gauss-Markov process can be fully characterized by a second-order linear differential operator like \mathcal{L} . Since all second-order linear ODEs can be recast to a Sturm-Liouville equation of form (6) below by a simple transformation (Arfken et al. 2012, Chapter 8), we impose the following regularity condition on such an ODE.

ASSUMPTION 1. Let $k(\mathbf{x}, \mathbf{x}') = \prod_{j=1}^d p_j(x_j \wedge x'_j) q_j(x_j \vee x'_j)$ be a TM kernel for $\mathbf{x}, \mathbf{x}' \in (0, 1)^d$. For each $j = 1, \dots, d$, both p_j and q_j are continuously differentiable and satisfy the ODE $(\mathcal{L}_j f)(x) = 0$ for all $x \in (0, 1)$, where

$$(\mathcal{L}_j f)(x) = \frac{d}{dx} \left(u_j(x) \frac{df}{dx}(x) \right) + v_j(x) f(x), \quad (6)$$

where u_j is a continuously differentiable function on $(0, 1)$ and v_j is a continuous function on $(0, 1)$.

It is straightforward to verify that Examples 4–6 all satisfy Assumption 1, so we omit the details.

3.2. Markov Property

Let \mathbf{Y} be a TMGP defined on $\mathcal{X} = \times_{j=1}^d \mathcal{X}_j$, with each $\mathcal{X}_j \subseteq \mathbb{R}$ an interval. It follows from Corollary 3.3 in Carnal and Walsh (1991) that \mathbf{Y} has the *sharp Markov property with respect to rectangular sets*, which is equivalent to the \mathbf{p} -order Markov property, introduced in Salemi et al. (2019a), with $\mathbf{p} = \mathbf{0}$. Specifically, let $\mathcal{J} = \times_{j=1}^d \mathcal{J}_j$ be a rectangular set in \mathcal{X} , where each $\mathcal{J}_j \subseteq \mathcal{X}_j$ is an interval. Then, $\varsigma(\{\mathbf{Y}(\mathbf{x}) : \mathbf{x} \in \mathcal{J}\})$ is conditionally independent of $\varsigma(\{\mathbf{Y}(\mathbf{x}) : \mathbf{x} \in \mathcal{X} \setminus \mathcal{J}\})$ given $\varsigma(\{\mathbf{Y}(\mathbf{x}) : \mathbf{x} \in \partial(\mathcal{J})\})$, where $\varsigma(\mathcal{S})$ denotes the sigma-algebra generated by \mathcal{S} , and $\partial(\mathcal{J})$ denotes the boundary of \mathcal{J} . Basically, the $\mathbf{0}$ -order Markov property indicates that given information about \mathbf{Y} on the boundary of a rectangular region, information about \mathbf{Y} outside the region provides no additional value for predicting \mathbf{Y} inside the region.

It is nontrivial to generalize the usual Markov property for stochastic processes on \mathbb{R} to random fields on \mathbb{R}^d . A particular challenge is to define properly the “past”, “present”, and “future” on a multidimensional space, analogously to the real line. Indeed, there are several different Markovian notions other than the sharp Markov property for random fields; see, e.g., the Appendix in Adler (1981). It is beyond the scope of the present paper to study these properties for TMGPs in detail. Our sample complexity analysis and development of computational algorithms do not directly rely on the multidimensional Markovian notions. Instead, it is the usual Markov property on the real line that is of great significance for us to develop relevant theory. In particular, for $d = 1$, by virtue of the Markov property of the underlying Gauss-Markov process, we show below that \mathbf{K}^{-1} is a tridiagonal matrix and its nonzero entries can be calculated analytically.

PROPOSITION 1. Let $k(x, x') = p(x \wedge x') q(x \vee x')$ be a TM kernel in one dimension. Let $n \geq 3$, $x_0 = -\infty$, $x_{n+1} = \infty$, and $\{x_1, \dots, x_n\}$ be an increasing sequence. Let $\mathbf{p}_0 = \mathbf{q}_{n+1} = 0$, $\mathbf{p}_{n+1} = \mathbf{q}_0 = 1$, and $\mathbf{p}_i = p(x_i)$ and $\mathbf{q}_i = q(x_i)$ for $i = 1, \dots, n$. Then, \mathbf{K}^{-1} and $\mathbf{K}^{-1}\mathbf{k}(x)$ are specified as follows.

(i) \mathbf{K}^{-1} is a tridiagonal matrix, i.e., $(\mathbf{K}^{-1})_{i,i+2} = (\mathbf{K}^{-1})_{i+2,i} = 0$ for all $i = 1, \dots, n-2$; moreover,

$$\begin{aligned} (\mathbf{K}^{-1})_{i,i} &= \frac{\mathbf{p}_{i+1}\mathbf{q}_{i-1} - \mathbf{p}_{i-1}\mathbf{q}_{i+1}}{(\mathbf{p}_i\mathbf{q}_{i-1} - \mathbf{p}_{i-1}\mathbf{q}_i)(\mathbf{p}_{i+1}\mathbf{q}_i - \mathbf{p}_i\mathbf{q}_{i+1})}, & i = 1, \dots, n, \\ (\mathbf{K}^{-1})_{i,i+1} &= (\mathbf{K}^{-1})_{i+1,i} = \frac{-1}{\mathbf{p}_{i+1}\mathbf{q}_i - \mathbf{p}_i\mathbf{q}_{i+1}}, & i = 1, \dots, n-1. \end{aligned} \quad (7)$$

(ii) Let $i^* = 0, 1, \dots, n$ such that $x \in [x_{i^*}, x_{i^*+1})$. Then,

$$(\mathbf{K}^{-1}\mathbf{k}(x))_i = \begin{cases} \frac{\mathbf{p}_{i^*+1}q(x) - p(x)\mathbf{q}_{i^*+1}}{\mathbf{p}_{i^*+1}\mathbf{q}_{i^*} - \mathbf{p}_{i^*}\mathbf{q}_{i^*+1}}, & \text{if } i = i^*, \\ \frac{p(x)\mathbf{q}_{i^*} - \mathbf{p}_{i^*}q(x)}{\mathbf{p}_{i^*+1}\mathbf{q}_{i^*} - \mathbf{p}_{i^*}\mathbf{q}_{i^*+1}}, & \text{if } i = i^* + 1, \\ 0, & \text{otherwise.} \end{cases} \quad (8)$$

REMARK 1. One should not confuse TMGPs with Gaussian Markov random fields (GMRFs). The former are GPs defined on a continuous domain in \mathbb{R}^d , whereas the latter are GPs defined on a discrete set, usually a graph with nodes representing the index and edges indicating the dependence structure. We refer to Rue and Held (2005) for a general introduction to GMRFs.

3.3. Non-differentiability

It can be shown that TMGPs can be represented by a time-changed Brownian field after proper possibly nonlinear scaling; see, e.g., Theorem 3.2 in Carnal and Walsh (1991) and Remark 5.1.11 in Marcus and Rosen (2006). In particular, if $\mathbf{Y} = \{\mathbf{Y}(\mathbf{x}) : \mathbf{x} \in \mathcal{X}\}$ is a TMGP with kernel (5), then \mathbf{Y} has the same distribution as

$$\left\{ \left(\prod_{j=1}^d q_j(x_j) \right) \mathbf{B}(p_1(x_1)/q_1(x_1), \dots, p_d(x_d)/q_d(x_d)) : \mathbf{x} \in \mathcal{X} \right\},$$

where \mathbf{B} is a standard Brownian field on $\mathbb{R}_{\geq 0}^d$. This representation suggests that like Brownian fields, the sample paths of TMGPs are continuous but nowhere differentiable.

From a modeling viewpoint, the nowhere-differentiability seems rather restrictive. After all, most response surfaces of interest in practice do exhibit some degree of smoothness: non-differentiability often appears in some but all parts of the design space. We discuss in Section 5.2 the prediction capability of TMGPs under such model misspecification. Somewhat surprisingly, we prove that the convergence rate of stochastic kriging with TM kernels for predicting smooth surfaces does not suffer much from the curse of dimensionality under mild conditions, provided that the experimental design is chosen to be a TSG.

4. Sparse Grid Experimental Designs

This section proceeds in two main steps. First, we introduce classical SGs. Then, we propose TSG designs that are much more flexible with regard to specifying the sampling budget.

4.1. Classical Sparse Grids

Recall that a lattice design is defined as the Cartesian product $\mathcal{X} = \prod_{j=1}^d \mathcal{X}_j$, where \mathcal{X}_j is a one-dimensional *component design* in the j -th dimension, having n_j points. Then, the kernel matrix of

size $\prod_{j=1}^d n_j \times \prod_{j=1}^d n_j$ can be expressed as a Kronecker product of much smaller matrices, each of size $n_j \times n_j$, provided that the kernel is of the product form (3).

Sparse grid (SG) designs extend the idea of lattice designs, retaining the computational advantage induced by the tensor structure while dramatically reducing the grid size in high dimensions. A key notion in constructing SG designs is the *level* that we denote by $\tau \geq 1$. Given τ , we specify, for each dimension, a *nested* sequence of one-dimensional designs $\emptyset = \mathcal{X}_{j,0} \subseteq \mathcal{X}_{j,1} \subseteq \mathcal{X}_{j,2} \subseteq \cdots \subseteq \mathcal{X}_{j,\tau}$. There are multiple ways to choose the nested sequences to construct an SG; see Bungartz and Griebel (2004). We adopt the “classical” approach in the present paper. Suppose that the design space is a hypercube $\mathcal{X} = (0,1)^d$. We construct the nested sequence for each dimension by recursive dyadic partitioning of the interval $(0,1)$. That is, for each $j = 1, \dots, d$,

$$\begin{aligned} \mathcal{X}_{j,1} &= \{1/2\}, \\ \mathcal{X}_{j,2} &= \{1/4, 1/2, 3/4\}, \\ &\vdots \\ \mathcal{X}_{j,\tau} &= \{1 \cdot 2^{-\tau}, 2 \cdot 2^{-\tau}, \dots, (2^\tau - 1) \cdot 2^{-\tau}\}. \end{aligned} \tag{9}$$

The parameter τ thus indicates the refinement level of the nested sequence of each dimension. Then, a SG of level τ is defined as

$$\mathcal{X}_\tau^{\text{SG}} = \bigcup_{|\mathbf{l}| \leq \tau + d - 1} \mathcal{X}_{1,l_1} \times \cdots \times \mathcal{X}_{d,l_d} \tag{10}$$

where $\mathbf{l} = (l_1, \dots, l_d) \in \mathbb{N}^d$ and $|\mathbf{l}| = \sum_{j=1}^d l_j$. Namely, an SG is the union of multiple lattices. We refer to the SGs constructed using the nested sequences in (9) as the classical SGs.

REMARK 2. The “full grid” that uses the same refinement level τ for each dimension can be expressed in a form similar to (10):

$$\bigtimes_{j=1}^d \mathcal{X}_{j,\tau} = \bigcup_{\|\mathbf{l}\|_\infty \leq \tau} \mathcal{X}_{1,l_1} \times \cdots \times \mathcal{X}_{d,l_d}, \tag{11}$$

where $\|\mathbf{l}\|_\infty = \max(l_1, \dots, l_d)$. Contrasting (10) with (11) reveals a key reason why SG designs have a much smaller grid size relative to lattice designs of the same refinement level. In the SG design (10), the size of each constituent lattice is small, because the refinement level of each dimension cannot be large simultaneously due to the condition $\sum_{j=1}^d l_j \leq \tau + d - 1$. For instance, if there exists a dimension in which $l_j = \tau$, then $l_{j'} = 1$ for all $j' \neq j$.

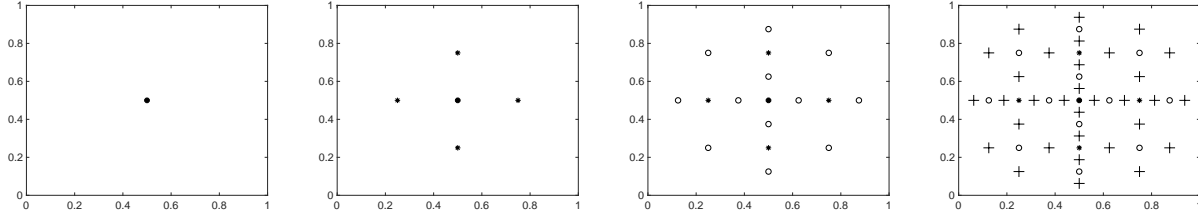
EXAMPLE 7 (TWO-DIMENSIONAL CLASSICAL SPARSE GRIDS). Assume $d = 2$ and $\tau = 2$. By the definition (10), the level multi-index satisfies $|\mathbf{l}| \leq 3$, so the two-dimensional classical SG of level 2 is a union of three smaller lattices with level indices $\mathbf{l} \in \{(1,1), (1,2), (2,1)\}$, i.e.,

$$\mathcal{X}_2^{\text{SG}} = (\mathcal{X}_{1,1} \times \mathcal{X}_{2,1}) \cup (\mathcal{X}_{1,1} \times \mathcal{X}_{2,2}) \cup (\mathcal{X}_{1,2} \times \mathcal{X}_{2,1})$$

$$\begin{aligned}
&= (\{1/2\} \times \{1/2\}) \cup (\{1/2\} \times \{1/4, 1/2, 3/4\}) \cup (\{1/4, 1/2, 3/4\} \times \{1/2\}) \\
&= \{(1/2, 1/4), (1/2, 1/2), (1/2, 3/4), (1/4, 1/2), (3/4, 1/2)\}.
\end{aligned}$$

Figure 1 shows the two-dimensional classical SGs of level 1 to 4.

Figure 1 Classical SGs of Level 1 to 4 in Two Dimensions.



Note. The new points added as the level increases are denoted by a different symbol.

Note that the constituent lattices of an SG have common points. For instance, in Example 7

$$(\mathcal{X}_{1,1} \times \mathcal{X}_{2,1}) \cap (\mathcal{X}_{1,1} \times \mathcal{X}_{2,2}) \cap (\mathcal{X}_{1,2} \times \mathcal{X}_{2,1}) = \{(1/2, 1/2)\}.$$

To facilitate theoretical analysis in later sections, we represent classical SGs as a union of non-overlapping sets of design points by defining the following notations. Let $\mathbf{c}_{l,i} := i \cdot 2^{-l}$ for $l \geq 1$ and $i = 1, \dots, 2^l - 1$, and let $\mathbf{c}_{\mathbf{l},\mathbf{i}} := (\mathbf{c}_{l_1,i_1}, \dots, \mathbf{c}_{l_d,i_d})$. For any level multi-index \mathbf{l} , we define a set for the multi-index \mathbf{i} as follows

$$\rho(\mathbf{l}) := \bigtimes_{j=1}^d \{i_j : i_j \text{ is an odd number between } 1 \text{ and } 2^{l_j}\} = \bigtimes_{j=1}^d \{1, 3, 5, \dots, 2^{l_j} - 1\}. \quad (12)$$

Then, we may write the component designs in (9) as $\mathcal{X}_{j,l} = \{\mathbf{c}_{l,i} : i = 1, \dots, 2^l - 1\}$ for all $j = 1, \dots, d$ and $l = 1, \dots, \tau$. Furthermore, it is easy to show that thanks to the nested structure, the classical SG can be represented as

$$\mathcal{X}_\tau^{\text{SG}} = \bigcup_{|\mathbf{l}| \leq \tau + d - 1} \{\mathbf{c}_{\mathbf{l},\mathbf{i}} : \mathbf{i} \in \rho(\mathbf{l})\}. \quad (13)$$

Moreover, when we augment the classical SG from level $\tau - 1$ to level τ , the new added points are exactly $\{\mathbf{c}_{\mathbf{l},\mathbf{i}} : |\mathbf{l}| = \tau + d - 1, \mathbf{i} \in \rho(\mathbf{l})\}$; see Figure 1 for an illustration in two dimensions. Hence, (13) represents the classical SG as a union of non-overlapping sets of design points.

Lemma 3.6 in Bungartz and Griebel (2004) stipulates that the sample size of $\mathcal{X}_\tau^{\text{SG}}$ is given by

$$|\mathcal{X}_\tau^{\text{SG}}| = \sum_{\ell=0}^{\tau-1} 2^\ell \binom{\ell + d - 1}{d - 1} = 2^\tau \cdot \left(\frac{\tau^{d-1}}{(d-1)!} + \mathcal{O}(\tau^{d-2}) \right) \asymp 2^\tau \tau^{d-1}, \quad (14)$$

where $a_n \asymp b_n$ denotes the relation that $\limsup_{n \rightarrow \infty} a_n/b_n < \infty$ and $\limsup_{n \rightarrow \infty} b_n/a_n < \infty$ for two sequences $\{a_n\}$ and $\{b_n\}$. In contrast, the sample size of a full grid of the same refinement level is $|\mathcal{X}_{j,\tau}|^d = (2^\tau - 1)^d \asymp 2^{\tau d}$, a dramatically larger number; see Table 1 for a stark contrast between full grids and classical SGs in terms of the sample size especially in high dimensions. In addition, Table 2 shows that the sample size of classical SGs of different levels and dimensions.

Table 1 Full Grids versus Classical Sparse Grids.

Dimension d	Full Grid	Sparse Grid of Level 4
1	15	15
2	225	49
5	759,375	351
10	5.77×10^{11}	2,001
20	3.33×10^{23}	13,201
50	6.38×10^{58}	182,001

The refinement level of each full grid is $\tau = 4$, so its sample size is $(2^\tau - 1)^d = 15^d$. The size of a classical SG is calculated by (14).

Table 2 Classical Sparse Grids of Different Dimensions and Levels.

Level τ	$d = 2$	$d = 5$	$d = 10$	$d = 20$	$d = 50$
2	5	11	21	41	101
3	17	71	241	881	5,201
4	49	351	2,001	13,201	182,001
5	129	1,471	13,441	154,881	4,867,201

The size of a classical SG is calculated by (14).

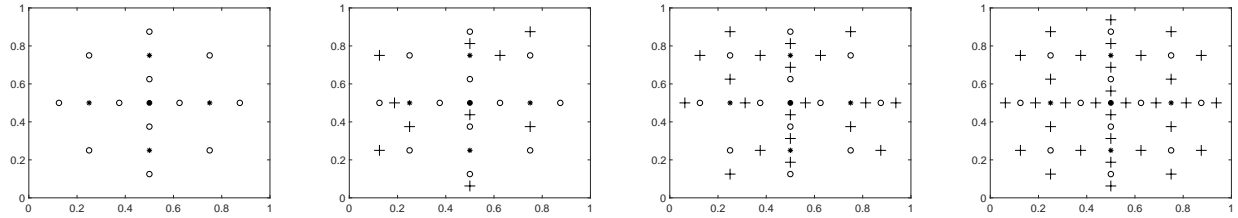
4.2. Truncated Sparse Grids

Despite the huge reduction in sample size and the significant computational savings that follow (see Section 6), SG designs lack sufficient flexibility that would allow them to be widely adopted in practice. This is because SGs are not defined directly via the sample size n but via the level τ . If n lies between $|\mathcal{X}_\tau^{\text{SG}}|$ and $|\mathcal{X}_{\tau+1}^{\text{SG}}|$ for some τ , then we are forced to choose between the two SGs. However, choosing $\mathcal{X}_\tau^{\text{SG}}$ would mean wasting the budget, while choosing $\mathcal{X}_{\tau+1}^{\text{SG}}$ would mean that one has to increase the budget which may not be possible. This issue becomes particularly serious in high dimensions, because the sample size of the classical SG increases very quickly as τ increases; see Table 2. To resolve the issue, we propose a new experimental design as follows.

DEFINITION 2 (TRUNCATED SPARSE GRID). Given a sampling budget n , there exists $\tau \geq 1$ such that $|\mathcal{X}_\tau^{\text{SG}}| \leq n < |\mathcal{X}_{\tau+1}^{\text{SG}}|$, which can be calculated via formula (14). Let $\tilde{n} = n - |\mathcal{X}_\tau^{\text{SG}}|$ and $\mathcal{D}_{\tau+1} := \mathcal{X}_{\tau+1}^{\text{SG}} \setminus \mathcal{X}_\tau^{\text{SG}}$. We construct $\mathcal{A}_{\tilde{n}}$, a set of points of size \tilde{n} , by arbitrarily selecting the design points in $\mathcal{D}_{\tau+1}$. Then, a *truncated sparse grid* (TSG) design of size n , denoted by $\mathcal{X}_n^{\text{TSG}}$, is the union of $\mathcal{X}_\tau^{\text{SG}}$ and $\mathcal{A}_{\tilde{n}}$, that is, $\mathcal{X}_n^{\text{TSG}} = \mathcal{X}_\tau^{\text{SG}} \cup \mathcal{A}_{\tilde{n}}$. Further, if $\mathcal{A}_{\tilde{n}}$ is constructed by selecting the design points in $\mathcal{D}_{\tau+1}$ uniformly at random without replacement, then the resulting design is called a *random truncated sparse grid* (RTSG) design.

Figure 2 presents examples of TSGs in two dimensions.

A natural question follows the simple construction of TSGs. Being “incomplete” SGs, can TSGs retain the computational tractability of classical SGs, yielding fast computation of kriging for tensor product kernels (3) as shown in Plumlee (2014)? This is a nontrivial question and the answer is

Figure 2 Examples of TSGs in Two Dimensions.

Note. (i) $\tau = 3$, $\tilde{n} = 0$; (ii) $\tau = 3$, $\tilde{n} = 10$; (iii) $\tau = 3$, $\tilde{n} = 20$; (iv) $\tau = 4$, $\tilde{n} = 0$. The first and last are classical SGs.

negative in general. However, we show later in Theorem 5 that the inverse kernel matrices induced by TM kernels and TSG designs possess a nice sparse structure, which facilitates fast computation of stochastic kriging. The proof depends critically on a deep connection between classical SGs and an orthogonal basis expansion of TM kernels that may not exist for general tensor product kernels.

5. Sample Efficiency

We analyze in this section the convergence rate of stochastic kriging with TM kernels in terms of MSE. We aim to answer a fundamental question regarding how many simulation samples are needed for stochastic kriging to produce good predictions of a high-dimensional response surface. Note that this section does not concern the computational issue of large matrix inversion that is involved in stochastic kriging. (One could use generic matrix inversion algorithms. It would not change the sample efficiency, but would result in a time complexity of $\mathcal{O}(n^3)$.) We present algorithms for fast computation of stochastic kriging with TM kernels and TSG designs in Section 6.

Our analysis on the sample efficiency comprises three parts as follows.

- (i) We first focus on the case of deterministic simulation. Assuming that the response surface is indeed a realization of a TMGP, we establish an upper bound on the convergence rate, if the design points form a TSG.
- (ii) We then consider model misspecification—the response surface is realized from a GP induced by a tensor product kernel having a higher degree of smoothness than the TM kernel. We prove that the convergence rate of the “misspecified” predictor is affected only mildly by the curse of dimensionality.
- (iii) Third, we generalize the above results to the stochastic setting.

5.1. Deterministic Simulation

In this section, we study the convergence rate of (deterministic) kriging with TM kernels and TSGs. Let $\hat{Y}_n(\mathbf{x})$ denote the kriging predictor with kernel k and design points $\{\mathbf{x}_1, \dots, \mathbf{x}_n\}$,

$$\hat{Y}_n(\mathbf{x}) = \mathbf{k}^\top(\mathbf{x})\mathbf{K}^{-1}\mathbf{y}, \quad (15)$$

where $\mathbf{y} = (Y(\mathbf{x}_1), \dots, Y(\mathbf{x}_n))^\top$. Our first main result establishes an upper bound on the MSE (2) uniformly in \mathbf{x} in the absence of simulation noise, assuming that the response surface is a realization of a TMGP and the experimental design forms a TSG.

THEOREM 1. *Let $\{Y(\mathbf{x}) : \mathbf{x} \in (0, 1)^d\}$ be a zero mean TMGP with kernel k that satisfies Assumption 1. Suppose that the true response surface is a realization of Y , the simulation has no noise, and the design points $\{\mathbf{x}_1, \dots, \mathbf{x}_n\}$ form a TSG. Let $\hat{Y}_n(\mathbf{x})$ be the kriging predictor with kernel k and the TSG design. Then, as $n \rightarrow \infty$,*

$$\sup_{\mathbf{x} \in (0, 1)^d} \mathbb{E}[(\hat{Y}_n(\mathbf{x}) - Y(\mathbf{x}))^2] = \mathcal{O}(n^{-1}(\log n)^{2(d-1)}). \quad (16)$$

Note that in the upper bound (16), the dimension d does not appear in the exponent of n , but only in the exponent of $\log n$. This suggests that for a fixed d , the MSE of the kriging predictor with TM kernels and TSGs can be upper bounded by a rate arbitrarily close to n^{-1} as $n \rightarrow \infty$, almost overcoming the curse of dimensionality on the sample complexity. Admittedly, the setting of Theorem 1 is somewhat restrictive: the simulation model is deterministic and the response surface is realized from a TMGP which suggests nowhere-differentiability. But these restrictions will be relaxed shortly, and the curse of dimensionality on the convergence rate is still not substantial.

Let us now contrast Theorem 1 with existing results. Tuo and Wang (2020) investigates thoroughly the convergence rate of deterministic kriging for the Matérn kernels. The authors prove that if the response surface y is realized from a GP with the Matérn(α) kernel, then for *any* experimental design, the kriging predictor with the Matérn(ν) kernel, where ν is allowed to be different from α , has the following lower bound on its MSE,

$$\sup_{\mathbf{x} \in (0, 1)^d} \mathbb{E}[(\hat{Y}_n(\mathbf{x}) - Y(\mathbf{x}))^2] \geq cn^{-2\alpha/d}, \quad (17)$$

for some constant $c > 0$ and all sufficiently large n . Unlike Theorem 1, in the above lower bound the dimension d appears in the exponent of n and it decreases the lower rate rapidly, manifesting the severity of the curse of dimensionality.

A fundamental reason behind the stark difference between the decay rates in (16) and (17) is that TM kernels are not isotropic but defined via a tensor structure, which can rule out some irregular functions that would be included in the function space that are formed by the GP sample paths induced by the Matérn kernel; see Evans (2010, Page 260) for one such irregular function that possesses certain smoothness properties but is unbounded on each open subset of the design space.

Meanwhile, the function space formed by TMGP sample paths is still broad in the sense that if the experimental design is not well chosen, the decay rate of the MSE of the kriging predictor with a TM kernel will suffer severely from the curse of dimensionality, as shown below.

PROPOSITION 2. Let $\{\mathbf{Y}(\mathbf{x}) : \mathbf{x} \in (0, 1)^d\}$ be a zero mean TMGP with kernel k that satisfies Assumption 1. Suppose that the true response surface is a realization of \mathbf{Y} , the simulation has no noise, and the design points $\{\mathbf{x}_1, \dots, \mathbf{x}_n\}$ form a lattice $\times_{j=1}^d \mathcal{X}_{j,\tau}$ for some $\tau \geq 1$, where $\mathcal{X}_{j,\tau} = \{i \cdot 2^{-\tau} : 1 \leq i \leq 2^\tau - 1\}$. Let $\hat{\mathbf{Y}}_n(\mathbf{x})$ be the kriging predictor with kernel k and the lattice design. Then, there exists a constant $c > 0$ such that for all sufficiently large n ,

$$\sup_{\mathbf{x} \in (0,1)^d} \mathbb{E}[(\hat{\mathbf{Y}}_n(\mathbf{x}) - \mathbf{Y}(\mathbf{x}))^2] \geq cn^{-1/d}.$$

5.2. Model Misspecification

As discussed in Section 3.3, samples paths of a TMGP are nowhere differentiable. However, most of the response surfaces of practical interest do possess certain level of smoothness. To postulate that the true surface is a TMGP sample path is restrictive. We study the model misspecification issue in this section. We show that if the true surface is realized from a GP with a tensor product kernel having a higher degree of differentiability than TM kernels, thereby inducing smoother sample paths than TMGPs, then kriging with TM kernels and TSGs still breaks the curse of dimensionality, which is obviously reassuring for practitioners.

To facilitate presentation, we will use the notion of reproducing kernel Hilbert space (RKHS); see Rasmussen and Williams (2006, Chapter 6) for an introduction. For a kernel k , we use \mathcal{H}_k to denote its associated RKHS and $\|\cdot\|_{\mathcal{H}_k}$ to denote the norm of the space.

ASSUMPTION 2. Let $k(\mathbf{x}, \mathbf{x}') = \prod_{j=1}^d k_j(x_j, x'_j)$ be a TM kernel that satisfies Assumption 1, and $k^*(\mathbf{x}, \mathbf{x}') = \prod_{j=1}^d k_j^*(x_j, x'_j)$ be a tensor product kernel for $\mathbf{x}, \mathbf{x}' \in (0, 1)^d$. For each $j = 1, \dots, d$, k_j^* satisfies $\sup_{x \in (0,1)} \|\mathcal{L}_j k_j^*(x, \cdot)\|_{\mathcal{H}_{k_j}} < \infty$, where the differential operator \mathcal{L}_j is defined in (6).

REMARK 3. It can be shown that Assumption 2 holds if for each j , $k_j^*(x, x')$ has a second-order weak derivative with respect to x and $\partial_x^2 k_j^*(x, x')$ has a first-order weak derivative with respect to x' for all $x, x' \in (0, 1)$. For example, k_j^* can be the Matérn(ν) kernel with $\nu \geq 3/2$ or the Gaussian kernel. For another example, k^* can be the GIBF(ℓ) kernel where $\ell = (\ell_1, \dots, \ell_d)$ with $\ell_j \geq 2$ for each j ; see Example 3.

THEOREM 2. Let k be a TM kernel that satisfies Assumption 1 and k^* be a tensor product kernel that satisfies Assumption 2. Let $\{\mathbf{Y}^*(\mathbf{x}) : \mathbf{x} \in (0, 1)^d\}$ be a zero mean GP with kernel k^* . Suppose that the true response surface is a realization of \mathbf{Y}^* , the simulation has no noise, and the design points $\{\mathbf{x}_1, \dots, \mathbf{x}_n\}$ form a TSG. Let $\hat{\mathbf{Y}}_n^{\text{mis}}(\mathbf{x}) = \mathbf{k}^\top(\mathbf{x})\mathbf{K}^{-1}\mathbf{y}^*$ be the misspecified kriging predictor with kernel k and the TSG design, where $\mathbf{y}^* = (\mathbf{Y}^*(\mathbf{x}_1), \dots, \mathbf{Y}^*(\mathbf{x}_n))^\top$. Then, as $n \rightarrow \infty$,

$$\sup_{\mathbf{x} \in (0,1)^d} \mathbb{E}[(\hat{\mathbf{Y}}_n^{\text{mis}}(\mathbf{x}) - \mathbf{Y}^*(\mathbf{x}))^2] = \mathcal{O}(n^{-2}(\log n)^{3(d-1)}). \quad (18)$$

Note that the upper bound (18) decays to zero at a rate that is substantially faster than the upper bound (16) in Theorem 1. This is somewhat surprising: it appears as if the convergence rate of kriging with TM kernels and TSG designs were benefiting positively from the model misspecification. The seemingly counterintuitive result stems from the fact that optimal convergence rates for estimating unknown functions, in general, depend on the properties of the true function rather than on those of the postulated model. For instance, the lower bound (17) does not depend on the smoothness parameter of the Matérn kernel used for kriging, but instead depends on the smoothness parameter of the GP that generates the true surface.

Clearly, the tensor product kernel k^* in Theorem 2 has a higher degree of differentiability than the TM kernel k , since each component of the latter, having the form $p_j(x \wedge \cdot)q_j(x \vee \cdot)$, is non-differentiable. Hence, the true surface is significantly smoother than TMGP sample paths. Conceivably, if one uses k^* for kriging so that the model is correctly specified, then one might be able to prove an even faster rate than (18), possibly under a different experimental design than TSGs. However, this is beyond the scope of the present paper, and we leave it to future research.

5.3. Stochastic Simulation and Budget Allocation

The rate results for deterministic simulation can be generalized to the stochastic setting as follows.

THEOREM 3. *Let $\{Y(\mathbf{x}) : \mathbf{x} \in (0, 1)^d\}$ be a zero mean TMGP with kernel k that satisfies Assumption 1. Suppose that the true response surface is a realization of Y , the simulation noise has variance $\sigma^2(\mathbf{x})$, the design points $\{\mathbf{x}_1, \dots, \mathbf{x}_n\}$ form a TSG, and the number of replications taken at each \mathbf{x}_i is m_i . Let $\hat{Y}_n(\mathbf{x})$ be the stochastic kriging predictor (1) with kernel k and the TSG design. If $(\log n)^d \max_{1 \leq i \leq n} m_i^{-1/2} \sigma(\mathbf{x}_i) \rightarrow 0$ as $n \rightarrow \infty$, then*

$$\sup_{\mathbf{x} \in (0, 1)^d} \mathbb{E}[(\hat{Y}_n(\mathbf{x}) - Y(\mathbf{x}))^2] = \mathcal{O} \left(n^{-1} (\log n)^{2(d-1)} + (\log n)^d \max_{1 \leq i \leq n} m_i^{-1/2} \sigma(\mathbf{x}_i) \right). \quad (19)$$

THEOREM 4. *Let k be a TM kernel that satisfies Assumption 1 and k^* be a tensor product kernel that satisfies Assumption 2. Let $\{Y^*(\mathbf{x}) : \mathbf{x} \in (0, 1)^d\}$ be a zero mean GP with kernel k^* . Suppose that the true response surface is a realization of Y^* , the simulation noise has variance $\sigma^2(\mathbf{x})$, the design points $\{\mathbf{x}_1, \dots, \mathbf{x}_n\}$ form a TSG, and the number of replications taken at each \mathbf{x}_i is m_i . Let $\hat{Y}_n^{\text{mis}}(\mathbf{x}) = \mathbf{k}^\top(\mathbf{x})(\mathbf{K} + \Sigma)^{-1} \bar{\mathbf{Y}}^*$ be the misspecified stochastic kriging predictor with kernel k and the TSG design, where $\bar{\mathbf{Y}}^*$ denotes the vector composed of entries $Y^*(\mathbf{x}_i) + m_i^{-1} \sum_{r=1}^{m_i} \epsilon_r(\mathbf{x}_i)$, for $i = 1, \dots, n$. If $(\log n)^d \max_{1 \leq i \leq n} m_i^{-1/2} \sigma(\mathbf{x}_i) \rightarrow 0$ as $n \rightarrow \infty$, then*

$$\sup_{\mathbf{x} \in (0, 1)^d} \mathbb{E}[(\hat{Y}_n^{\text{mis}}(\mathbf{x}) - Y^*(\mathbf{x}))^2] = \mathcal{O} \left(n^{-2} (\log n)^{3(d-1)} + (\log n)^d \max_{1 \leq i \leq n} m_i^{-1/2} \sigma(\mathbf{x}_i) \right). \quad (20)$$

Comparing the above results with their deterministic counterparts (Theorems 1 and 2), we can easily see that the MSE upper bounds (19) and (20) can both be decomposed into two parts—the function approximation error and the simulation error, thereby reflecting the bias-variance tradeoff. Intuitively, in order for the MSE to diminish, the number of replications at each design point needs to grow to infinity to reduce the simulation error to zero. The upper bounds (19) and (20) further suggest that each m_i needs to grow fast enough as $n \rightarrow \infty$.

In a stochastic simulation experiment, one is usually constrained by a sampling budget B . For simplicity, we assume that the sample cost is the same for all \mathbf{x} and write $B = \sum_{i=1}^n m_i$. To gain insights into the implication of budget allocation, we further assume homoscedasticity, i.e., $\sigma(\mathbf{x}) \approx \sigma$ for all \mathbf{x} , and equal number of replications at the design points, i.e., $m_i \approx m$ for all $i = 1, \dots, m$. Then, $B = mn$ and the upper bound (19) becomes $n^{-1}(\log n)^{2(d-1)} + \sigma m^{-1/2}(\log n)^d$, which is minimized when the two summands are approximately equal, resulting in $m \approx (n/(\log n)^{d-2})^2$. Further, for a fixed d , the relation is approximately reduced to $m \approx n^2$ for large n . Therefore, the budget allocation minimizing the upper convergence rate is roughly $m \approx B^{2/3}$ and $n \approx B^{1/3}$, leading to an MSE upper bound approximately of order $B^{-1/3}$.

The above heuristic analysis can be applied to the model misspecification case as well. In this case, the asymptotically optimal budget allocation is such that $m \approx B^{4/5}$ and $n \approx B^{1/5}$, and the corresponding MSE upper bound is approximately of order $B^{-2/5}$.

6. Fast Computation

Plumlee (2014) develops fast algorithms for kriging of tensor product kernels and classical SG designs. However, they are only valid if (i) the simulation model is deterministic, so that the matrix to invert is \mathbf{K} rather than $(\mathbf{K} + \mathbf{\Sigma})$, and (ii) the design points must form a (complete) SG. In this section, we relax the above two restrictions to cover the case of stochastic simulation and allow design points to form an TSG.

6.1. Kernel Matrix Inversion

In this section, we develop a fast algorithm for exact computation of \mathbf{K}^{-1} for TSGs. The development takes four steps, each analyzing a case that is more general than the last. The four cases are: (i) one-dimensional grids, (ii) lattices, (iii) classical SGs, and (iv) TSGs, resulting in Algorithms 1–4, respectively. The algorithm developed in an earlier step becomes a subroutine for the more general cases in later steps.

The computation of $\mathbf{K}^{-1}\mathbf{k}(\mathbf{x})$ for classical SGs is an important building block for the inversion of the kernel matrix for TSGs. It turns out that by taking advantage of special structures related to TM kernels, we may directly compute this vector without going through the two-step approach that

computes \mathbf{K}^{-1} first and does matrix-vector multiplication later. We therefore present Algorithms 1–3 to include both the methods for computing \mathbf{K}^{-1} and that for $\mathbf{K}^{-1}\mathbf{k}(\mathbf{x})$.

For the ease of presentation in the sequel, given two sets of design points \mathcal{X}' and \mathcal{X}'' , we use $k(\mathcal{X}', \mathcal{X}'')$ to denote the matrix consisting of entries $k(\mathbf{x}', \mathbf{x}'')$ for all $\mathbf{x}' \in \mathcal{X}'$ and $\mathbf{x}'' \in \mathcal{X}''$. With this notation, for example, we have $\mathbf{K} = k(\mathcal{X}, \mathcal{X})$ and $\mathbf{k}(\mathbf{x}) = k(\mathcal{X}, \{\mathbf{x}\})$.

6.1.1. Computation in One Dimension With $d = 1$, kernel matrices for TM kernels are particularly tractable, with the inverse being specified explicitly in Proposition 1, which immediately suggests Algorithm 1 for computing \mathbf{K}^{-1} and $\mathbf{K}^{-1}\mathbf{k}(x)$.

Algorithm 1: Computing \mathbf{K}^{-1} and $\mathbf{K}^{-1}\mathbf{k}(x)$ for One-Dimensional Grids

Input : TM kernel k in one dimension, design points $x_1 < \dots < x_n$, and prediction point x

Output : \mathbf{K}^{-1} and $\mathbf{K}^{-1}\mathbf{k}(x)$

- 1 Initialize $\mathbf{A} \leftarrow \mathbf{0} \in \mathbb{R}^{n \times n}$ and $\mathbf{b} \leftarrow \mathbf{0} \in \mathbb{R}^{n \times 1}$
 - 2 Update the tridiagonal entries of \mathbf{A} using (7)
 - 3 Search for $i^* \in \{0, 1, \dots, n\}$ such that $x \in [x_{i^*}, x_{i^*+1})$, where $x_0 = -\infty$ and $x_{n+1} = \infty$
 - 4 Update \mathbf{b}_{i^*} and \mathbf{b}_{i^*+1} using (8)
 - 5 Return $\mathbf{K}^{-1} \leftarrow \mathbf{A}$ and $\mathbf{K}^{-1}\mathbf{k}(x) \leftarrow \mathbf{b}$
-

6.1.2. Computation on Lattices In light of the tensor structure of TM kernels, it is straightforward to generalize the computation of \mathbf{K}^{-1} and $\mathbf{K}^{-1}\mathbf{k}(\mathbf{x})$ from one-dimensional grids to multidimensional lattices (O'Hagan 1991). In Algorithm 2, \mathbf{K}_j denotes the matrix composed of entries $k_j(x, x')$ for all $x, x' \in \mathcal{X}_j$, $\mathbf{k}_j(x)$ denotes the vector composed of entries $k_j(x, x')$ for all $x' \in \mathcal{X}_j$, and $\text{vec}(\cdot)$ denotes the vectorization of a matrix.

Algorithm 2: Computing \mathbf{K}^{-1} and $\mathbf{K}^{-1}\mathbf{k}(\mathbf{x})$ for Lattices

Input : TM kernel k in d dimensions, lattice design $\mathcal{X} = \bigotimes_{j=1}^d \mathcal{X}_j$ with $|\mathcal{X}_j| = n_j$, and prediction point $\mathbf{x} = (x_1, \dots, x_d)$

Output : \mathbf{K}^{-1} and $\mathbf{K}^{-1}\mathbf{k}(\mathbf{x})$

- 1 **for** $j \leftarrow 1$ **to** d **do**
 - 2 | Compute $\mathbf{K}_j^{-1} \in \mathbb{R}^{n_j \times n_j}$ and $\mathbf{K}_j^{-1}\mathbf{k}_j(x_j) \in \mathbb{R}^{n_j \times 1}$ via Algorithm 1 with inputs $(k_j, \mathcal{X}_j, x_j)$
 - 3 **end**
 - 4 Return $\mathbf{K}^{-1} = \bigotimes_{j=1}^d \mathbf{K}_j^{-1}$ and $\mathbf{K}^{-1}\mathbf{k}(\mathbf{x}) = \text{vec} \left(\bigotimes_{j=1}^d \mathbf{K}_j^{-1}\mathbf{k}_j(x_j) \right)$
-

6.1.3. Computation on Classical Sparse Grids Algorithms for computing quantities involved in kriging with SG designs have been developed in Plumlee (2014) for general tensor product kernels. We now tailor them to our context, resulting in Algorithm 3 which we briefly explain below; see Appendix B of Plumlee (2014) for the proof of its validity.

Let $\mathcal{X}_{j,l} = \{\mathbf{c}_{l,i} : 1 \leq i \leq 2^l - 1\}$ with $\mathbf{c}_{l,i} = i \cdot 2^{-l}$ be a component design defined in (9). For any multi-index $\mathbf{l} \in \mathbb{N}^d$, $\mathcal{X}_1^{\text{FG}} := \bigtimes_{j=1}^d \mathcal{X}_{j,l_j}$ defines a full grid (i.e., lattice). By its definition in (10), the classical SG of level τ is expressed as $\mathcal{X}_\tau^{\text{SG}} = \bigcup_{|\mathbf{l}| \leq \tau+d-1} \mathcal{X}_1^{\text{FG}}$, which drives the updating schemes in Algorithm 3. Let $\mathbf{K}_1 := k(\mathcal{X}_1^{\text{FG}}, \mathcal{X}_1^{\text{FG}})$ and $\mathbf{k}_1(\mathbf{x}) := k(\mathcal{X}_1^{\text{FG}}, \{\mathbf{x}\})$. In general, for any matrix $\mathbf{A} \in \mathbb{R}^{n \times n}$ with $n = |\mathcal{X}_\tau^{\text{SG}}|$ whose entries are indexed by $(\mathbf{x}, \mathbf{x}')$ for $\mathbf{x}, \mathbf{x}' \in \mathcal{X}_\tau^{\text{SG}}$, we may write \mathbf{A}_1 to denote the part of \mathbf{A} having entries indexed by $(\mathbf{x}, \mathbf{x}')$ for all $\mathbf{x}, \mathbf{x}' \in \mathcal{X}_1^{\text{FG}}$. Likewise, we may define \mathbf{b}_1 for any vector $\mathbf{b} \in \mathbb{R}^n$. In each iteration \mathbf{l} of Algorithm 3, the part of \mathbf{K}^{-1} that corresponds to $\mathcal{X}_1^{\text{FG}}$ is updated; so is $\mathbf{K}^{-1}\mathbf{k}(\mathbf{x})$. Note that both \mathbf{K}_1 and $\mathbf{k}_1(\mathbf{x})$ are defined on a lattice. Thus, they can be computed via Algorithm 2.

Algorithm 3: Computing \mathbf{K}^{-1} and $\mathbf{K}^{-1}\mathbf{k}(\mathbf{x})$ for Classical Sparse Grids

Input : TM kernel k in d dimensions, classical SG design $\mathcal{X}_\tau^{\text{SG}}$ with size n , and prediction point \mathbf{x}

Output : \mathbf{K}^{-1} and $\mathbf{K}^{-1}\mathbf{k}(\mathbf{x})$

1 Initialize $\mathbf{A} \leftarrow \mathbf{0} \in \mathbb{R}^{n \times n}$ and $\mathbf{b} \leftarrow \mathbf{0} \in \mathbb{R}^{n \times 1}$

2 **for** all $\mathbf{l} \in \mathbb{N}^d$ with $\tau \leq |\mathbf{l}| \leq \tau + d - 1$ **do**

3 Compute \mathbf{K}_1^{-1} and $\mathbf{K}_1^{-1}\mathbf{k}_1(\mathbf{x})$ via Algorithm 2 with inputs $(k, \bigtimes_{j=1}^d \mathcal{X}_{j,l_j}, \mathbf{x})$

4 Update \mathbf{A}_1 and \mathbf{b}_1 via

$$\mathbf{A}_1 \leftarrow \mathbf{A}_1 + (-1)^{\tau+d-1-|\mathbf{l}|} \binom{d-1}{\tau+d-1-|\mathbf{l}|} \mathbf{K}_1^{-1} \quad (21)$$

$$\mathbf{b}_1 \leftarrow \mathbf{b}_1 + (-1)^{\tau+d-1-|\mathbf{l}|} \binom{d-1}{\tau+d-1-|\mathbf{l}|} \mathbf{K}_1^{-1}\mathbf{k}_1(\mathbf{x}) \quad (22)$$

5 **end**

6 Return $\mathbf{K}^{-1} \leftarrow \mathbf{A}$ and $\mathbf{K}^{-1}\mathbf{k}(\mathbf{x}) \leftarrow \mathbf{b}$

6.1.4. Computation on Truncated Sparse Grids Being part of a larger classical SG by definition, an TSG can be viewed as an “incomplete” SG. The lack of completeness breaks the tensor structure of SGs, meaning that an TSG cannot be expressed as a union of tensor products of one-dimensional designs, in the same way as SGs can in (10). This is the key reason why Algorithm 3 as well as those proposed in Plumlee (2014) cease to work for TSGs.

To address the issue, we take advantage of the fact that an TSG is the union of a classical SG and a set of design points belonging to the classical SG of the next level, that is, $\mathcal{X}_n^{\text{TSG}} = \mathcal{X}_\tau^{\text{SG}} \cup \mathcal{A}_{\bar{n}}$ with $\mathcal{A}_{\bar{n}} \subseteq \mathcal{D}_{\tau+1} = \mathcal{X}_{\tau+1}^{\text{SG}} \setminus \mathcal{X}_\tau^{\text{SG}}$. In other words, the “incompleteness” only occurs to the highest level of the

SG involved. It can be shown that TMGPs possess a nice conditional independence structure which specifies that the samples taken at design points belonging to $\mathcal{D}_{\tau+1}$ are conditionally independent given the observations made at all the design points of $\mathcal{X}_\tau^{\text{SG}}$. This conditional independence structure then induces the sparseness of \mathbf{K}^{-1} . Particularly, part (i) of Theorem 5 asserts that \mathbf{K}^{-1} can be expressed as a 2×2 block matrix, in which the bottom-right block is a diagonal submatrix and the other blocks are all sparse as well. We characterize the sparse structure explicitly in part (ii) of Theorem 5, providing sufficient conditions for entries of \mathbf{K}^{-1} to be zero. Knowing which entries are guaranteed to be zero, we only need to compute those that are likely to be nonzero, which yields substantial computational savings. Since the computational efficiency for computing \mathbf{K}^{-1} is essentially determined by its sparsity, we give an estimate of the proportion of nonzero entries in \mathbf{K}^{-1} in part (iii) of Theorem 5.

THEOREM 5. *Let $k(\mathbf{x}, \mathbf{x}') = \prod_{j=1}^d p_j(x_j \wedge x'_j) q_j(x_j \vee x'_j)$ be a TM kernel that satisfies Assumption 1 and $n \geq 3$. Suppose that the design points $\{\mathbf{x}_1, \dots, \mathbf{x}_n\}$ form a TSG $\mathcal{X}_n^{\text{TSG}} = \mathcal{X}_\tau^{\text{SG}} \cup \mathcal{A}_{\tilde{n}}$.*

(i) *The inverse of the kernel matrix on $\mathcal{X}_n^{\text{TSG}}$ can be expressed as the following block matrix,*

$$\mathbf{K}^{-1} = \begin{pmatrix} \mathbf{E} & -\mathbf{BD} \\ -\mathbf{DB}^\top & \mathbf{D} \end{pmatrix}, \quad (23)$$

where $\mathbf{E} = \mathbf{A}^{-1} + \mathbf{BDB}^\top$, $\mathbf{A} = k(\mathcal{X}_\tau^{\text{SG}}, \mathcal{X}_\tau^{\text{SG}})$, $\mathbf{B} = \mathbf{A}^{-1}k(\mathcal{X}_\tau^{\text{SG}}, \mathcal{A}_{\tilde{n}})$, and \mathbf{D} is a $\tilde{n} \times \tilde{n}$ diagonal matrix whose diagonal entries are given by

$$\mathbf{D}_{(\mathbf{l}, \mathbf{i}), (\mathbf{l}, \mathbf{i})} = \prod_{j=1}^d \left(\frac{p_{j, l_j, i_j+1} q_{j, l_j, i_j-1} - p_{j, l_j, i_j-1} q_{j, l_j, i_j+1}}{(p_{j, l_j, i_j} q_{j, l_j, i_j-1} - p_{j, l_j, i_j-1} q_{j, l_j, i_j}) (p_{j, l_j, i_j+1} q_{j, l_j, i_j} - p_{j, l_j, i_j} q_{j, l_j, i_j+1})} \right), \quad (24)$$

for all (\mathbf{l}, \mathbf{i}) such that $\mathbf{c}_{\mathbf{l}, \mathbf{i}} \in \mathcal{A}_{\tilde{n}}$, where $p_{j, l, i} = p_j(c_{l, i})$ and $q_{j, l, i} = q_j(c_{l, i})$ for all j, l , and i .

(ii) For each (\mathbf{l}, \mathbf{i}) , define a hyperrectangle $\mathcal{R}_{(\mathbf{l}, \mathbf{i})} := \times_{j=1}^d (c_{l_j, i_j-1}, c_{l_j, i_j+1})$. Suppose that one of the following conditions is satisfied:

- (a.) $\mathbf{c}_{\mathbf{l}', \mathbf{i}'}, \mathbf{c}_{\mathbf{l}'', \mathbf{i}''} \in \mathcal{X}_{\tau+1}^{\text{SG}}$, and $\mathbf{c}_{\mathbf{l}', \mathbf{i}'} \neq \mathbf{c}_{\mathbf{l}'', \mathbf{i}''}$;
- (b.) $\mathbf{c}_{\mathbf{l}', \mathbf{i}'} \in \mathcal{X}_\tau^{\text{SG}}$, $\mathbf{c}_{\mathbf{l}'', \mathbf{i}''} \in \mathcal{A}_{\tilde{n}}$, and $\mathbf{c}_{\mathbf{l}'', \mathbf{i}''} \notin \mathcal{R}_{\mathbf{l}', \mathbf{i}'}$;
- (c.) $\mathbf{c}_{\mathbf{l}', \mathbf{i}'}, \mathbf{c}_{\mathbf{l}'', \mathbf{i}''} \in \mathcal{X}_\tau^{\text{SG}}$,

$$\left| i'_j \cdot 2^{l'_j \vee l''_j - l'_j} - i''_j \cdot 2^{l'_j \vee l''_j - l''_j} \right| \geq 2, \quad \text{for some } j = 1, \dots, d, \quad (25)$$

and

$$\mathbf{c}_{\mathbf{l}, \mathbf{i}} \notin \mathcal{R}_{\mathbf{l}', \mathbf{i}'} \cap \mathcal{R}_{\mathbf{l}'', \mathbf{i}''}, \quad \text{for all } \mathbf{c}_{\mathbf{l}, \mathbf{i}} \in \mathcal{A}_{\tilde{n}}. \quad (26)$$

Then, $(\mathbf{K}^{-1})_{(\mathbf{l}', \mathbf{i}'), (\mathbf{l}'', \mathbf{i}'')} = (\mathbf{K}^{-1})_{(\mathbf{l}'', \mathbf{i}''), (\mathbf{l}', \mathbf{i}')} = 0$.

(iii) The number of nonzero entries in \mathbf{E} is $\mathcal{O}(|\mathcal{X}_\tau^{\text{SG}}| + \tilde{n}\tau^{2d})$, and that in \mathbf{BD} is $\mathcal{O}(\tilde{n} \log(|\mathcal{X}_\tau^{\text{SG}}|)^{d-1})$. Overall, the density of \mathbf{K}^{-1} , i.e., the proportion of nonzero entries therein, is $\mathcal{O}(n^{-1}(\log n)^{2d})$.

The three conditions in part (ii) of Theorem 5 correspond to different blocks of \mathbf{K}^{-1} in (23), namely, the bottom-right, off-diagonal, and top-left blocks, respectively. Each block can be computed efficiently. First, the diagonal entries of \mathbf{D} can be computed via (24). Second, \mathbf{A} is simply the kernel matrix on the classical SG $\mathcal{X}_\tau^{\text{SG}}$, and each column of \mathbf{B} is of the form $\mathbf{A}^{-1}k(\mathcal{X}_\tau^{\text{SG}}, \{\mathbf{x}\})$ for $\mathbf{x} \in \mathcal{A}_{\tilde{n}}$, so both \mathbf{A}^{-1} and \mathbf{B} can be computed via Algorithm 3. It is also easy to compute \mathbf{BDB}^\top since \mathbf{D} is diagonal and \mathbf{B} is a sparse matrix by part (iii) of Theorem 5. This gives rise to Algorithm 4.

Algorithm 4: Computing \mathbf{K}^{-1} for Truncated Sparse Grids

Input : TM kernel k in d dimensions, TSG design $\mathcal{X}_n^{\text{TSG}} = \mathcal{X}_\tau^{\text{SG}} \cup \mathcal{A}_{\tilde{n}}$, observations $\bar{\mathbf{y}}$, and prediction point \mathbf{x}

Output : \mathbf{K}^{-1}

- 1 With $\mathbf{A} := k(\mathcal{X}_\tau^{\text{SG}}, \mathcal{X}_\tau^{\text{SG}})$, compute \mathbf{A}^{-1} via Algorithm 3 with inputs $(k, \mathcal{X}_\tau^{\text{SG}})$
 - 2 Initialize $\mathbf{B} \leftarrow \mathbf{0} \in \mathbb{R}^{|\mathcal{X}_\tau^{\text{SG}}| \times \tilde{n}}$ and $\mathbf{D} \leftarrow \mathbf{0} \in \mathbb{R}^{\tilde{n} \times \tilde{n}}$
 - 3 **for** all $\mathbf{x} \in \mathcal{A}_{\tilde{n}}$ **do**
 - 4 Compute $\mathbf{b} \leftarrow \mathbf{A}^{-1}k(\mathcal{X}_\tau^{\text{SG}}, \{\mathbf{x}\})$ via Algorithm 3 with inputs $(k, \mathcal{X}_\tau^{\text{SG}}, \mathbf{x})$
 - 5 Update the \mathbf{x} -th column of \mathbf{B} to \mathbf{b}
 - 6 Update the \mathbf{x} -th diagonal entry of \mathbf{D} via (24)
 - 7 **end**
 - 8 Compute \mathbf{K}^{-1} via (23)
-

REMARK 4. The validity of Theorem 5 relies on two critical conditions. First, the kernel is a TM kernel, so Algorithm 4 does not work for general tensor product kernels. Second, the experimental design is a TSG, so the algorithm does not work for “incomplete” SGs in general.

6.2. Computing Stochastic Kriging with TM Kernels and TSGs

Since fast computation of \mathbf{K}^{-1} is made available by Algorithm 4 and $\mathbf{\Sigma}$ is a diagonal matrix, we can apply the Woodbury matrix identity

$$(\mathbf{K} + \mathbf{\Sigma})^{-1} = \mathbf{\Sigma}^{-1} - \mathbf{\Sigma}^{-1}(\mathbf{K}^{-1} + \mathbf{\Sigma}^{-1})^{-1}\mathbf{\Sigma}^{-1},$$

and take advantage of the fact that $(\mathbf{K}^{-1} + \mathbf{\Sigma}^{-1})$ is a sparse matrix so computing its inverse can benefit from sparse linear algebra. Indeed, the specific sparse structure of \mathbf{K}^{-1} in (23) permits fast Cholesky decomposition $(\mathbf{K}^{-1} + \mathbf{\Sigma}^{-1}) = \mathbf{L}\mathbf{L}^\top$, where \mathbf{L} is a lower triangular matrix. Then, the stochastic kriging predictor (1) and its MSE (2) can be expressed as

$$\hat{\mathbf{Y}}(\mathbf{x}) = \mathbf{k}^\top(\mathbf{x})\mathbf{\Sigma}^{-1}\bar{\mathbf{Y}} - \mathbf{b}_1^\top\mathbf{b}_2, \quad (27)$$

$$\text{MSE}[\hat{\mathbf{Y}}(\mathbf{x})] = k(\mathbf{x}, \mathbf{x}) - \mathbf{k}^\top(\mathbf{x})\mathbf{\Sigma}^{-1}\mathbf{k}(\mathbf{x}) + \mathbf{b}_1^\top\mathbf{b}_1, \quad (28)$$

where \mathbf{b}_1 and \mathbf{b}_2 are the solutions of the following systems of linear equations,

$$\mathbf{L}^\top \mathbf{b}_1 = \boldsymbol{\Sigma}^{-1} \mathbf{k}(\mathbf{x}) \quad \text{and} \quad \mathbf{L}^\top \mathbf{b}_2 = \boldsymbol{\Sigma}^{-1} \bar{\mathbf{Y}}. \quad (29)$$

We summarize the above discussion in Algorithm 5.

Algorithm 5: Computing Stochastic Kriging with TM Kernels and TSGs

Input : TM kernel k in d dimensions, TSG design $\mathcal{X}_n^{\text{TSG}}$, observations $\bar{\mathbf{Y}}$, covariance matrix $\boldsymbol{\Sigma}$, and prediction point \mathbf{x}

Output : $\hat{\mathbf{Y}}(\mathbf{x})$ and $\text{MSE}[\hat{\mathbf{Y}}(\mathbf{x})]$

- 1 Compute \mathbf{K}^{-1} via Algorithm 4
 - 2 Perform the Cholesky decomposition $\mathbf{L}\mathbf{L}^\top = \mathbf{K}^{-1} + \boldsymbol{\Sigma}^{-1}$
 - 3 Solve the equations (29) for \mathbf{b}_1 and \mathbf{b}_2
 - 4 Compute $\hat{\mathbf{Y}}(\mathbf{x})$ and $\text{MSE}[\hat{\mathbf{Y}}(\mathbf{x})]$ via (27) and (28), respectively
-

7. Numerical Experiments

We conduct extensive numerical experiments to assess both the prediction capability and the computational efficiency of our methodology, with a focus on high-dimensional problems. We present three sets of experiments in the order of increasing dimensions—artificial test functions in 10 dimensions in Section 7.2, the expected revenue of a production line problem in 20 dimensions in Section 7.3, the expected profit of an assortment problem in 50 dimensions in Section 7.4, and the optimal value of a linear program as a function of 16675 relevant parameters in Section 7.5.

7.1. General Setup

In each experiment, the TM kernel we use is the tensor product of the Laplace kernel, i.e.,

$$k(\mathbf{x}, \mathbf{x}') = \prod_{j=1}^d \exp(-|x_j - x'_j|) = \exp\left(-\sum_{j=1}^d |x_j - x'_j|\right). \quad (30)$$

We have also tried other TM kernels, e.g., replacing the Laplace kernel with the Brownian motion kernel, and the numerical results are similar. Moreover, we use RTSG designs for simplicity.

We assess the prediction accuracy via the root mean squared error (RMSE) of a predictor with respect to a set of prediction points $\{\mathbf{p}_j\}_{j=1}^{n_{\text{pred}}}$,

$$\widehat{\text{RMSE}} = \left(\frac{1}{n_{\text{pred}}} \sum_{i=1}^{n_{\text{pred}}} [\hat{\mathbf{M}}(\mathbf{p}_i) - y(\mathbf{p}_i)]^2 \right)^{1/2},$$

where $\hat{\mathbf{M}}(\mathbf{p}_i)$ is the value of a simulation metamodel predictor $\hat{\mathbf{M}}$ at \mathbf{p}_i . We sample the prediction points randomly from the design space with $n_{\text{pred}} = 1000$. We repeat the process $R = 100$ times,

each called a macro-replication, and obtain $\widehat{\text{RMSE}}_r$, $r = 1, \dots, R$. Then, we calculate the standard deviation (SD) of these estimated RMSEs to assess the error in estimating the RMSE,

$$\widehat{\text{SD}} = \left(\frac{1}{R-1} \sum_{r=1}^R \widehat{\text{RMSE}}_r \right)^{1/2}.$$

In each macro-replication r , we also record the elapsed time to complete the prediction over all the prediction points. Then, we report the average time over the $R = 100$ macro-replications. All the experiments are implemented in MATLAB (version 2018a) on a laptop computer with macOS, 3.3 GHz Intel Core i5 CPU, and 8 GB of RAM (2133Mhz).

7.2. Test Functions in 10 Dimensions

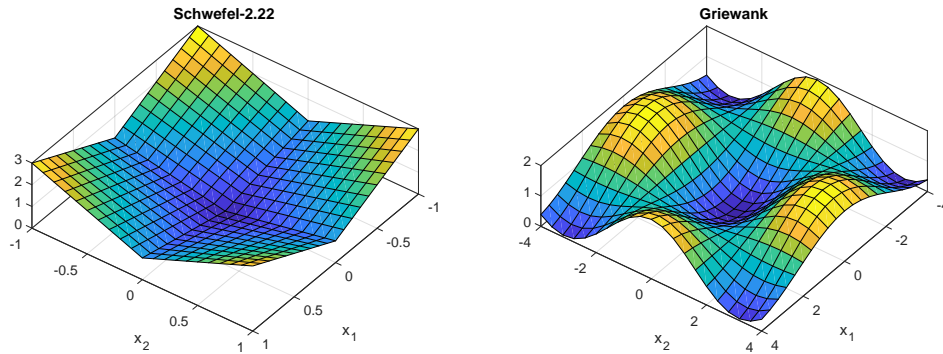
In this section, we use the following two 10-dimensional test functions with different smoothness to determine the sample and computational efficiency of our methodology:

$$y_{\text{Schwefel-2.22}}(\mathbf{x}) = \sum_{j=1}^d |x_j| + \prod_{j=1}^d |x_j|, \quad \mathbf{x} \in (-1, 1)^d,$$

$$y_{\text{Griewank}}(\mathbf{x}) = \sum_{j=1}^d \frac{x_j^2}{4000} - \prod_{j=1}^d \cos\left(\frac{x_j}{\sqrt{j}}\right) + 1, \quad \mathbf{x} \in (-4, 4)^d,$$

where $d = 10$. The two-dimensional versions of these functions are shown in Figure 3. The Schwefel-2.22 function is non-differentiable, having “wedges” on the surface, due to the presence of the absolute value functions in its definition. In contrast, the Griewank function is infinitely differentiable in the test region $(-4, 4)^{10}$.

Figure 3 The Griewank and Schwefel-2.22 Functions in Two Dimensions.



We compare our approach (the TM kernel (30) plus the RTSG design), denoted by **TM-RTSG** in the sequel, against the following methods, having different combinations of kernels and designs.

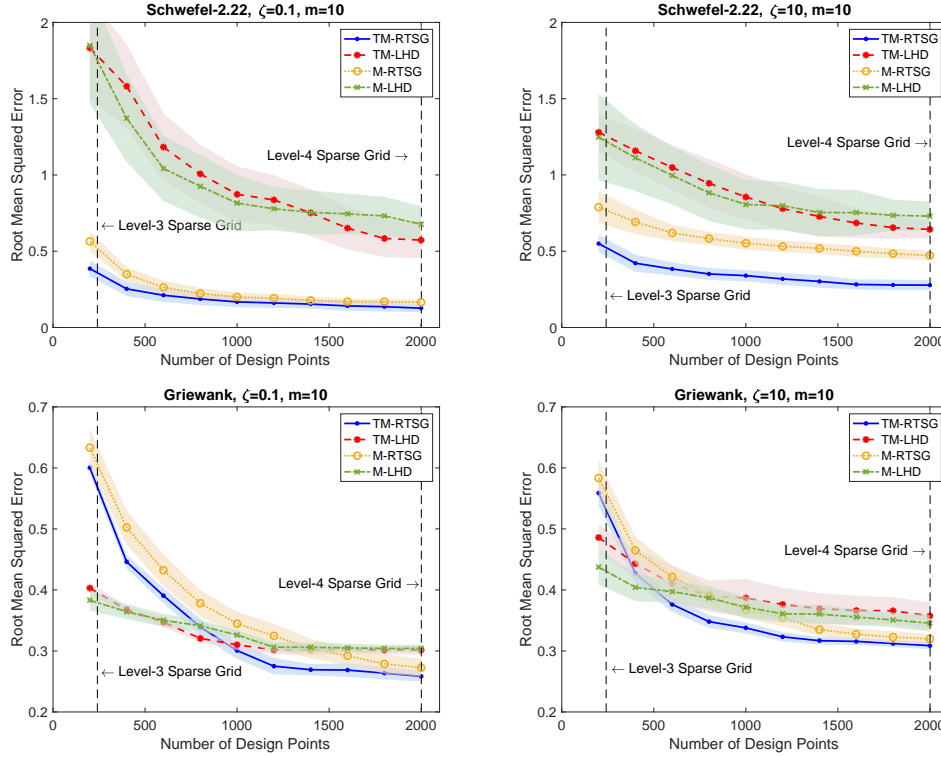
- (i) **M-LHD**: the Matérn($5/2$) kernel plus the maximin Latin hypercube design (LHD) that maximizes the minimum distance between points (van Dam et al. 2007). It is shown in Tuo and Wang (2020) that the maximin LHD design is the optimal design in an asymptotic sense with respect to the L_p norm for kriging with Matérn kernels.
- (ii) **M-RTSG**: the Matérn($5/2$) kernel plus the RTSG design.
- (iii) **TM-LHD**: the TM kernel plus the maximin LHD design.

We investigate the prediction performance and the computational cost of each method as the sampling budget increases. Given a sampling budget n , we construct the set of prediction points of size $n_{\text{pred}} = 1000$ by selecting randomly from a 10-dimensional lattice with 4 equally spaced points in each dimension, i.e., a lattice of size 4^{10} . (We do not randomly sample the prediction points from the entire design space because the points would mostly be sampled from areas close to the boundary of the design space, making it difficult to differentiate the prediction performance of the competing methods.) We compute $\widehat{\text{RMSE}}$ of the predictor of each method, its associated $\widehat{\text{SD}}$, and the average time to complete the n_{pred} predictions based on $R = 100$ macro-replications, as detailed in Section 7.1.

For both functions, the sampling budget is set to be $n = 200, 400, \dots, 2000$. We consider the case of noisy observations by adding to the test function value $y(\mathbf{x})$ a zero mean Gaussian random variable with standard deviation that is proportional to $y(\mathbf{x})$. That is, the observations are heteroscedastic Gaussian random variables: $Y_r(\mathbf{x}_i) \sim \mathcal{N}(y(\mathbf{x}_i), \zeta y^2(\mathbf{x}_i))$, for all $r = 1, \dots, m_i$ and $i = 1, \dots, n$. The experiments are run under two scenarios with different noise levels: a low-noise scenario with $\zeta = 0.1$ and the high-noise scenario with $\zeta = 10$. We set $m_i \equiv 10$ for all i , and use the estimated variance in stochastic kriging. The experiment results are shown in Figure 4.

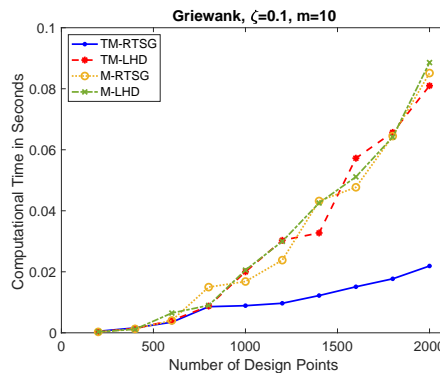
There are several observations from Figure 4. We first focus on the results for the low-noise scenario (i.e., the left column of Figure 4). For the Schwefel-2.22 function, our approach **TM-RTSG**, in general, outperforms the others significantly in prediction accuracy, having the lowest $\widehat{\text{RMSE}}$, for all the sample sizes used in the experiment. It also yields the lowest $\widehat{\text{SD}}$ with a similar pattern, which is visualized via the shaded areas in the figure. Since $\widehat{\text{SD}}$ is computed via many macro-replications, each of which a random set of prediction points are sampled, this suggests that the prediction given by **TM-RTSG** is more stable than the competing approaches.

For the Griewank function (i.e., the bottom-left block of Figure 4), however, the advantage of **TM-RTSG** in prediction accuracy is lost for the cases of relatively small number of design points ($n < 1000$). But our approach regains its superiority as n increases. The difference in performance of **TM-RTSG** between being applied to the Schwefel-2.22 function and to the Griewank function may be attributed to the different levels of smoothness of the two test functions—the former has non-differentiable regions whereas the latter is infinitely differentiable.

Figure 4 Prediction Errors for the Test Functions.

Note. Left column: $\widehat{\text{RMSE}}$ with $\zeta = 0.1$; Right column: $\widehat{\text{RMSE}}$ with $\zeta = 10$. Top panel: Schwefel-2.22 function; Bottom panel: Griewank function. The black dashed vertical lines indicate the number of design points for which RTSG is identical to a classical SG. The shaded areas have a half-width that equals $\widehat{\text{SD}}$.

Finally, under the high-noise scenario (i.e., the right column of Figure 4), except for the case that combines small n and the Griewank function, TM-RTSG still mostly outperforms the other approaches significantly in both prediction accuracy and stability, although the margins relative to the others are no the same as before.

Figure 5 Computational Time for Predicting the Griewank Function with $\zeta = 0.1$.

In Figure 5, we compare the computational time of different approaches in predicting the Griewank function with $\zeta = 0.1$. The computational time comparisons in other settings are similar. The advantage of TM-RTSG in terms of computational efficiency is dominant, requiring a computational expense that is substantially lower than the other approaches. The stark difference in computational time stems from the careful design of the algorithms that leverage the sparseness of the inverse kernel matrix associated with TM kernels and RTSG designs. We can see from Theorem 5 that the sparseness is increasing as the sample size grows, with the proportion of nonzero entries decaying to zero at the rate $n^{-1}(\log n)^{2d}$. In contrast, the other approaches suffers heavily from the numerical inversion of dense matrices.

7.3. A Production Line with 20 Servers

In this section, we consider an a production line problem from the SimOpt Library (www.simopt.org). It is a queueing system with $d = 20$ servers in tandem, each having exponentially distributed service times. The response surface of interest is the expected revenue of the production line as a function of the vector of service rates $\mathbf{x} \in (0, 2)^d$.

Parts arrive to the first server of the production line following a Poisson process with rate λ . The parts are processed at each queue on a first-come-first-serve basis. All servers have a finite capacity K . Upon completion of the service at server i , a part will be transferred to server $i + 1$, if there is room at the next server. Otherwise, if there are already K parts at server $i + 1$, sever i is said to be blocked, and the part being served at server i cannot leave even if its service is completed. The throughput of the production line, denoted by $\text{Th}(\mathbf{x})$, is defined as the number of parts leaving the last server within a given time horizon T . The expected revenue is defined as

$$y(\mathbf{x}) = \mathbb{E} \left[\frac{r \cdot \text{Th}(\mathbf{x})}{c_0 + \mathbf{c}^\top \mathbf{x}} \right].$$

The parameters are specified as follows:

- (i) The design space is $\mathcal{X} = (0, 2)^d$.
- (ii) Capacity $K = 10$, unit $r = 2 \times 10^5$, and time horizon $T = 200$.
- (iii) The vector $\mathbf{c} = (c_1, c_2, \dots, c_d)$ with $c_i = i$ denotes the cost to run server i and the initial cost $c_0 = 1$.

We set the sampling budget to be $n = 100, 200, \dots, 1500$. In this example, the simulation noise has an unknown variance. We run $m = 10$ replications at each design point during the training process to estimate the variance $\sigma^2(\mathbf{x})$ and use the sample estimate in stochastic kriging. We construct the set of prediction points of size $n_{\text{pred}} = 1000$ by sampling randomly from the 20-dimensional hypercube $(0, 2)^{20}$. Since $y(\mathbf{x})$ has no closed-form, for each prediction point, we run 100 replications to compute the “true” value of the response there. Moreover, we run the experiments for two value

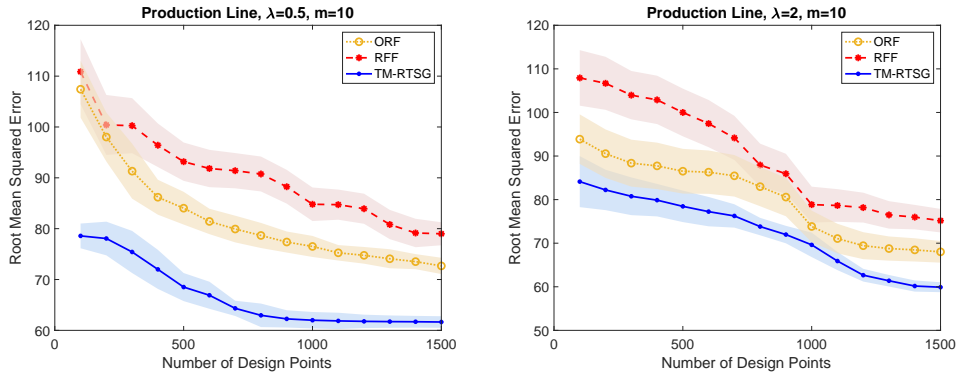
of the arrival rate: $\lambda = 0.5$ and $\lambda = 2$. The variances of the simulation outputs for the former case are lower than those for the latter. Thus, similar to Section 7.2, we call them the low-noise scenario and the high-noise scenario, respectively.

We now compare TM-RTSG with two kernel approximation methods that are popular benchmarks in machine learning literature. Both belong to the random features method; see Section 2.3.3 for an overview and Liu et al. (2021) for a recent survey which also provides the MATLAB code for the two methods, available at www.lfhsgre.org.

- (i) **RFF**: Random Fourier Feature (Rahimi and Recht 2007) constructs a low-rank approximation of the kernel matrix by randomly sampling a small set of the Fourier components of the kernel.
- (ii) **ORF**: Orthogonal Random Feature (Yu et al. 2016) is a refined variant of RFF in that certain orthogonality condition is enforced when sampling the relevant Fourier components.

For both methods, we set the number of random Fourier components to be \sqrt{n} , a standard choice in the literature; see, e.g., Yen et al. (2014). In addition, we set the experimental design to be the maximin LHD design, similar to Section 7.2. We use the Laplace kernel for RFF and use Gaussian kernel ORF, respectively. Recall that the TM kernel in TM-RTSG is also the Laplace kernel. Hence, to some extent, RFF is a variant of TM-LHD in terms of prediction accuracy, while ORF is a variant of stochastic kriging with the Gaussian kernel and the maximin LHD design.

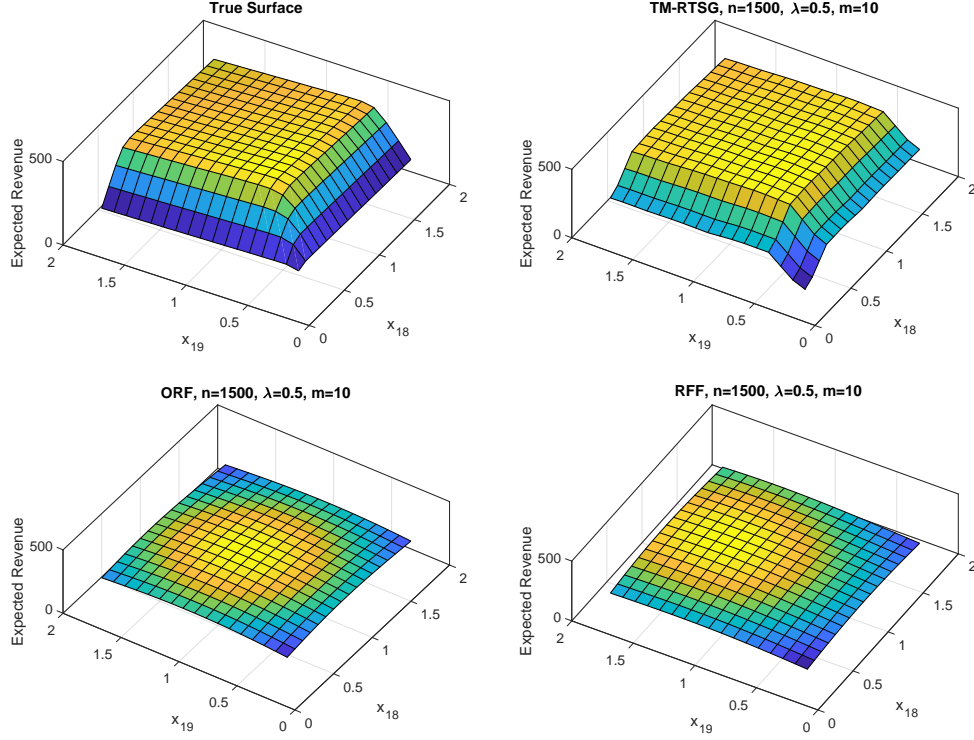
Figure 6 Prediction Errors for the Production Line Problem.



Note. Left: $\widehat{\text{RMSE}}$ with $\lambda = 0.5$, $m = 10$; Right: $\widehat{\text{RMSE}}$ with $\lambda = 2$, $m = 10$. The shaded areas have a half-width that equals $\widehat{\text{SD}}$.

Figure 6 exhibits $\widehat{\text{RMSE}}$ and $\widehat{\text{SD}}$ of the three approaches (TM-RTSG, RFF, and ORF) for both the low-noise and high-noise scenarios. TM-RTSG obviously dominates the other two approaches in prediction accuracy for this 20-dimensional problem.

In Figure 7, for the case of $\lambda = 0.5$, we visualize the true surface and the predicted surfaces by TM-RTSG, ORF and RFF that are projected onto the dimensions spanned by x_{18} and x_{19} of the design space. Specifically, the projections are formed by fixing $x_j = 1$ for $j \neq 18, 19$. We can see that

Figure 7 Two-Dimensional Projections of the True and Predicted Surfaces of the Production Line Problem.

Note. Top-left: True surface; Top-right: Predicted surface by TM-RTSG; Bottom-left: Predicted surface by ORF; Bottom-right: Predicted surface by RFF.

TM-RTSG successfully captures the shape of the true surface, whereas the projections formed by other approaches fail to do so. We have also examined projections onto other dimensions and the results are similar.

We omit the computational times, since they are basically determined by the sample size and has little to do with what the true response surface is. The computational time of TM-RTSG of similar sample sizes have been reported in Figure 5. Moreover, the comparison on computational time would be less meaningful here, since TM-RTSG performs *exact* computation of stochastic kriging, whereas both RFF and ORF produce approximations whose computational time heavily depends on the approximation level.

7.4. A 50-Product Assortment Problem

In this section, we follow the formulation in Aydin and Porteus (2008) to consider an assortment problem involving $d = 50$ products with joint inventory and pricing decisions in a newsvendor model. The response surface of interest is the expected profit as a function of the price vector $\mathbf{x} \in \mathbb{R}^d$ with the inventory levels set optimally. Let c_j denote the unit procurement cost of product j , $j = 1, \dots, d$. Suppose that the products' demand follows the multinomial logit choice model, namely, the

demand for product j is $D_j(\mathbf{x}) = Q_j(\mathbf{x})\varepsilon_j$, where ε_j 's are i.i.d. random variables having the uniform distribution $\text{Unif}(a, b)$, and $Q_j(\mathbf{x}) = e^{\alpha_j - x_j} / [1 + \sum_{i=1}^d e^{\alpha_i - x_i}]$. Then, it is shown in Section 3 in Aydin and Porteus (2008) that the expected profit is given by

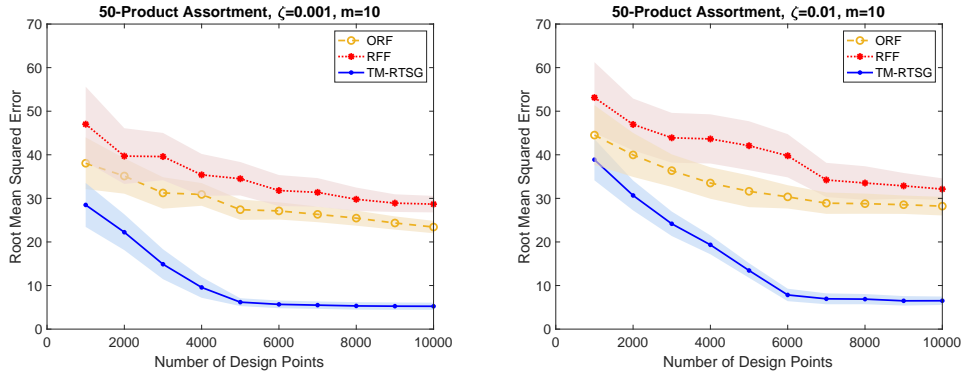
$$y(\mathbf{x}) = \frac{1}{2(b-a)} \sum_{j=1}^d \left[(b-a) \left(\frac{x_j - c_j}{x_j} \right) + a \right]^2 Q_j^2(\mathbf{x}).$$

The parameters are specified as follows:

- (i) The design space is $\mathcal{X} = \prod_{j=1}^d (h_j, h_j + 10)$, where $h_j = 9 + 0.5(j-1)$. Note that the profit maximizer is contained in this region.
- (ii) $c_j = 6.5 + 0.5(j-1)$ and $\alpha_j = 10.5 + 0.5(j-1)$, for $j = 1, \dots, d$.
- (iii) $a = 100$, $b = 400$.

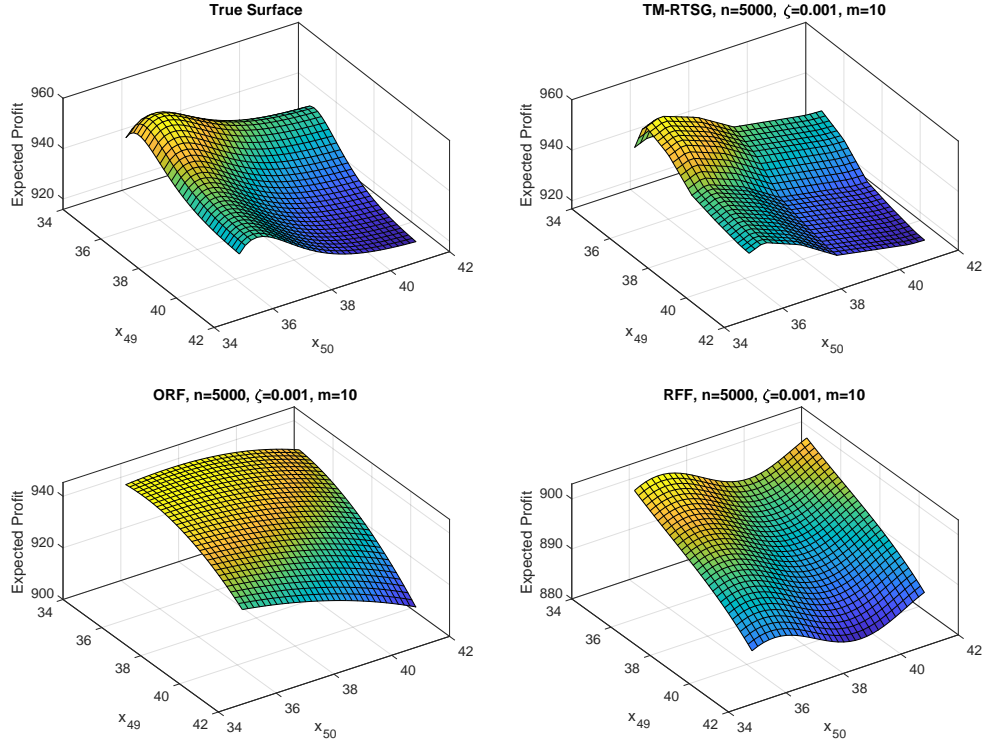
We set the sampling budget to be $n = 1000, 2000, \dots, 10000$, and construct the set of prediction points of size $n_{\text{pred}} = 1000$ by sampling randomly from a 50-dimensional lattice of with 3 equally spaced points in each dimension. Noisy simulation outputs are generated by adding to the true response surface Gaussian noise with heterogeneous variance $\sigma^2(\mathbf{x}) = \zeta|y(\mathbf{x})|$. That is, $Y_r(\mathbf{x}_i) \sim \mathcal{N}(y(\mathbf{x}_i), \zeta|y(\mathbf{x}_i)|)$, for all $r = 1, \dots, m_i$ and $i = 1, \dots, n$. Similar to the experiments in Section 7.2, we run the experiments for both $\zeta = 0.001$ and $\zeta = 0.01$, representing different levels of simulation noise. We set $m_i \equiv 10$ to estimate $\sigma^2(\mathbf{x}_i)$ for all i .

Figure 8 Prediction Errors for the Assortment Problem.



Note. Left: $\widehat{\text{RMSE}}$ with $\zeta = 0.001$; Right: $\widehat{\text{RMSE}}$ with $\zeta = 0.01$. The shaded areas have a half-width that equals $\widehat{\text{SD}}$.

The prediction errors of the three approaches (TM-RTSG, RFF, and ORF) are presented in Figure 8. (Note that all the three competing approaches in Section 7.2 (i.e., M-LHD, M-LHD, and M-RTSG) fail to predict the surface to an acceptable level of accuracy with the above sampling budget, due to the curse of dimensionality.) The specifications of RFF and ORF are the same as those in Section 7.3. Figure 9 presents the true surface and the predicted surfaces by TM-RTSG, ORF and RFF that are projected onto the last two dimensions of the design space. Similar to the experiments in Section 7.3, the advantage of our approach relative to the others is substantial in high-dimensional settings.

Figure 9 Two-Dimensional Projections of the True and Predicted Surfaces of the Assortment Problem.

Note. Top-left: True surface; Top-right: Predicted surface by TM-RTSG; Bottom-left: Predicted surface by ORF; Bottom-right: Predicted surface by RFF.

7.5. A Large Linear Program

In this section, we challenge the prediction capability of TM-RTSG with a very high-dimensional example with $d = 16675$. The response surface of interest is the optimal value of STOCFOR3, a linear programming (LP) model—the largest one available in the NETLIB Library (netlib.org/lp)—to decide what parts of a forest should be harvested to prevent wildfires. The design variable $\mathbf{x} \in (0, 1)^d$ is taken to be the right-hand-side terms of the constraints of the LP model. Specifically, the LP model is of the form

$$\begin{aligned} y(\mathbf{x}) &:= \text{Minimize}_{\mathbf{w}} \quad \mathbf{c}^\top \mathbf{w} \\ &\text{subject to} \quad \mathbf{A} \mathbf{w} = \mathbf{x} \\ &\quad \mathbf{l} \leq \mathbf{w} \leq \mathbf{u}, \end{aligned}$$

where the values of \mathbf{c} , \mathbf{A} , \mathbf{l} , and \mathbf{u} are publicly available. The value of $y(\mathbf{x})$ can be computed with the LP solver in MATLAB. Similar to Sections 7.2 and 7.4, we add artificial Gaussian noise to $y(\mathbf{x})$, but with equal variance $\sigma^2(\mathbf{x}) \equiv 1$. For simplicity, we assume the variance is given without estimation and take one replication at each design point.

The sampling budget is set to be $n = 3000, 6000, \dots, 30000$. We construct the set of prediction points as follows. First, we randomly draw 4 different dimensions $[d_1, d_2, d_3, d_4]$ among the total d dimensions; then, we randomly draw a $(d - 4)$ -dimensional random vector \mathbf{v} from $[\frac{1}{4}, \frac{3}{4}]^{d-4}$; at last, the prediction points are chosen to be

$$\{\mathbf{x} \in (0, 1)^d : x_{d_i} = 1/8, 2/8, \dots, 7/8, \forall i = 1, \dots, 4, \text{ and } [x_i]_{i \neq d_1, d_2, d_3, d_4} = \mathbf{v}\}.$$

In other words, for each $i = 1, \dots, 4$, the d_i -th entry of each prediction point takes value from $\{1/8, 2/8, \dots, 7/8\}$, while the other $(d - 4)$ entries are fixed to be \mathbf{v} . By doing so, we can avoid the situation where most of the prediction points are near the boundary of the design space, which would be the case if we do uniform random sampling on the hypercube $(0, 1)^d$ for such a large value of d . In total, we have $n_{\text{pred}} = 7^4 = 2401$ prediction points.

We compare TM-RTSG with the following two approaches.

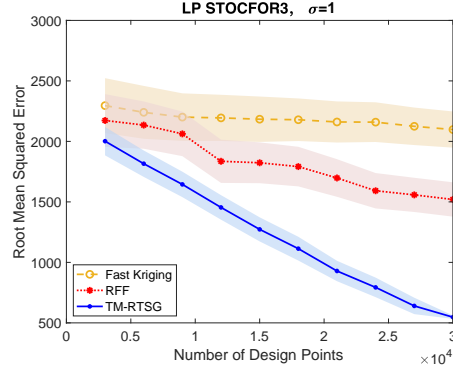
- (i) **RFF**: Random Fourier features with the Laplace kernel. The number of random Fourier components is set to be $\frac{n}{10}$. The experimental design is set to be the RTSG design.
- (ii) **FK**: Fast Kriging (Lu et al. 2020) is a recent development of the Nyström method (see Section 2.3.3). The number of Nyström centers is set to be $\frac{n}{10}$. The design points are uniformly drawn from the hypercube $(0, 1)^d$. The MATLAB code is made public by the authors of Lu et al. (2020), available at github.com/LuXuefei/FastKriging.

We do not include ORF here, however, because it involves doing computations on a $d \times d$ matrix, which exceeds the capacity of our computer for $d = 16675$. By contrast, RFF is not subject to this limitation. We use the RTSG design instead of an LHD design for RFF because it is computationally prohibitive—both in time and space—to generate a LHD in $d = 16675$ dimensions. Moreover, because the dimensionality of this example is substantially higher than those in Sections 7.3 and 7.4, RFF needs a larger number of random Fourier components to produce reasonable predictions. Hence, we set the number to be $\frac{n}{10}$ instead of \sqrt{n} as in the previous sections.

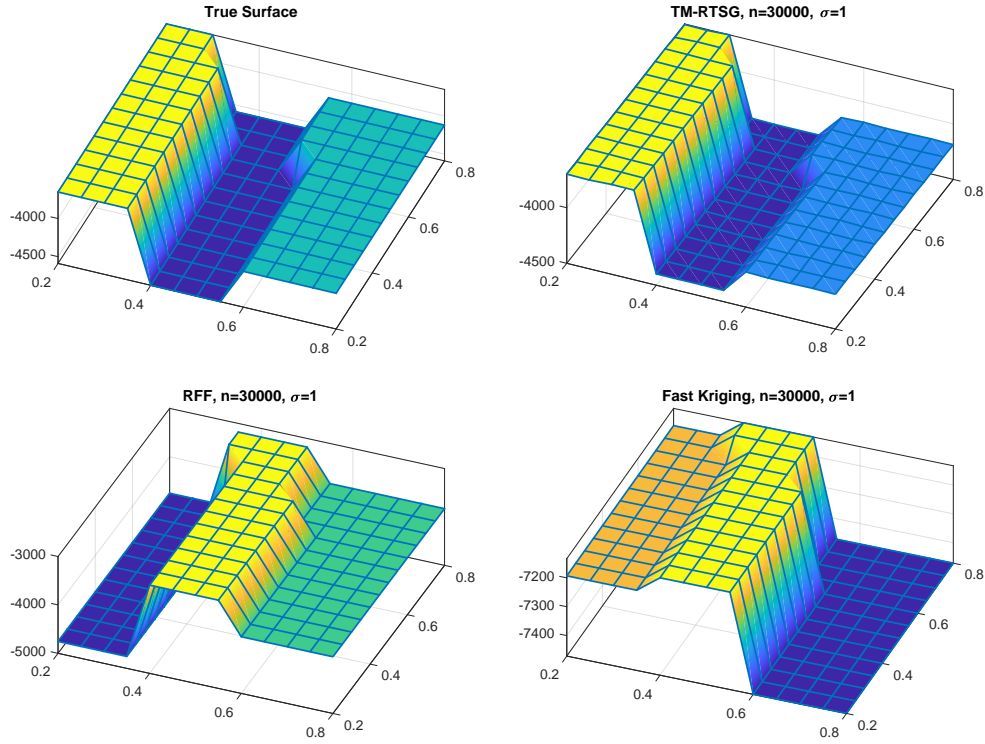
We can see from Figure 10 that TM-RTSG outperforms RFF and FK in prediction accuracy by a large margin. Further, the advantage of TM-RTSG appears to be increasing as the number of design points increases. Such an advantage in prediction accuracy is also reflected clearly in Figure 11. It shows projections of the true response surface and the predicted surfaces onto two arbitrarily chosen dimensions, with the values of the design variable in the other dimensions being randomly chosen from $1/4$, $1/2$, and $3/4$.

8. Concluding Remarks

We develop in this paper a new methodology for simulation metamodeling in high dimensions. We show that stochastic kriging with TM kernels and TSG designs is both sample-efficient and

Figure 10 Prediction Errors for the STOCFOR3 Problem.

Note. The shaded areas have a half-width that equals \widehat{SD} .

Figure 11 Two-Dimensional Projections of the True and Predicted Surfaces of the STOCFOR3 Problem.

Note. Top-left: True surface; Top-right: Predicted surface by TM-RTSG; Bottom-left: Predicted surface by RFF; Bottom-right: Predicted surface by FK.

computationally efficient. First, we establish an upper bound on the convergence rate under both correct model specification and model misspecification. The upper bounds imply that for both cases, the sample complexity of our methodology is almost free of the curse of dimensionality. The convergence analysis under model misspecification is particularly reassuring for practitioners, as it provides strong robustness of our methodology.

Second, we develop algorithms that perform fast, exact computation of stochastic kriging with TM kernels and TSG designs. They are fundamentally driven by our explicit characterization of the sparse structure of the inverse kernel matrix, which hold only for TM kernels. Compared to existing algorithms for kriging with SG designs, our algorithms allow simulation noise and are not restricted to “complete” SG designs. But our algorithms do not apply to general tensor product kernels, which may not possess the sparse structure.

The present paper can potentially be extended in several ways. First, we only establish upper bounds on the convergence rate and whether they are tight is unknown. It is of great interest to establish minimax lower bounds, although new theoretical tools may be needed for this purpose.

Second, kriging metamodels often suffer from the numerical instability due to the ill-conditionedness of the kernel matrix. The kernel matrices associated with TM kernels and TSGs appear to be well-conditioned in our numerical experiments, but we do not analyze it theoretically. Further studies on the eigenvalues of these kernel matrices would be insightful.

Third, this paper focuses on prediction of the response surface. Another main use of simulation metamodeling is simulation optimization. Given a sampling budget, a simple algorithm for computing the global optimal solution of an unknown response surface would be to take samples following the TSG design, construct the predicted surface using stochastic kriging with TM kernels, and then select from the TSG the design point that has the optimal predicted value as the solution. Since the upper convergence rates that we establish are uniform in the design variable, it is conceivable that this algorithm may be affected only mildly by the curse of dimensionality. One might devise a more efficient algorithm that adaptively selects sampling locations from a SG design, which is made possible by the theory developed for the TSG designs here.

References

- Ababou R, Bagtzoglou AC, Wood EF (1994) On the condition number of covariance matrices in kriging, estimation, and simulation of random fields. *Math. Geol.* 26(1):99–133.
- Adler RJ (1981) *The Geometry of Random Fields* (Wiley).
- Ankenman B, Nelson BL, Staum J (2010) Stochastic kriging for simulation metamodeling. *Oper. Res.* 58(2):371–382.
- Arfken GB, Weber HJ, Harris FE (2012) *Mathematical Methods for Physicists: A Comprehensive Guide* (Academic Press), 7th edition.
- Aydin G, Porteus E (2008) Joint inventory and pricing decisions for an assortment. *Oper. Res.* 56(5):1247–1255.
- Barton RR (2015) Tutorial: Simulation metamodeling. *Proc. 2015 Winter Simulation Conf.*, 1765–1779.
- Barton RR, Nelson BL, Xie W (2014) Quantifying input uncertainty via simulation confidence intervals. *INFORMS J. Comput.* 26(1):74–87.

- Bungartz HJ, Griebel M (2004) Sparse grids. *Acta Numerica* 13:147–269.
- Burt DR, Rasmussen CE, van der Wilk M (2020) Convergence of sparse variational inference in Gaussian processes regression. *J. Mach. Learn. Res.* 21(131):1–63.
- Caponnetto A, De Vito E (2007) Optimal rates for the regularized least-squares algorithm. *Found. Comput. Math.* 7(3):331–368.
- Carnal E, Walsh J (1991) Markov properties for certain random fields. Mayer-Wolf E, Merzbach E, Shwartz A, eds., *Stochastic Analysis: Liber Amicorum for Moshe Zakai*, 91–110 (Academic Press).
- Chen X, Ankenman B, Nelson BL (2012) The effects of common random numbers on stochastic kriging metamodels. *ACM Trans. Model. Comput. Simul.* 22(2):Article 7.
- Dolph CL, Woodbury MA (1952) On the relation between Green’s functions and covariances of certain stochastic processes and its application to unbiased linear prediction. *Trans. Amer. Math. Soc.* 72:519–550.
- Evans LC (2010) *Partial Differential Equations* (American Mathematical Society), 2nd edition.
- Garcke J, Griebel M, eds. (2013) *Sparse Grids and Applications* (Springer-Verlag).
- Gramacy RB (2020) *Surrogates: Gaussian Process Modeling, Design and Optimization for the Applied Sciences* (CRC Press).
- Gramacy RB, Apley DW (2015) Local Gaussian process approximation for large computer experiments. *J. Comput. Graph. Stat.* 24(2):561–578.
- Haaland B, Qian PZG (2011) Accurate emulators for large-scale computer experiments. *Ann. Stat.* 39(6):2974–3002.
- Haaland B, Wang W, Maheshwari V (2018) A framework for controlling sources of inaccuracy in Gaussian process emulation of deterministic computer experiments. *SIAM/ASA J. Uncertainty Quantification* 6(2):497–521.
- Horn RA, Johnson CR (2012) *Matrix Analysis* (Cambridge University Press), 2nd edition.
- Jalali H, Van Nieuwenhuyse I, Picheny V (2017) Comparison of Kriging-based algorithms for simulation optimization with heterogeneous noise. *Eur. J. Oper. Res.* 261(1):279 – 301.
- Karatzas I, Shreve SE (1991) *Brownian Motion and Stochastic Calculus* (Springer), 2nd edition.
- Kleijnen JPC (2017) Regression and kriging metamodels with their experimental designs in simulation: A review. *Eur. J. Oper. Res.* 256(1):1–16.
- Liu F, Huang X, Chen Y, Suykens JA (2021) Random features for kernel approximation: A survey on algorithms, theory, and beyond. Preprint available at *arXiv:2004.11154*.
- Liu H, Ong YS, Shen X, Cai J (2020) When Gaussian process meets big data: A review of scalable GPs. *IEEE Trans. Neural Netw. Learn. Syst.* 31(11):4405–4423.

- Lu X, Rudi A, Borgonovo E, Rosasco L (2020) Faster kriging: Facing high-dimensional simulators. *Oper. Res.* 68(1):233–249.
- Marcus MB, Rosen J (2006) *Markov Processes, Gaussian Processes, and Local Times* (Cambridge University Press).
- Matheron G (1963) Principles of geostatistics. *Econ. Geol.* 58(8):1246–1266.
- McKay MD, Beckman RJ, Conover WJ (1979) A comparison of three methods for selecting values of input variables in the analysis of output from a computer code. *Technometrics* 21(2):239–245.
- Moura JMF, Goswami S (1997) Gauss–Markov random fields (GMrf) with continuous indices. *IEEE Trans. Inf. Theory* 43(5):1560–1573.
- O’Hagan A (1991) Bayes–Hermite quadrature. *J. Stat. Plann. Infer.* 29(3):245–260.
- Pati D, Bhattacharya A, Cheng G (2015) Optimal Bayesian estimation in random covariate design with a rescaled Gaussian process prior. *J. Mach. Learn. Res.* 16(87):2837–2851.
- Pearce M, Poloczek M, Branke J (2019) Bayesian simulation optimization with common random numbers. *Proc. 2019 Winter Simulation Conf.*, 3492–3503.
- Plumlee M (2014) Fast prediction of deterministic functions using sparse grid experimental designs. *J. Amer. Statist. Assoc.* 109(508):1581–1591.
- Rahimi A, Recht B (2007) Random features for large-scale kernel machines. *Advances in Neural Information Processing Systems 20*, 1177–1184.
- Rasmussen CE, Williams KI (2006) *Gaussian Processes for Machine Learning* (MIT Press).
- Rudi A, Rosasco L (2017) Generalization properties of learning with random features. *Advances in Neural Information Processing Systems*, 3218–3228.
- Rue H, Held L (2005) *Gaussian Markov Random Fields: Theory and Applications* (CRC Press).
- Sacks J, Welch WJ, Mitchell TJ, Wynn HP (1989) Design and analysis of computer experiments. *Stat. Sci.* 409–423.
- Salemi P, Staum J, Nelson BL (2019a) Generalized integrated Brownian fields for simulation metamodeling. *Oper. Res.* 67(3):874–891.
- Salemi PL, Song E, Nelson BL, Staum J (2019b) Gaussian Markov random fields for discrete optimization via simulation: Framework and algorithms. *Oper. Res.* 67(1):250–266.
- Santner TJ, Williams BJ, Notz WI (2003) *The Design and Analysis of Computer Experiments* (Springer).
- Schölkopf B, Smola AJ (2002) *Learning with Kernels: Support Vector Machines, Regularization, Optimization, and Beyond* (MIT Press).
- Shahriari B, Swersky K, Wang Z, Adams RP, de Freitas N (2016) Taking the human out of the loop: A review of Bayesian optimization. *Proc. IEEE* 104(1):148–175.

- Smola AJ, Schölkopf B (2000) Sparse greedy matrix approximation for machine learning. *Proceedings of the 17th International Conference on Machine Learning*, 911–918.
- Stone CJ (1980) Optimal rates of convergence for nonparametric estimators. *Ann. Stat.* 8(6):1348–1360.
- Sun L, Hong LJ, Hu Z (2014) Balancing exploitation and exploration in discrete optimization via simulation through a Gaussian process-based search. *Oper. Res.* 62(6):1416–1438.
- Tsybakov AB (2009) *Introduction to Nonparametric Estimation* (Springer, New York).
- Tuo R, Wang W (2020) Kriging prediction with isotropic Matérn correlations: Robustness and experimental design. *J. Mach. Learn. Res.* 21(187):1–38.
- Tuo R, Wang Y, Jeff Wu CF (2020) On the improved rates of convergence for Matérn-type kernel ridge regression with application to calibration of computer models. *SIAM/ASA J. Uncertainty Quantification* 8(4):1522–1547.
- van Dam ER, Husslage B, den Hertog D, Melissen H (2007) Maximin Latin hypercube designs in two dimensions. *Oper. Res.* 55(1):158–169.
- van der Vaart A, van Zanten H (2011) Information rates of nonparametric Gaussian process methods. *J. Mach. Learn. Res.* 12:2095–2119.
- Wang W, Haaland B (2019) Controlling sources of inaccuracy in stochastic kriging. *Technometrics* 61(3):309–321.
- Wang W, Tuo R, Wu CFJ (2020) On prediction properties of kriging: Uniform error bounds and robustness. *J. Amer. Statist. Assoc.* 115(530):920–930.
- Williams C, Seeger M (2001) Using the Nyström method to speed up kernel machines. *Advances in Neural Information Processing Systems 13*, 682–688.
- Xie W, Nelson BL, Barton RR (2014) A Bayesian framework for quantifying uncertainty in stochastic simulation. *Oper. Res.* 62(6):1439–1452.
- Yen IEH, Lin TW, Lin SD, Ravikumar PK, Dhillon IS (2014) Sparse random feature algorithm as coordinate descent in Hilbert space. *Advances in Neural Information Processing Systems 27*, 2456–2464.
- Ylvisaker D (1987) Prediction and design. *Ann. Statist.* 15(1):1–19.
- Yu FX, Suresh AT, Choromanski KM, Holtmann-Rice DN, Kumar S (2016) Orthogonal random features. *Advances in Neural Information Processing Systems 29*, 1975–1983.
- Zenger C (1991) Sparse grids. Hackbusch W, ed., *Parallel Algorithms for Partial Differential Equations*, volume 31 of *Notes on Numerical Fluid Mechanics*, 241–251 (Vieweg-Verlag).

Supplemental Material

EC.1. An Orthogonal Expansion of TM Kernels

We first introduce a technical result that is fundamental for both the convergence rate analysis and the kernel matrix inversion. It summarizes Theorem 2 and Corollary 1 in Ding et al. (2020).

LEMMA EC.1. *Let $k(\mathbf{x}, \mathbf{x}') = \prod_{j=1}^d p_j(x_j \wedge x'_j) q_j(x_j \vee x'_j)$ be a TM kernel that satisfies Assumption 1. Let $\mathbf{c}_{l,i} := i \cdot 2^{-l}$ for $l \geq 1$ and $i = 1, \dots, 2^l - 1$. For each $j = 1, \dots, d$, define the following continuous function with support $(\mathbf{c}_{l,i-1}, \mathbf{c}_{l,i+1}) = ((i-1) \cdot 2^{-l}, (i+1) \cdot 2^{-l})$:*

$$\phi_{j,l,i}(x) := \begin{cases} \frac{p_j(x) \mathbf{q}_{j,l,i-1} - \mathbf{p}_{j,l,i-1} q_j(x)}{\mathbf{p}_{j,l,i} \mathbf{q}_{j,l,i-1} - \mathbf{p}_{j,l,i-1} \mathbf{q}_{j,l,i}}, & \text{if } x \in (\mathbf{c}_{l,i-1}, \mathbf{c}_{l,i}], \\ \frac{\mathbf{p}_{j,l,i+1} q_j(x) - p_j(x) \mathbf{q}_{j,l,i+1}}{\mathbf{p}_{j,l,i+1} \mathbf{q}_{j,l,i} - \mathbf{p}_{j,l,i} \mathbf{q}_{j,l,i+1}}, & \text{if } x \in (\mathbf{c}_{l,i}, \mathbf{c}_{l,i+1}), \\ 0, & \text{otherwise,} \end{cases} \quad (\text{EC.1.1})$$

where $\mathbf{p}_{j,l,i} = p_j(\mathbf{c}_{l,i})$ and $\mathbf{q}_{j,l,i} = q_j(\mathbf{c}_{l,i})$. For any multi-indices $\mathbf{l}, \mathbf{i} \in \mathbb{N}^d$, define

$$\phi_{\mathbf{l},\mathbf{i}}(\mathbf{x}) := \prod_{j=1}^d \phi_{j,l_j,i_j}(x_j). \quad (\text{EC.1.2})$$

Let \mathcal{H}_k denote the reproducing kernel Hilbert space (RKHS) generated by the kernel k , with inner product $\langle \cdot, \cdot \rangle_{\mathcal{H}_k}$ and norm $\|\cdot\|_{\mathcal{H}_k}$. Then, $\{\phi_{\mathbf{l},\mathbf{i}} : \mathbf{l} \in \mathbb{N}^d, \mathbf{i} \in \rho(\mathbf{l})\}$ is an orthogonal basis for \mathcal{H}_k with respect to $\langle \cdot, \cdot \rangle_{\mathcal{H}_k}$, where $\rho(\mathbf{l}) = \bigtimes_{j=1}^d \{i_j : 1 \leq i_j \leq 2^{l_j} - 1, i_j \text{ odd}\}$. In particular, we have the following expansion for k :

$$k(\mathbf{x}, \mathbf{x}') = \sum_{\mathbf{l} \in \mathbb{N}^d} \sum_{\mathbf{i} \in \rho(\mathbf{l})} \frac{\phi_{\mathbf{l},\mathbf{i}}(\mathbf{x}) \phi_{\mathbf{l},\mathbf{i}}(\mathbf{x}')}{\|\phi_{\mathbf{l},\mathbf{i}}\|_{\mathcal{H}_k}^2}, \quad (\text{EC.1.3})$$

for all $\mathbf{x}, \mathbf{x}' \in (0, 1)^d$.

The following result calculates the RKHS norm of $\phi_{\mathbf{l},\mathbf{i}}$ and establishes its decay rate as $|\mathbf{l}| \rightarrow \infty$. This result will be used in the analysis of convergence rates of stochastic kriging with TM kernels and TSGs.

LEMMA EC.2. *Let $k(\mathbf{x}, \mathbf{x}') = \prod_{j=1}^d p_j(x_j \wedge x'_j) q_j(x_j \vee x'_j)$ be a TM kernel that satisfies Assumption 1. Let $\{\phi_{\mathbf{l},\mathbf{i}} : \mathbf{l} \in \mathbb{N}^d, \mathbf{i} \in \rho(\mathbf{l})\}$ be the orthogonal basis defined by (EC.1.2) for \mathcal{H}_k . Then,*

$$\|\phi_{\mathbf{l},\mathbf{i}}\|_{\mathcal{H}_k}^2 = \prod_{j=1}^d \left(\frac{\mathbf{p}_{j,l_j,i_j+1} \mathbf{q}_{j,l_j,i_j-1} - \mathbf{p}_{j,l_j,i_j-1} \mathbf{q}_{j,l_j,i_j+1}}{(\mathbf{p}_{j,l_j,i_j} \mathbf{q}_{j,l_j,i_j-1} - \mathbf{p}_{j,l_j,i_j-1} \mathbf{q}_{j,l_j,i_j}) (\mathbf{p}_{j,l_j,i_j+1} \mathbf{q}_{j,l_j,i_j} - \mathbf{p}_{j,l_j,i_j} \mathbf{q}_{j,l_j,i_j+1})} \right), \quad (\text{EC.1.4})$$

where $\mathbf{p}_{j,l,i} = p_j(\mathbf{c}_{l,i})$ and $\mathbf{q}_{j,l,i} = q_j(\mathbf{c}_{l,i})$ for all j, l , and i . Moreover, as $|\mathbf{l}| \rightarrow \infty$,

$$\|\phi_{\mathbf{l},\mathbf{i}}\|_{\mathcal{H}_k}^2 \asymp 2^{|\mathbf{l}|}. \quad (\text{EC.1.5})$$

Proof. If $d = 1$, we suppress the dependence on j and write $k(x, x') = p(x \wedge x')q(x \vee x')$ for all $x, x' \in [0, 1]$. Then, (EC.1.4) is reduced to

$$\|\phi_{l,i}\|_{\mathcal{H}_k}^2 = \frac{\mathbf{p}_{l,i+1}\mathbf{q}_{l,i-1} - \mathbf{p}_{j,l,i-1}\mathbf{q}_{l,i+1}}{(\mathbf{p}_{l,i}\mathbf{q}_{l,i-1} - \mathbf{p}_{l,i-1}\mathbf{q}_{l,i})(\mathbf{p}_{l,i+1}\mathbf{q}_{l,i} - \mathbf{p}_{l,i}\mathbf{q}_{l,i+1})}, \quad (\text{EC.1.6})$$

where $\phi_{l,i}$ is defined as (EC.1.1), and $\mathbf{p}_{l,i} = p(\mathbf{c}_{l,i})$ and $\mathbf{q}_{l,i} = q(\mathbf{c}_{l,i})$ for all l and i . Moreover, (EC.1.5) is reduced to

$$\|\phi_{l,i}\|_{\mathcal{H}_k}^2 \asymp 2^l, \quad (\text{EC.1.7})$$

as $l \rightarrow \infty$. To prove (EC.1.6), we show that $\phi_{l,i}(x)$ can be expressed as a linear combination of $k(x, \mathbf{c}_{l,i-1})$, $k(x, \mathbf{c}_{l,i})$, and $k(x, \mathbf{c}_{l,i+1})$, and then apply the definition of the RKHS norm. Specifically, it can be shown by direct, albeit tedious, calculation that

$$\phi_{l,i}(x) = \eta_{l,i-1}k(x, \mathbf{c}_{l,i-1}) + \eta_{l,i}k(x, \mathbf{c}_{l,i}) + \eta_{l,i+1}k(x, \mathbf{c}_{l,i+1}), \quad (\text{EC.1.8})$$

for all $x \in [0, 1]$, $l \geq 1$, and $i \in \rho(l)$, where

$$\begin{aligned} \eta_{l,i} &= \frac{\mathbf{p}_{l,i+1}\mathbf{q}_{l,i-1} - \mathbf{p}_{l,i-1}\mathbf{q}_{l,i+1}}{(\mathbf{p}_{l,i}\mathbf{q}_{l,i-1} - \mathbf{p}_{l,i-1}\mathbf{q}_{l,i})(\mathbf{p}_{l,i+1}\mathbf{q}_{l,i} - \mathbf{p}_{l,i}\mathbf{q}_{l,i+1})}, \\ \eta_{l,i-1} &= \frac{-1}{\mathbf{p}_{l,i}\mathbf{q}_{l,i-1} - \mathbf{p}_{l,i-1}\mathbf{q}_{l,i}}, \\ \eta_{l,i+1} &= \frac{-1}{\mathbf{p}_{l,i+1}\mathbf{q}_{l,i} - \mathbf{p}_{l,i}\mathbf{q}_{l,i+1}}. \end{aligned} \quad (\text{EC.1.9})$$

Hence, by the definition of the RKHS norm,

$$\|\phi_{l,i}\|_{\mathcal{H}_k}^2 = \sum_{i'=i-1}^{i+1} \sum_{i''=i-1}^{i+1} \eta_{l,i'}\eta_{l,i''}k(\mathbf{c}_{l,i'}, \mathbf{c}_{l,i''}) = \eta_{l,i},$$

where the second equality, again, follows direct calculation. This proves (EC.1.6).

To prove (EC.1.7), we notice that

$$\begin{aligned} \mathbf{p}_{l,i+1}\mathbf{q}_{l,i} - \mathbf{p}_{l,i}\mathbf{q}_{l,i+1} &= (\mathbf{p}_{l,i+1} - \mathbf{p}_{l,i})\mathbf{q}_{l,i} - \mathbf{p}_{l,i}(\mathbf{q}_{l,i+1} - \mathbf{q}_{l,i}) \\ &= [p(\mathbf{c}_{l,i+1}) - p(\mathbf{c}_{l,i})]q(\mathbf{c}_{l,i}) - p(\mathbf{c}_{l,i})[q(\mathbf{c}_{l,i+1}) - q(\mathbf{c}_{l,i})]. \end{aligned}$$

Hence,

$$\begin{aligned} 2^{-l}(\mathbf{p}_{l,i+1}\mathbf{q}_{l,i} - \mathbf{p}_{l,i}\mathbf{q}_{l,i+1}) &= \frac{p((i+1) \cdot 2^{-l}) - p(i \cdot 2^{-l})}{2^l}q(\mathbf{c}_{l,i}) - p(\mathbf{c}_{l,i})\frac{q((i+1) \cdot 2^{-l}) - q(i \cdot 2^{-l})}{2^l} \\ &\asymp p'(\mathbf{c}_{l,i})q(\mathbf{c}_{l,i}) - p(\mathbf{c}_{l,i})q'(\mathbf{c}_{l,i}), \end{aligned}$$

as $l \rightarrow \infty$, where p' and q' denote the derivatives of p and q , respectively. Similarly, we have

$$\begin{aligned} 2^{-l}(\mathbf{p}_{l,i}\mathbf{q}_{l,i-1} - \mathbf{p}_{l,i-1}\mathbf{q}_{l,i}) &\asymp p'(\mathbf{c}_{l,i-1})q(\mathbf{c}_{l,i-1}) - p(\mathbf{c}_{l,i-1})q'(\mathbf{c}_{l,i-1}), \\ 2^{-(l-1)}(\mathbf{p}_{l,i+1}\mathbf{q}_{l,i-1} - \mathbf{p}_{l,i-1}\mathbf{q}_{l,i+1}) &\asymp p'(\mathbf{c}_{l,i-1})q(\mathbf{c}_{l,i-1}) - p(\mathbf{c}_{l,i-1})q'(\mathbf{c}_{l,i-1}), \end{aligned} \quad (\text{EC.1.10})$$

as $l \rightarrow \infty$. It follows that, by (EC.1.6),

$$\|\phi_{l,i}\|_{\mathcal{H}_k}^2 \asymp \frac{2^{l+1}}{p'(\mathbf{c}_{l,i})q(\mathbf{c}_{l,i}) - p(\mathbf{c}_{l,i})q'(\mathbf{c}_{l,i})}, \quad (\text{EC.1.11})$$

as $l \rightarrow \infty$. Furthermore, by Lemma 1, $p(x)/q(x)$ is strictly increasing in x on $(0,1)$. Thus,

$$\left(\frac{p(x)}{q(x)}\right)' = \frac{p'(x)q(x) - p(x)q'(x)}{q^2(x)} > 0$$

for all $x \in [0,1]$. Therefore, $|p'(x)q(x) - p(x)q'(x)| \in [a,b]$ for some positive constants a and b , since p and q are continuously differentiable by Assumption 1. We thus conclude from (EC.1.11) that $\|\phi_{l,i}\|_{\mathcal{H}_k}^2 \asymp 2^l$, proving (EC.1.6).

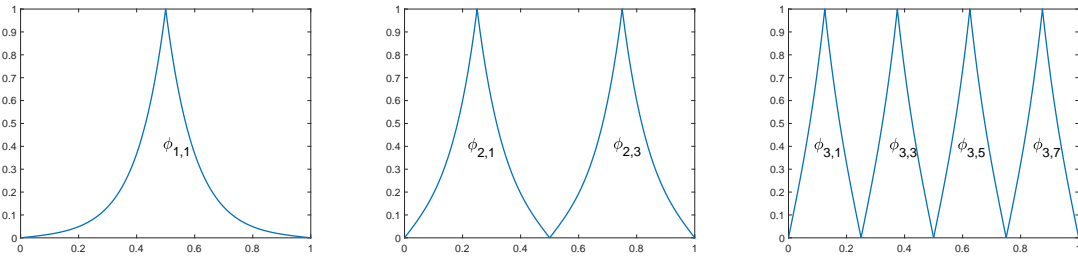
For $d > 1$, in light of the tensor structure of both k and $\phi_{\mathbf{l},\mathbf{i}}$, the RKHS norm of $\phi_{\mathbf{l},\mathbf{i}}$ possesses a product form as follows,

$$\|\phi_{\mathbf{l},\mathbf{i}}\|_{\mathcal{H}_k}^2 = \prod_{j=1}^d \|\phi_{l_j,i_j}\|_{\mathcal{H}_{k_j}}^2,$$

where \mathcal{H}_{k_j} denotes the RKHS induced by the component kernel k_j . Then, (EC.1.4) and (EC.1.5) follow immediately from (EC.1.6) and (EC.1.7), respectively, to each dimension $j = 1, \dots, d$. \square

Next, we establish an important connection between the functions $\{\phi_{\mathbf{l},\mathbf{i}} : \mathbf{l} \in \mathbb{N}^d, \mathbf{i} \in \rho(\mathbf{l})\}$ and classical SGs. In particular, given a design point $\mathbf{c}_{\mathbf{l}',\mathbf{i}'}$ on a classical SG, $\phi_{\mathbf{l},\mathbf{i}}(\mathbf{c}_{\mathbf{l}',\mathbf{i}'}) = 0$ for most of the pairs (\mathbf{l},\mathbf{i}) with $|\mathbf{l}| \geq |\mathbf{l}'|$. Since the notation is a bit involved, we use a one-dimensional example for illustration before presenting the formal statement.

Figure EC.1 The one-dimensional orthogonal basis $\{\phi_{l,i} : l \geq 1, 1 \leq i \leq 2^l - 1, i \text{ odd}\}$ associated with the TM kernel $k(x, x') = \exp(-5|x - x'|)$ on $(0,1)$.



Note. Left: $l = 1$; Middle: $l = 2$; Right: $l = 3$.

In Figure EC.1, we plot the first few functions of the orthogonal basis $\{\phi_{l,i}(x) : l \geq 1, 1 \leq i \leq 2^l - 1, i \text{ odd}\}$ associated with the TM kernel $k(x, x') = \exp(-5|x - x'|)$ on $[0,1]$. Recall that when $d = 1$, the classical SG of level τ is simply the one-dimensional dyadic grid $\{i \cdot 2^{-\tau} : 1 \leq i \leq 2^{-\tau} - 1\}$. For $\tau = 1$, $\mathcal{X}_1^{\text{SG}} = \{1/2\}$. It is straightforward to see that $\phi_{2,1}(1/2) = \phi_{2,3}(1/2) = 0$, and $\phi_{3,1}(1/2) = \phi_{3,3}(1/2) = \phi_{3,5}(1/2) = \phi_{3,7}(1/2) = 0$. Likewise, for $\tau = 2$, consider the design point $1/4 \in \mathcal{X}_2^{\text{SG}}$. Clearly,

$\phi_{3,i}(1/4) = 0$ for all $i = 1, 3, 5, 7$. In general, we have $\phi_{l,i}(\mathbf{c}_{\tau,i'}) = 0$ if $l > \tau$. This is because in this case, $\mathbf{c}_{\tau,i'}$ happens to be outside the support of $\phi_{l,i}$ by definition. We now present formally the general result regarding the function $\phi_{1,i}$ evaluated at design points on a classical SG.

LEMMA EC.3. *Consider the functions $\{\phi_{1,i} : \mathbf{l} \in \mathbb{N}^d, \mathbf{i} \in \rho(\mathbf{l})\}$ defined by (EC.1.2), and design points on a classical SG that are of the form $\mathbf{c}_{1,i} = (\mathbf{c}_{l_1,i_1}, \dots, \mathbf{c}_{l_d,i_d})$. Then,*

- (i) $\phi_{1,i}(\mathbf{c}_{1,i}) = 1$ for all $\mathbf{l} \in \mathbb{N}^d$ and $\mathbf{i} \in \rho(\mathbf{l})$;
- (ii) $\phi_{1,i}(\mathbf{c}_{1',i'}) = 0$ for all $\mathbf{l}, \mathbf{l}' \in \mathbb{N}^d$, $\mathbf{i} \in \rho(\mathbf{l})$, and $\mathbf{i}' \in \rho(\mathbf{l}')$ with $l_j > l'_j$ for some $j = 1, \dots, d$.
- (iii) $\phi_{1,i}(\mathbf{c}_{1',i'}) = 0$ for all $\mathbf{l}, \mathbf{l}' \in \mathbb{N}^d$, $\mathbf{i} \in \rho(\mathbf{l})$, and $\mathbf{i}' \in \rho(\mathbf{l}')$ with $\mathbf{l} = \mathbf{l}'$ and $\mathbf{i} \neq \mathbf{i}'$.

Proof of Lemma EC.3. These properties are essentially a result of the tensor structure and the nested structure of $\phi_{1,i}$'s and classical SGs.

Part (i). By the definition (EC.1.1), for each tuple (j, l, i) ,

$$\phi_{j,l,i}(\mathbf{c}_{l,i}) = \frac{p_j(\mathbf{c}_{l,i})\mathbf{q}_{j,l,i-1} - \mathbf{p}_{j,l,i-1}q_j(\mathbf{c}_{l,i})}{\mathbf{p}_{j,l,i}\mathbf{q}_{j,l,i-1} - \mathbf{p}_{j,l,i-1}q_{j,l,i}} = 1,$$

since $p_j(\mathbf{c}_{l,i}) = \mathbf{p}_{j,l,i}$ and $q_j(\mathbf{c}_{l,i}) = \mathbf{q}_{j,l,i}$. Hence, $\phi_{1,i}(\mathbf{c}_{1,i}) = \prod_{j=1}^d \phi_{j,l_j,i_j}(\mathbf{c}_{l_j,i_j}) = 1$.

Part (ii). Without loss of generality, assume $j = 1$, i.e., $l_1 > l'_1$. Note that $\mathbf{c}'_{l'_1,i'_1} = i'_1 \cdot 2^{-l'_1} = (i'_1 \cdot 2^{l_1-l'_1}) \cdot 2^{-l_1}$. Since i'_1 is an odd number between 1 and $2^{l'_1} - 1$, we know that $i'_1 \cdot 2^{l_1-l'_1}$ is an even number between $2^{l_1-l'_1}$ and $2^{l_1} - 2^{l_1-l'_1}$. Hence, there does not exist an odd number i_1 between 1 and $2^{l_1} - 1$ such that $i_1 - 1 < i'_1 \cdot 2^{l_1-l'_1} < i_1 + 1$. This implies that

$$\mathbf{c}'_{l'_1,i'_1} = (i'_1 \cdot 2^{l_1-l'_1}) \cdot 2^{-l_1} \notin ((i_1 - 1) \cdot 2^{-l_1}, (i_1 + 1) \cdot 2^{-l_1}),$$

for any odd number i_1 between 1 and $2^{l_1} - 1$. It follows that $\phi_{1,l_1,i_1}(\mathbf{c}_{l_1,i_1}) = 0$, since the support of ϕ_{1,l_1,i_1} is $((i_1 - 1) \cdot 2^{-l_1}, (i_1 + 1) \cdot 2^{-l_1})$. Therefore, $\phi_{1,i}(\mathbf{c}_{1',i'}) = \phi_{1,l_1,i_1}(\mathbf{c}'_{l'_1,i'_1}) \cdot \prod_{j=2}^d \phi_{j,l_j,i_j}(\mathbf{c}'_{l'_j,i'_j}) = 0$.

Part (iii). Since $\mathbf{i} \neq \mathbf{i}'$, there must exist j such that $i_j \neq i'_j$. Without loss of generality, assume $j = 1$. Note that $l_1 = l'_1$, so i'_1 is an odd number between 1 and $2^{l_1} - 1$. It follows that $i'_1 \notin (i_1 - 1, i_1 + 1)$, the only odd number in the open interval is i_1 , which is not i'_1 . Thus, $\mathbf{c}'_{l'_1,i'_1} = i'_1 \cdot 2^{-l'_1} = i'_1 \cdot 2^{-l_1}$ does not belong to $((i_1 - 1) \cdot 2^{-l_1}, (i_1 + 1) \cdot 2^{-l_1})$, the support of ϕ_{j,l_j,i_j} . Hence, $\phi_{1,i}(\mathbf{c}_{1',i'}) = \phi_{1,l_1,i_1}(\mathbf{c}'_{l'_1,i'_1}) \cdot \prod_{j=2}^d \phi_{j,l_j,i_j}(\mathbf{c}'_{l'_j,i'_j}) = 0$. \square

At last, we show that the orthogonal basis $\{\phi_{1,i} : \mathbf{l} \in \mathbb{N}^d, \mathbf{i} \in \rho(\mathbf{l})\}$ associated with the TM kernel k induces an expansion of the TMGP with the same kernel in terms of i.i.d. standard normal random variables. This is an immediate consequence of Theorems 3.1.1 and 3.1.2 in Adler and Taylor (2009).

LEMMA EC.4. *Let $\{Y(\mathbf{x}) : \mathbf{x} \in (0, 1)^d\}$ be a mean zero TMGP with kernel k that satisfies Assumption 1. Let $\{\phi_{1,i} : \mathbf{l} \in \mathbb{N}^d, \mathbf{i} \in \rho(\mathbf{l})\}$ be the orthogonal basis defined by (EC.1.2) for \mathcal{H}_k . Then,*

$$Y(\mathbf{x}) = \sum_{\mathbf{l} \in \mathbb{N}^d} \sum_{\mathbf{i} \in \rho(\mathbf{l})} \frac{\phi_{1,i}(\mathbf{x})}{\|\phi_{1,i}\|_{\mathcal{H}_k}} Z_{1,i}, \quad (\text{EC.1.12})$$

where $Z_{\mathbf{l},\mathbf{i}}$'s are i.i.d. standard normal variables, and the sum converges almost surely and the convergence is uniform over $x \in (0,1)^d$.

We can apply Lemmas EC.3 and EC.4 to express $Y(\mathbf{c}_{\mathbf{l},\mathbf{i}})$ as a linear combination of a *finite* set of i.i.d normal random variables.

LEMMA EC.5. *Let $\{Y(\mathbf{x}) : \mathbf{x} \in (0,1)^d\}$ be a mean zero TMGP with kernel k that satisfies Assumption 1. Let $\{\phi_{\mathbf{l},\mathbf{i}} : \mathbf{l} \in \mathbb{N}^d, \mathbf{i} \in \rho(\mathbf{l})\}$ be the orthogonal basis defined by (EC.1.2) for \mathcal{H}_k . Then,*

$$Y(\mathbf{c}_{\mathbf{l}',\mathbf{i}'}) = \sum_{|\mathbf{l}| \leq \tau+d-1} \sum_{\mathbf{i} \in \rho(\mathbf{l})} \frac{\phi_{\mathbf{l},\mathbf{i}}(\mathbf{c}_{\mathbf{l}',\mathbf{i}'})}{\|\phi_{\mathbf{l},\mathbf{i}}\|_{\mathcal{H}_k}} Z_{\mathbf{l},\mathbf{i}} + \frac{1}{\|\phi_{\mathbf{l}',\mathbf{i}'}\|_{\mathcal{H}_k}} Z_{\mathbf{l}',\mathbf{i}'}, \quad (\text{EC.1.13})$$

for all $\mathbf{c}_{\mathbf{l}',\mathbf{i}'} \in \mathcal{D}_{\tau+1} = \mathcal{X}_{\tau+1}^{\text{SG}} \setminus \mathcal{X}_{\tau}^{\text{SG}}$, where $Z_{\mathbf{l},\mathbf{i}}$'s are i.i.d. standard normal variables.

Proof of Lemma EC.5. By the definition of classical SGs, particularly the formula (13), we know that $|\mathbf{l}'| = \tau + d$ if $\mathbf{c}_{\mathbf{l}',\mathbf{i}'} \in \mathcal{D}_{\tau+1}$. Hence, if $|\mathbf{l}| \geq \tau + d + 1$, then there must exist j such that $l_j > l'_j$, and thus $\phi_{\mathbf{l},\mathbf{i}}(\mathbf{c}_{\mathbf{l}',\mathbf{i}'}) = 0$ by part (ii) of Lemma EC.3. In addition, it follows from part (ii) and part (iii) of Lemma EC.3 that for all \mathbf{l} such that $|\mathbf{l}| = |\mathbf{l}'|$, $\phi_{\mathbf{l},\mathbf{i}}(\mathbf{c}_{\mathbf{l}',\mathbf{i}'}) = 0$ unless $(\mathbf{l}, \mathbf{i}) = (\mathbf{l}', \mathbf{i}')$. Consequently, all the terms in the expansion (EC.1.12) with $|\mathbf{l}| \geq |\mathbf{l}'|$ are zero except for $(\mathbf{l}, \mathbf{i}) = (\mathbf{l}', \mathbf{i}')$, yielding that

$$Y(\mathbf{c}_{\mathbf{l}',\mathbf{i}'}) = \sum_{|\mathbf{l}| \leq \tau+d-1} \sum_{\mathbf{i} \in \rho(\mathbf{l})} \frac{\phi_{\mathbf{l},\mathbf{i}}(\mathbf{c}_{\mathbf{l}',\mathbf{i}'})}{\|\phi_{\mathbf{l},\mathbf{i}}\|_{\mathcal{H}_k}} Z_{\mathbf{l},\mathbf{i}} + \frac{\phi_{\mathbf{l}',\mathbf{i}'}(\mathbf{c}_{\mathbf{l}',\mathbf{i}'})}{\|\phi_{\mathbf{l}',\mathbf{i}'}\|_{\mathcal{H}_k}} Z_{\mathbf{l}',\mathbf{i}'}.$$

Then, (EC.1.13) follows immediately from part (i) of Lemma EC.3. \square

Following Lemma EC.5, we show that given a TSG $\mathcal{X}_n^{\text{TSG}}$, observing $\{Y(\mathbf{c}_{\mathbf{l},\mathbf{i}}) : \mathbf{c}_{\mathbf{l},\mathbf{i}} \in \mathcal{X}_n^{\text{TSG}}\}$ is equivalent to observing $\{Z_{\mathbf{l},\mathbf{i}} : \mathbf{c}_{\mathbf{l},\mathbf{i}} \in \mathcal{X}_n^{\text{TSG}}\}$.

LEMMA EC.6. *Let $\{Y(\mathbf{x}) : \mathbf{x} \in (0,1)^d\}$ be a mean zero TMGP with kernel k that satisfies Assumption 1. Consider the expansion (EC.1.12). Then,*

$$\varsigma(Y(\mathbf{c}_{\mathbf{l},\mathbf{i}}) : \mathbf{c}_{\mathbf{l},\mathbf{i}} \in \mathcal{X}_n^{\text{TSG}}) = \varsigma(Z_{\mathbf{l},\mathbf{i}} : \mathbf{c}_{\mathbf{l},\mathbf{i}} \in \mathcal{X}_n^{\text{TSG}}), \quad (\text{EC.1.14})$$

for all $n \geq 1$, where $\varsigma(\mathcal{S})$ denotes the sigma-algebra generated by \mathcal{S} .

Proof of Lemma EC.6. We first prove a weaker result as follows,

$$\varsigma(Y(\mathbf{c}_{\mathbf{l},\mathbf{i}}) : \mathbf{c}_{\mathbf{l},\mathbf{i}} \in \mathcal{X}_{\tau}^{\text{SG}}) = \varsigma(Z_{\mathbf{l},\mathbf{i}} : \mathbf{c}_{\mathbf{l},\mathbf{i}} \in \mathcal{X}_{\tau}^{\text{SG}}), \quad (\text{EC.1.15})$$

for all $\tau \geq 1$. We do so by induction on τ . If $\tau = 1$, then $\mathcal{X}_{\tau}^{\text{SG}} = \{\mathbf{c}_{\bar{\mathbf{l}},\bar{\mathbf{l}}}\}$, where $\bar{\mathbf{l}}$ is the d -dimensional vector of ones. Thus, by (EC.1.13), $Z_{\bar{\mathbf{l}},\bar{\mathbf{l}}} = \|\phi_{\bar{\mathbf{l}},\bar{\mathbf{l}}}\|_{\mathcal{H}_k} Y(\mathbf{c}_{\bar{\mathbf{l}},\bar{\mathbf{l}}})$, so (EC.1.15) follows immediately.

Assume that (EC.1.15) holds for some $\tau \geq 1$. That is, $\{Z_{\mathbf{l},\mathbf{i}} : \mathbf{c}_{\mathbf{l},\mathbf{i}} \in \mathcal{X}_{\tau}^{\text{SG}}\}$ are uniquely determined by $\{Y(\mathbf{c}_{\mathbf{l},\mathbf{i}}) : \mathbf{c}_{\mathbf{l},\mathbf{i}} \in \mathcal{X}_{\tau}^{\text{SG}}\}$, and vice versa. By (EC.1.13),

$$Z_{\mathbf{l}',\mathbf{i}'} = \|\phi_{\mathbf{l}',\mathbf{i}'}\|_{\mathcal{H}_k} \left[Y(\mathbf{c}_{\mathbf{l}',\mathbf{i}'}) - \sum_{(\mathbf{l},\mathbf{i}) : \mathbf{c}_{\mathbf{l},\mathbf{i}} \in \mathcal{X}_{\tau}^{\text{SG}}} \frac{\phi_{\mathbf{l},\mathbf{i}}(\mathbf{c}_{\mathbf{l}',\mathbf{i}'})}{\|\phi_{\mathbf{l},\mathbf{i}}\|_{\mathcal{H}_k}} Z_{\mathbf{l},\mathbf{i}} \right], \quad (\text{EC.1.16})$$

for all $\mathbf{c}_{l',i'} \in \mathcal{X}_{\tau+1}^{\text{SG}} \setminus \mathcal{X}_{\tau}^{\text{SG}}$. Hence, $\{Z_{l,i} : \mathbf{c}_{l,i} \in \mathcal{X}_{\tau+1}^{\text{SG}}\}$ are uniquely determined by $\{Y(\mathbf{c}_{l,i}) : \mathbf{c}_{l,i} \in \mathcal{X}_{\tau+1}^{\text{SG}}\}$, and vice versa, completing the induction. So, (EC.1.15) holds for all $\tau \geq 1$.

To prove (EC.1.14), let τ be such that $\mathcal{X}_{\tau}^{\text{SG}} \subseteq \mathcal{X}_n^{\text{TSG}} \subset \mathcal{X}_{\tau+1}^{\text{SG}}$. It follows from (EC.1.13) and (EC.1.16) that for any $\mathcal{S} \subseteq \mathcal{X}_{\tau+1}^{\text{SG}} \setminus \mathcal{X}_{\tau}^{\text{SG}}$, $\{Z_{l,i} : \mathbf{c}_{l,i} \in \mathcal{X}_{\tau}^{\text{SG}} \cup \mathcal{S}\}$ are uniquely determined by $\{Y(\mathbf{c}_{l,i}) : \mathbf{c}_{l,i} \in \mathcal{X}_{\tau}^{\text{SG}} \cup \mathcal{S}\}$, and vice versa. Since $\mathcal{X}_n^{\text{TSG}} = \mathcal{X}_{\tau}^{\text{SG}} \cup \mathcal{A}_{\bar{n}}$ with $\mathcal{A}_{\bar{n}} \subset \mathcal{X}_{\tau+1}^{\text{SG}}$, we conclude that (EC.1.14) holds. \square

We now prove a general result regarding the conditional distribution of $Y(\cdot)$ given $\{Y(\mathbf{x}) : \mathbf{x} \in \mathcal{X}_n^{\text{TSG}}\}$. This result will be used later in convergence rate analysis and the kernel matrix inversion.

PROPOSITION EC.1. *Let $\{Y(\mathbf{x}) : \mathbf{x} \in (0,1)^d\}$ be a zero mean TMGP with kernel k that satisfies Assumption 1. Let $\{z_{l,i} : \mathbf{c}_{l,i} \in \mathcal{X}_n^{\text{TSG}}\}$ denote the realization of $Z_{l,i}$'s that are uniquely determined by observations of $\{Y(\mathbf{c}_{l,i}) : \mathbf{c}_{l,i} \in \mathcal{X}_n^{\text{TSG}}\}$ via (EC.1.16). Then, conditioning on $\{Y(\mathbf{c}_{l,i}) : \mathbf{c}_{l,i} \in \mathcal{X}_n^{\text{TSG}}\}$, $Y(\cdot)$ is a GP with mean function μ_n^{TSG} and kernel function k_n^{TSG} as follows,*

$$\mu_n^{\text{TSG}}(\mathbf{x}') = \sum_{(l,i) : \mathbf{c}_{l,i} \in \mathcal{X}_n^{\text{TSG}}} \frac{\phi_{l,i}(\mathbf{x}')}{\|\phi_{l,i}\|_{\mathcal{H}_k}} z_{l,i}, \quad (\text{EC.1.17})$$

$$k_n^{\text{TSG}}(\mathbf{x}', \mathbf{x}'') = \sum_{(l,i) : l \in \mathbb{N}^d, i \in \rho(l), \mathbf{c}_{l,i} \notin \mathcal{X}_n^{\text{TSG}}} \frac{\phi_{l,i}(\mathbf{x}') \phi_{l,i}(\mathbf{x}'')}{\|\phi_{l,i}\|_{\mathcal{H}_k}^2}, \quad (\text{EC.1.18})$$

for all $\mathbf{x}', \mathbf{x}'' \in (0,1)^d$.

Proof of Proposition EC.1. Note that conditioning on $\{Y(\mathbf{x}) : \mathbf{x} \in \mathcal{X}_n^{\text{TSG}}\}$,

$$Y(\mathbf{x}') = \sum_{(l,i) : \mathbf{c}_{l,i} \in \mathcal{X}_n^{\text{TSG}}} \frac{\phi_{l,i}(\mathbf{x}')}{\|\phi_{l,i}\|_{\mathcal{H}_k}} z_{l,i} + \sum_{(l,i) : l \in \mathbb{N}^d, i \in \rho(l), \mathbf{c}_{l,i} \notin \mathcal{X}_n^{\text{TSG}}} \frac{\phi_{l,i}(\mathbf{x}')}{\|\phi_{l,i}\|_{\mathcal{H}_k}} Z_{l,i}, \quad (\text{EC.1.19})$$

by (EC.1.12) and (EC.1.14). It is straightforward to see that $\mu_n^{\text{TSG}}(\mathbf{x}') = \mathbb{E}[Y(\mathbf{x}') | Y(\mathbf{x}) : \mathbf{x} \in \mathcal{X}_n^{\text{TSG}}]$ is given by (EC.1.17). Moreover, $k_n^{\text{TSG}}(\mathbf{x}', \mathbf{x}'') = \text{Cov}[Y(\mathbf{x}'), Y(\mathbf{x}'') | Y(\mathbf{x}) : \mathbf{x} \in \mathcal{X}_n^{\text{TSG}}]$ equals

$$\begin{aligned} & \mathbb{E} \left[\left(\sum_{(l,i) : l \in \mathbb{N}^d, i \in \rho(l), \mathbf{c}_{l,i} \notin \mathcal{X}_n^{\text{TSG}}} \frac{\phi_{l,i}(\mathbf{x}') Z_{l,i}}{\|\phi_{l,i}\|_{\mathcal{H}_k}} \right) \left(\sum_{(l,i) : l \in \mathbb{N}^d, i \in \rho(l), \mathbf{c}_{l,i} \notin \mathcal{X}_n^{\text{TSG}}} \frac{\phi_{l,i}(\mathbf{x}'') Z_{l,i}}{\|\phi_{l,i}\|_{\mathcal{H}_k}} \right) \right] \\ &= \sum_{(l,i) : l \in \mathbb{N}^d, i \in \rho(l), \mathbf{c}_{l,i} \notin \mathcal{X}_n^{\text{TSG}}} \frac{\phi_{l,i}(\mathbf{x}') \phi_{l,i}(\mathbf{x}'')}{\|\phi_{l,i}\|_{\mathcal{H}_k}^2}, \end{aligned}$$

proving (EC.1.18). \square

We further show that TMGPs possess a nice structure of conditional independence between observations at design points on $\mathcal{D}_{\tau+1}$.

PROPOSITION EC.2. *Let $\{Y(\mathbf{x}) : \mathbf{x} \in (0,1)^d\}$ be a zero mean TMGP with kernel k that satisfies Assumption 1. Consider a TSG $\mathcal{X}_n^{\text{TSG}} = \mathcal{X}_{\tau}^{\text{SG}} \cup \mathcal{A}_{\bar{n}}$. For all $\mathbf{x}', \mathbf{x}'' \in \mathcal{A}_{\bar{n}}$ with $\mathbf{x}' \neq \mathbf{x}''$, $Y(\mathbf{x}')$ and $Y(\mathbf{x}'')$ are conditionally independent given $\{Y(\mathbf{x}) : \mathbf{x} \in \mathcal{X}_n^{\text{TSG}} \setminus \{\mathbf{x}', \mathbf{x}''\}\}$. Moreover, for all $\mathbf{c}_{l,i} \in \mathcal{A}_{\bar{n}}$,*

$$\text{Var}[Y(\mathbf{c}_{l,i}) | Y(\mathbf{x}) : \mathbf{x} \in \mathcal{X}_n^{\text{TSG}} \setminus \{\mathbf{c}_{l,i}\}] = \|\phi_{l,i}\|_{\mathcal{H}_k}^{-2}. \quad (\text{EC.1.20})$$

Proof of Proposition EC.2. Fix arbitrary $\mathbf{c}_{l',i'}, \mathbf{c}_{l'',i''} \in \mathcal{A}_{\bar{n}}$ and assume that $(l', i') \neq (l'', i'')$. Let $\mathcal{X}_{n-2}^{\text{TSG}} := \mathcal{X}_n^{\text{TSG}} \setminus \{\mathbf{c}_{l',i'}, \mathbf{c}_{l'',i''}\}$. Since $\mathcal{X}_{n-2}^{\text{TSG}}$ is a TSG, it follows from Proposition EC.1, particularly (EC.1.18) therein, that

$$\text{Cov}[Y(\mathbf{c}_{l',i'}), Y(\mathbf{c}_{l'',i''}) | Y(\mathbf{x}), \mathbf{x} \in \mathcal{X}_{n-2}^{\text{TSG}}] = \sum_{(\mathbf{l}, \mathbf{i}): \mathbf{l} \in \mathbb{N}^d, \mathbf{i} \in \rho(\mathbf{l}), \mathbf{c}_{\mathbf{l}, \mathbf{i}} \notin \mathcal{X}_{n-2}^{\text{TSG}}} \frac{\phi_{\mathbf{l}, \mathbf{i}}(\mathbf{c}_{l',i'}) \phi_{\mathbf{l}, \mathbf{i}}(\mathbf{c}_{l'',i''})}{\|\phi_{\mathbf{l}, \mathbf{i}}\|_{\mathcal{H}_k}^2}.$$

Further, note that for any (\mathbf{l}, \mathbf{i}) such that $\mathbf{l} \in \mathbb{N}^d$, $\mathbf{i} \in \rho(\mathbf{l})$, and $(\mathbf{l}, \mathbf{i}) \notin \mathcal{X}_{n-2}^{\text{TSG}}$, it must satisfy one of the following conditions:

- (i) $(\mathbf{l}, \mathbf{i}) \in \mathcal{X}_{\tau+1}^{\text{SG}} \setminus \mathcal{X}_{\tau}^{\text{SG}}$, in which case $|\mathbf{l}| = |\mathbf{l}'| = |\mathbf{l}''| = \tau + d$;
- (ii) $(\mathbf{l}, \mathbf{i}) \in \mathcal{X}_{\tilde{\tau}}^{\text{SG}} \setminus \mathcal{X}_{\tau+1}^{\text{SG}}$ for some $\tilde{\tau} \geq \tau + 2$, in which case $|\mathbf{l}| \geq \tau + d + 1$.

In either case, we can invoke Lemma EC.3 to deduce that $\phi_{\mathbf{l}, \mathbf{i}}(l', i') = \phi_{\mathbf{l}, \mathbf{i}}(l'', i'') = 0$ unless $(\mathbf{l}, \mathbf{i}) \in \{(l', i'), (l'', i'')\}$. Therefore,

$$\text{Cov}[Y(\mathbf{c}_{l',i'}), Y(\mathbf{c}_{l'',i''}) | Y(\mathbf{x}), \mathbf{x} \in \mathcal{X}_{n-2}^{\text{TSG}}] = \sum_{(\mathbf{l}, \mathbf{i}) \in \{(l', i'), (l'', i'')\}} \frac{\phi_{\mathbf{l}, \mathbf{i}}(\mathbf{c}_{l',i'}) \phi_{\mathbf{l}, \mathbf{i}}(\mathbf{c}_{l'',i''})}{\|\phi_{\mathbf{l}, \mathbf{i}}\|_{\mathcal{H}_k}^2} = 0,$$

where the second equality can be easily seen from part (iii) of Lemma EC.3.

Likewise, we can calculate the conditional variance of $Y(\mathbf{c}_{l',i'})$. Let $\mathcal{X}_{n-1}^{\text{TSG}} := \mathcal{X}_n^{\text{TSG}} \setminus \{\mathbf{c}_{l',i'}\}$. Then,

$$\text{Var}[Y(\mathbf{c}_{l',i'}) | Y(\mathbf{x}) : \mathbf{x} \in \mathcal{X}_{n-1}^{\text{TSG}}] = \sum_{(\mathbf{l}, \mathbf{i}): \mathbf{l} \in \mathbb{N}^d, \mathbf{i} \in \rho(\mathbf{l}), \mathbf{c}_{\mathbf{l}, \mathbf{i}} \notin \mathcal{X}_{n-1}^{\text{TSG}}} \frac{\phi_{\mathbf{l}, \mathbf{i}}^2(\mathbf{c}_{l',i'})}{\|\phi_{\mathbf{l}, \mathbf{i}}\|_{\mathcal{H}_k}^2} = \frac{\phi_{l',i'}^2(\mathbf{c}_{l',i'})}{\|\phi_{l',i'}\|_{\mathcal{H}_k}^2} = \frac{1}{\|\phi_{l',i'}\|_{\mathcal{H}_k}^2}. \quad \square$$

EC.2. Convergence Rate Analysis for Deterministic Simulation

In this section, we analyze the convergence rates for the (deterministic) kriging predictor with TM kernels and TSG designs. Specifically, we prove Theorem 1, Proposition 2, and Theorem 2.

EC.2.1. Proof of Theorem 1

The proof consists of two main steps. First, we establish the convergence rate if the design points happen to form a classical SG $\mathcal{X}_{\tau}^{\text{SG}}$. Second, we generalize the result to the TSG $\mathcal{X}_n^{\text{TSG}}$, by studying the asymptotic difference between the MSE conditioned on $\mathcal{X}_{\tau}^{\text{SG}}$ and that on $\mathcal{X}_{\tau+1}^{\text{SG}}$, the two classical SGs of consecutive levels that enclose $\mathcal{X}_n^{\text{TSG}}$.

PROPOSITION EC.3. *Let $\{Y(\mathbf{x}) : \mathbf{x} \in (0, 1)^d\}$ be a zero mean TMGP with kernel k that satisfies Assumption 1. Suppose that the true response surface is a realization of Y , the simulation has no noise, and the design points $\{\mathbf{x}_1, \dots, \mathbf{x}_n\}$ form a classical SG. Let $\hat{Y}_n(\mathbf{x})$ be the kriging predictor with kernel k and the classical SG design. Then, as $n \rightarrow \infty$,*

$$\sup_{\mathbf{x} \in (0, 1)^d} \mathbb{E}[(\hat{Y}_n(\mathbf{x}) - Y(\mathbf{x}))^2] = \mathcal{O}(n^{-1}(\log n)^{2(d-1)}). \quad (\text{EC.2.1})$$

Proof of Proposition EC.3. In the absence of simulation noise, the MSE of $\hat{Y}_n(\mathbf{x})$ is simply the posterior variance of $Y(\mathbf{x})$ given the observations of Y on the classical SG $\mathcal{X}_\tau^{\text{SG}}$. It then follows from Proposition EC.1 that

$$\mathbb{E}[(\hat{Y}_n(\mathbf{x}) - Y(\mathbf{x}))^2] = \sum_{|\mathbf{l}| > \tau + d - 1} \sum_{\mathbf{i} \in \rho(\mathbf{l})} \frac{\phi_{\mathbf{l}, \mathbf{i}}^2(\mathbf{x})}{\|\phi_{\mathbf{l}, \mathbf{i}}\|_{\mathcal{H}_k}^2}. \quad (\text{EC.2.2})$$

Note that for a fixed \mathbf{l} , $\phi_{\mathbf{l}, \mathbf{i}}$'s have disjoint supports by definition, and they form a partition of the design space $(0, 1)^d$. Thus, there exists one and only one $\mathbf{i}^*(\mathbf{l})$ such that $\mathbf{x} \in \text{supp}(\phi_{\mathbf{l}, \mathbf{i}^*(\mathbf{l})})$, implying that $\phi_{\mathbf{l}, \mathbf{i}^*(\mathbf{l})}(\mathbf{x}) = 0$ for all $\mathbf{i} \neq \mathbf{i}^*(\mathbf{l})$. Hence, by (EC.2.2),

$$\sup_{\mathbf{x} \in (0, 1)^d} \mathbb{E}[(\hat{Y}_n(\mathbf{x}) - Y(\mathbf{x}))^2] = \sup_{\mathbf{x} \in (0, 1)^d} \sum_{|\mathbf{l}| > \tau + d - 1} \frac{\phi_{\mathbf{l}, \mathbf{i}^*(\mathbf{l})}^2(\mathbf{x})}{\|\phi_{\mathbf{l}, \mathbf{i}^*(\mathbf{l})}\|_{\mathcal{H}_k}^2} \leq \sum_{|\mathbf{l}| > \tau + d - 1} \frac{1}{\|\phi_{\mathbf{l}, \mathbf{i}^*(\mathbf{l})}\|_{\mathcal{H}_k}^2}, \quad (\text{EC.2.3})$$

where the inequality holds because $\phi_{\mathbf{l}, \mathbf{i}}(\mathbf{x}) \in [0, 1]$ for all (\mathbf{l}, \mathbf{i}) , which can be easily seen from its definition. We now apply Lemma EC.2 to obtain the following estimate,

$$\sum_{|\mathbf{l}| > \tau + d - 1} \frac{1}{\|\phi_{\mathbf{l}, \mathbf{i}^*(\mathbf{l})}\|_{\mathcal{H}_k}^2} \asymp \sum_{|\mathbf{l}| > \tau + d - 1} 2^{-|\mathbf{l}|} = \mathcal{O}(2^{-\tau} \tau^{d-1}), \quad (\text{EC.2.4})$$

where the last equality follows from Lemma 3.7 in Bungartz and Griebel (2004). At last, note that $n = |\mathcal{X}_\tau^{\text{SG}}| \asymp 2^\tau \tau^{d-1}$ by (14), so

$$\mathcal{O}(2^{-\tau} \tau^{d-1}) = \mathcal{O}(n^{-1} \tau^{2(d-1)}) = \mathcal{O}(n^{-1} (\log n)^{2(d-1)}). \quad (\text{EC.2.5})$$

We combine (EC.2.2)–(EC.2.5) to conclude that

$$\sup_{\mathbf{x} \in (0, 1)^d} \mathbb{E}[(\hat{Y}_n(\mathbf{x}) - Y(\mathbf{x}))^2] = \mathcal{O}(n^{-1} (\log n)^{2(d-1)}). \quad \square$$

Recall that classical SGs are not specified directly via the sample size n but via the level. We now relax this restriction and generalize Proposition EC.3 to Theorem 1. The key is to analyze the change in MSE between two classical SGs of consecutive levels.

Proof of Theorem 1. Fix an arbitrary $\mathbf{x}' \in (0, 1)^d$. By definition, $\mathcal{X}_\tau^{\text{SG}} \subseteq \mathcal{X}_n^{\text{TSG}} \subset \mathcal{X}_{\tau+1}^{\text{SG}}$. Hence,

$$\underbrace{\text{Var}[Y(\mathbf{x}') | Y(\mathbf{x}), \mathbf{x} \in \mathcal{X}_{\tau+1}^{\text{SG}}]}_{V(\mathbf{x}'; \mathcal{X}_{\tau+1}^{\text{SG}})} \leq \underbrace{\text{Var}[Y(\mathbf{x}') | Y(\mathbf{x}), \mathbf{x} \in \mathcal{X}_n^{\text{TSG}}]}_{V(\mathbf{x}'; \mathcal{X}_n^{\text{TSG}})} \leq \underbrace{\text{Var}[Y(\mathbf{x}') | Y(\mathbf{x}), \mathbf{x} \in \mathcal{X}_\tau^{\text{SG}}]}_{V(\mathbf{x}'; \mathcal{X}_\tau^{\text{SG}})}.$$

Now, we provide an upper bound on the difference between the conditional variances. Specifically, following Proposition EC.1,

$$V(\mathbf{x}'; \mathcal{X}_\tau^{\text{SG}}) - V(\mathbf{x}'; \mathcal{X}_{\tau+1}^{\text{SG}}) = \sum_{|\mathbf{l}| = \tau + d} \sum_{\mathbf{i} \in \rho(\mathbf{l})} \frac{\phi_{\mathbf{l}, \mathbf{i}}^2(\mathbf{x}')}{\|\phi_{\mathbf{l}, \mathbf{i}}\|_{\mathcal{H}_k}^2} \leq \sum_{|\mathbf{l}| = \tau + d} \frac{1}{\|\phi_{\mathbf{l}, \mathbf{i}}\|_{\mathcal{H}_k}^2}, \quad (\text{EC.2.6})$$

where the inequality can be shown with an argument similar to that for (EC.2.3). By Lemma EC.2,

$$\sum_{|\mathbf{l}| = \tau + d} \frac{1}{\|\phi_{\mathbf{l}, \mathbf{i}}\|_{\mathcal{H}_k}^2} \asymp \sum_{|\mathbf{l}| = \tau + d} 2^{-|\mathbf{l}|} = 2^{-(\tau + d)} \binom{\tau + d - 1}{d - 1} = \mathcal{O}(2^{-\tau} \tau^{d-1}), \quad (\text{EC.2.7})$$

where the last step can be shown via Stirling's approximation for factorials. Therefore, combining (EC.2.9) and (EC.2.6) yields

$$V(\mathbf{x}'; \mathcal{X}_n^{\text{TSG}}) - V(\mathbf{x}'; \mathcal{X}_{\tau+1}^{\text{SG}}) \leq V(\mathbf{x}'; \mathcal{X}_\tau^{\text{SG}}) - V(\mathbf{x}'; \mathcal{X}_{\tau+1}^{\text{SG}}) = \mathcal{O}(2^{-\tau} \tau^{d-1}).$$

Moreover, we know from the proof of Proposition EC.3, particularly (EC.2.2)–(EC.2.4), that $V(\mathbf{x}'; \mathcal{X}_{\tau+1}^{\text{SG}}) = \mathcal{O}(2^{-(\tau+1)}(\tau+1)^{d-1})$. Hence,

$$V(\mathbf{x}'; \mathcal{X}_n^{\text{TSG}}) = \mathcal{O}(2^{-\tau} \tau^{d-1}) + \mathcal{O}(2^{-(\tau+1)}(\tau+1)^{d-1}) = \mathcal{O}(2^{-\tau} \tau^{d-1}) = \mathcal{O}(n^{-1}(\log n)^{2(d-1)}).$$

Note that by (EC.2.6), the upper bound is independent of \mathbf{x}' . Hence,

$$\sup_{\mathbf{x} \in (0,1)^d} \mathbb{E}[(\hat{Y}_n(\mathbf{x}) - Y(\mathbf{x}))^2] = \sup_{\mathbf{x} \in (0,1)^d} V(\mathbf{x}; \mathcal{X}_n^{\text{TSG}}) = \mathcal{O}(n^{-1}(\log n)^{2(d-1)}). \quad \square$$

EC.2.2. Proof of Proposition 2

Proof of Proposition 2. Let $\mathcal{X}_\tau^{\text{FG}} = \times_{j=1}^d \mathcal{X}_{j,\tau}$ denote the full grid (i.e., lattice) of level τ . Note that $\mathcal{X}_\tau^{\text{FG}}$ can be expressed as

$$\mathcal{X}_\tau^{\text{FG}} = \bigcup_{\|\mathbf{l}\|_\infty \leq \tau} \{\mathbf{c}_{\mathbf{l},\mathbf{i}} : \mathbf{i} \in \rho(\mathbf{l})\},$$

where $\|\mathbf{l}\|_\infty = \max(l_1, \dots, l_d)$. Then, following the expansion (EC.1.12) and a proof similar to that of Proposition EC.2, it can be shown that the conditional variance of $Y(\mathbf{x})$ given the observations of Y on the full grid $\mathcal{X}_\tau^{\text{FG}}$ is given by

$$\mathbb{E}[(\hat{Y}_n(\mathbf{x}) - Y(\mathbf{x}))^2] = \sum_{\|\mathbf{l}\|_\infty > \tau} \sum_{\mathbf{i} \in \rho(\mathbf{l})} \frac{\phi_{\mathbf{l},\mathbf{i}}^2(\mathbf{x})}{\|\phi_{\mathbf{l},\mathbf{i}}\|_{\mathcal{H}_k}^2}, \quad (\text{EC.2.8})$$

for all $\mathbf{x} \in (0,1)^d$.

We fix an $\tilde{\mathbf{x}} \notin \mathcal{X}_\tau^{\text{FG}}$. Let $\tilde{\mathbf{l}} = (\tau+1, 1, \dots, 1)$ and $\tilde{\mathbf{i}}$ be the index such that $\tilde{\mathbf{x}} \in \text{supp}(\phi_{\tilde{\mathbf{l}},\tilde{\mathbf{i}}})$. Then, $\|\tilde{\mathbf{l}}\|_\infty = \tau+1$, $|\tilde{\mathbf{l}}| = \tau+d$, and $\phi_{\tilde{\mathbf{l}},\tilde{\mathbf{i}}}(\tilde{\mathbf{x}}) > 0$. Hence, by (EC.2.8),

$$\sup_{\mathbf{x} \in (0,1)^d} \mathbb{E}[(\hat{Y}_n(\mathbf{x}) - Y(\mathbf{x}))^2] \geq \mathbb{E}[(\hat{Y}_n(\tilde{\mathbf{x}}) - Y(\tilde{\mathbf{x}}))^2] \geq \frac{\phi_{\tilde{\mathbf{l}},\tilde{\mathbf{i}}}^2(\tilde{\mathbf{x}})}{\|\phi_{\tilde{\mathbf{l}},\tilde{\mathbf{i}}}\|_{\mathcal{H}_k}^2} \asymp \phi_{\tilde{\mathbf{l}},\tilde{\mathbf{i}}}^2(\tilde{\mathbf{x}}) \cdot 2^{-|\tilde{\mathbf{l}}|} = \phi_{\tilde{\mathbf{l}},\tilde{\mathbf{i}}}^2(\tilde{\mathbf{x}}) \cdot 2^{-(\tau+d)}, \quad (\text{EC.2.9})$$

where the asymptotic equivalence follows from Lemma EC.2. At last, note that $n = |\mathcal{X}_\tau^{\text{FG}}| = (2^\tau - 1)^d \asymp 2^{\tau d}$, so $2^\tau \asymp n^{1/d}$ as $n \rightarrow \infty$. Hence, the proof is completed by using (EC.2.9). \square

EC.2.3. Proof of Theorem 2

To simplify the notation, for each n we define an operator \mathcal{P}_n that takes effect on a function $f : (0,1)^d \mapsto \mathbb{R}$ as follows,

$$(\mathcal{P}_n f)(\mathbf{x}) := \mathbf{k}^\top(\mathbf{x}) \mathbf{K}^{-1} \mathbf{f}, \quad (\text{EC.2.10})$$

where $\mathbf{k}(\cdot) = (k(\mathbf{x}_1, \cdot), \dots, k(\mathbf{x}_n, \cdot))^\top$, $\mathbf{f} = (f(\mathbf{x}_1), \dots, f(\mathbf{x}_n))^\top$.

We also define an operator $\mathcal{L}_{\mathbf{x}}$ that take effect on a function $f(\mathbf{x}, \tilde{\mathbf{x}}) : (0, 1)^d \times (0, 1)^d \rightarrow \mathbb{R}$ as follows,

$$(\mathcal{L}_{\mathbf{x}}f(\cdot, \tilde{\mathbf{x}}))(\mathbf{x}) := (\mathcal{L}_{1,x_1} \cdots \mathcal{L}_{d,x_d}f(\cdot, \tilde{\mathbf{x}}))(\mathbf{x}), \quad (\text{EC.2.11})$$

where \mathcal{L}_{j,x_j} is the differential operator \mathcal{L}_j , defined in (6), acting on the j -th variable x_j of \mathbf{x} , i.e.,

$$(\mathcal{L}_{j,x_j}f(\cdot, \tilde{\mathbf{x}}))(\mathbf{x}) = \left(\frac{d}{dx_j} u_j(x_j) \frac{d}{dx_j} + v_j(x_j) f(\cdot, \tilde{\mathbf{x}}) \right)(\mathbf{x}).$$

Proof of Theorem 2. Note that the misspecified kriging predictor $\hat{Y}_n^{\text{mis}}(\mathbf{x}) = (\mathcal{P}_n Y^*)(\mathbf{x})$, so

$$\begin{aligned} & \mathbb{E}[(Y^*(\mathbf{x}) - (\mathcal{P}_n Y^*)(\mathbf{x}))^2] \\ &= \underbrace{\mathbb{E}[(Y^*(\mathbf{x}))^2 - Y^*(\mathbf{x})(\mathcal{P}_n Y^*)(\mathbf{x})]}_{I_1(\mathbf{x})} - \underbrace{\mathbb{E}[Y^*(\mathbf{x})(\mathcal{P}_n Y^*)(\mathbf{x}) - ((\mathcal{P}_n Y^*)(\mathbf{x}))^2]}_{I_2(\mathbf{x})}. \end{aligned} \quad (\text{EC.2.12})$$

We first consider $I_1(\mathbf{x})$. Note that $\mathbb{E}[(Y^*(\mathbf{x}))^2] = \text{Var}[Y^*(\mathbf{x})] = k^*(\mathbf{x}, \mathbf{x})$, since Y^* is a zero mean GP with kernel k^* ; moreover,

$$\begin{aligned} \mathbb{E}[Y^*(\mathbf{x})(\mathcal{P}_n Y^*)(\mathbf{x})] &= \mathbb{E}[\mathbf{k}^\top(\mathbf{x}) \mathbf{K}^{-1} (Y^*(\mathbf{x}_1), \dots, Y^*(\mathbf{x}_n))^\top Y^*(\mathbf{x})] \\ &= \mathbf{k}^\top(\mathbf{x}) \mathbf{K}^{-1} (k^*(\mathbf{x}_1, \mathbf{x}), \dots, k^*(\mathbf{x}_n, \mathbf{x}))^\top \\ &= (\mathcal{P}_n k^*(\cdot, \mathbf{x}))(\mathbf{x}). \end{aligned} \quad (\text{EC.2.13})$$

Since we assume that k^* has a product form with twice differentiable factor, we have that $k^* \in \mathcal{H}_k$.

For all $f \in \mathcal{H}_k$, note that $(\mathcal{P}_n f)(\cdot)$ can be expressed as a linear combination of $\{k(\mathbf{x}_i, \cdot) : i = 1, \dots, n\}$, so it lies in \mathcal{F}_n , the span of $\{k(\mathbf{x}_i, \cdot) : i = 1, \dots, n\}$. Since the design points $\{\mathbf{x}_1, \dots, \mathbf{x}_n\}$ form a TSG $\mathcal{X}_n^{\text{TSG}}$, by the orthogonal expansion (EC.1.3), \mathcal{F}_n is identical to \mathcal{G}_n , the span of $\{\phi_{1,i} : \mathbf{c}_{1,i} \in \mathcal{X}_n^{\text{TSG}}\}$. Thus, $(\mathcal{P}_n f)(\cdot) \in \mathcal{G}_n$, and it can decomposed as follows.

$$(\mathcal{P}_n f)(\cdot) = \sum_{(\mathbf{l}, \mathbf{i}) : \mathbf{c}_{1,i} \in \mathcal{X}_n^{\text{TSG}}} \frac{\langle \mathcal{P}_n f, \phi_{1,i} \rangle_{\mathcal{H}_k}}{\|\phi_{1,i}\|_{\mathcal{H}_k}^2} \phi_{1,i}(\cdot) = \sum_{(\mathbf{l}, \mathbf{i}) : \mathbf{c}_{1,i} \in \mathcal{X}_n^{\text{TSG}}} \frac{\langle f, \phi_{1,i} \rangle_{\mathcal{H}_k}}{\|\phi_{1,i}\|_{\mathcal{H}_k}^2} \phi_{1,i}(\cdot). \quad (\text{EC.2.14})$$

It follows from Lemma EC.1 and (EC.2.14) that for all $\mathbf{x}, \mathbf{x}' \in (0, 1)^d$,

$$\begin{aligned} & |k^*(\mathbf{x}, \mathbf{x}') - (\mathcal{P}_n k^*(\cdot, \mathbf{x}'))(\mathbf{x})| \\ &= \left| \sum_{(\mathbf{l}, \mathbf{i}) : \mathbf{l} \in \mathbb{N}^d, \mathbf{i} \in \rho(\mathbf{l})} \frac{\langle k^*(\cdot, \mathbf{x}'), \phi_{1,i} \rangle_{\mathcal{H}_k}}{\|\phi_{1,i}\|_{\mathcal{H}_k}^2} \phi_{1,i}(\mathbf{x}) - \sum_{(\mathbf{l}, \mathbf{i}) : \mathbf{c}_{1,i} \in \mathcal{X}_n^{\text{TSG}}} \frac{\langle k^*(\cdot, \mathbf{x}'), \phi_{1,i} \rangle_{\mathcal{H}_k}}{\|\phi_{1,i}\|_{\mathcal{H}_k}^2} \phi_{1,i}(\mathbf{x}) \right| \\ &\leq \sum_{(\mathbf{l}, \mathbf{i}) : \mathbf{l} \in \mathbb{N}^d, \mathbf{i} \in \rho(\mathbf{l}), \mathbf{c}_{1,i} \notin \mathcal{X}_n^{\text{TSG}}} \frac{|\langle k^*(\cdot, \mathbf{x}'), \phi_{1,i} \rangle_{\mathcal{H}_k}|}{\|\phi_{1,i}\|_{\mathcal{H}_k}^2} \phi_{1,i}(\mathbf{x}) \\ &\leq \sum_{|\mathbf{l}| > \tau + d - 1} \sum_{\mathbf{i} \in \rho(\mathbf{l})} \frac{|\langle k^*(\cdot, \mathbf{x}'), \phi_{1,i} \rangle_{\mathcal{H}_k}|}{\|\phi_{1,i}\|_{\mathcal{H}_k}^2} \phi_{1,i}(\mathbf{x}) \end{aligned}$$

$$\begin{aligned}
&= \sum_{|\mathbf{l}| > \tau + d - 1} \frac{|\langle k^*(\cdot, \mathbf{x}'), \phi_{\mathbf{l}, \mathbf{i}^*(\mathbf{l})} \rangle_{\mathcal{H}_k}|}{\|\phi_{\mathbf{l}, \mathbf{i}^*(\mathbf{l})}\|_{\mathcal{H}_k}^2} \phi_{\mathbf{l}, \mathbf{i}^*(\mathbf{l})}(\mathbf{x}) \\
&\leq \sum_{|\mathbf{l}| > \tau + d - 1} \frac{|\langle k^*(\cdot, \mathbf{x}'), \phi_{\mathbf{l}, \mathbf{i}^*(\mathbf{l})} \rangle_{\mathcal{H}_k}|}{\|\phi_{\mathbf{l}, \mathbf{i}^*(\mathbf{l})}\|_{\mathcal{H}_k}^2}, \tag{EC.2.15}
\end{aligned}$$

where the second inequality holds because $\mathcal{X}_n^{\text{TSG}} \supseteq \mathcal{X}_\tau^{\text{SG}} = \{\mathbf{c}_{\mathbf{l}, \mathbf{i}} : |\mathbf{l}| \leq \tau + d - 1, \mathbf{i} \in \rho(\mathbf{l})\}$; the last equality holds because given \mathbf{l} , there exists a unique $\mathbf{i}^*(\mathbf{l})$ such that $\mathbf{x}' \in \text{supp}(\phi_{\mathbf{l}, \mathbf{i}^*(\mathbf{l})})$, implying that $\phi_{\mathbf{l}, \mathbf{i}}(\mathbf{x}') = 0$ for all $\mathbf{i} \neq \mathbf{i}^*(\mathbf{l})$, since $\phi_{\mathbf{l}, \mathbf{i}}$'s have disjoint supports by definition, and they form a partition of the design space $(0, 1)^d$; the last inequality holds because $\phi_{\mathbf{l}, \mathbf{i}} \in [0, 1]$ by definition. In the following, we give an estimate of the inner product $\langle k^*(\cdot, \mathbf{x}'), \phi_{\mathbf{l}, \mathbf{i}} \rangle_{\mathcal{H}_k}$.

Since both k^* and $\phi_{\mathbf{l}, \mathbf{i}}$ are of product form, for all (\mathbf{l}, \mathbf{i}) and $\mathbf{x}' = (x'_1, \dots, x'_d) \in (0, 1)^d$,

$$\begin{aligned}
|\langle k^*(\cdot, \mathbf{x}'), \phi_{\mathbf{l}, \mathbf{i}} \rangle_{\mathcal{H}_k}| &= \left| \int_{(0, 1)^d} (\mathcal{L}_{\mathbf{x}} k^*(\cdot, \mathbf{x}'))(\mathbf{x}) \phi_{\mathbf{l}, \mathbf{i}}(\mathbf{x}) d\mathbf{x} \right| \\
&= \left| \prod_{j=1}^d \int_0^1 \phi_{l_j, i_j}(x_j) (\mathcal{L}_{j, x_j} k_j^*(\cdot, x'_j))(x_j) dx_j \right| \\
&\leq \prod_{j=1}^d \int_0^1 \phi_{l_j, i_j}(x) dx \cdot \sup_{x_j \in (0, 1)} \left| (\mathcal{L}_{j, x_j} k_j^*(\cdot, x'_j))(x_j) \right|. \tag{EC.2.16}
\end{aligned}$$

By the Cauchy–Schwarz inequality, for all $x'_j \in [0, 1]$,

$$\begin{aligned}
\sup_{x_j \in (0, 1)} |(\mathcal{L}_{j, x_j} k_j^*(\cdot, x'_j))(x_j)| &= \sup_{x_j \in (0, 1)} |\langle (\mathcal{L}_{j, x_j} k_j^*(\cdot, x'_j)), k(\cdot, x'_j) \rangle_{\mathcal{H}_k}| \\
&\leq \sup_{x'_j \in (0, 1)} \sqrt{k_j(x'_j, x'_j)} \cdot \sup_{x_j \in (0, 1)} \|(\mathcal{L}_{j, x_j} k_j^*(x_j, \cdot))\|_{\mathcal{H}_{k_j}} \\
&:= C_1 < \infty, \tag{EC.2.17}
\end{aligned}$$

where the last step holds because of Assumption 2.

Further, note that

$$\prod_{j=1}^d \int_0^1 \phi_{l_j, i_j}(x) dx \leq \prod_{j=1}^d \int_{(i-1) \cdot 2^{-l_j}}^{(i+1) \cdot 2^{-l_j}} dx = \prod_{j=1}^d 2^{-(l_j-1)} = 2^{d-|\mathbf{l}|}, \tag{EC.2.18}$$

since $\phi_{l_j, i_j} \in [0, 1]$ with support $((i-1) \cdot 2^{-l_j}, (i+1) \cdot 2^{-l_j})$.

Hence, by (EC.2.16), (EC.2.17), and (EC.2.18),

$$|\langle k^*(\cdot, \mathbf{x}'), \phi_{\mathbf{l}, \mathbf{i}} \rangle_{\mathcal{H}_k}| \leq C_1 2^{d-|\mathbf{l}|}, \tag{EC.2.19}$$

for all $\mathbf{x}' \in (0, 1)^d$. Applying (EC.2.15) and Lemma EC.2,

$$|k^*(\mathbf{x}, \mathbf{x}') - (\mathcal{P}_n k^*(\cdot, \mathbf{x}'))(\mathbf{x})| \leq \sum_{|\mathbf{l}| > \tau + d - 1} C_2 2^{d-2|\mathbf{l}|} \leq C_3 2^{-2\tau} \tau^{d-1} \leq C_4 n^{-2} (\log n)^{3(d-1)}, \tag{EC.2.20}$$

for all $\mathbf{x}, \mathbf{x}' \in (0, 1)^d$ and some constants $C_i > 0$, $i = 2, 3, 4$, where the second equality follows from Lemma 3.7 in Bungartz and Griebel (2004), while the last from an argument similar to (EC.2.5). By (EC.2.20),

$$|I_1(\mathbf{x})| = |k^*(\mathbf{x}, \mathbf{x}) - (\mathcal{P}_n k^*(\cdot, \mathbf{x}))(\mathbf{x})| \leq C_4 n^{-2} (\log n)^{3(d-1)}. \quad (\text{EC.2.21})$$

We now consider $I_2(\mathbf{x})$ in (EC.2.12). Let $h(\mathbf{x}, \mathbf{x}') := (\mathcal{P}_n k^*(\cdot, \mathbf{x}'))(\mathbf{x})$. Then,

$$h(\mathbf{x}, \mathbf{x}') - (\mathcal{P}_n h(\mathbf{x}', \cdot))(\mathbf{x}) = \left(\mathcal{P}_n (k^*(\cdot, \mathbf{x}') - h(\mathbf{x}', \cdot)) \right)(\mathbf{x}). \quad (\text{EC.2.22})$$

Applying (EC.2.14) to expand $k^*(\mathbf{x}, \mathbf{x}') - h(\mathbf{x}', \mathbf{x})$ as a function in the variable \mathbf{x} , and switching the order of summation and \mathcal{P}_n , (EC.2.22) then reads:

$$h(\mathbf{x}, \mathbf{x}') - (\mathcal{P}_n h(\mathbf{x}', \cdot))(\mathbf{x}) = \sum_{(\mathbf{l}, \mathbf{i}): \mathbf{l} \in \mathbb{N}^d, \mathbf{i} \in \rho(\mathbf{l}), \mathbf{c}_{\mathbf{l}, \mathbf{i}} \notin \mathcal{X}_n^{\text{TSG}}} \frac{\mathcal{P}_n (\langle k^*(\cdot, \cdot), \phi_{\mathbf{l}, \mathbf{i}} \rangle_{\mathcal{H}_k})(\mathbf{x})}{\|\phi_{\mathbf{l}, \mathbf{i}}\|_{\mathcal{H}_k}^2} \phi_{\mathbf{l}, \mathbf{i}}(\mathbf{x}'), \quad (\text{EC.2.23})$$

where

$$\begin{aligned} & \mathcal{P}_n (\langle k^*(\cdot, \cdot), \phi_{\mathbf{l}, \mathbf{i}} \rangle_{\mathcal{H}_k})(\mathbf{x}) \\ &= \mathcal{P}_n \left(\int_{(0,1)^d} \phi_{\mathbf{l}, \mathbf{i}}(\tilde{\mathbf{x}}) (\mathcal{L}_{\tilde{\mathbf{x}}} k^*(\cdot, \tilde{\mathbf{x}})) d\tilde{\mathbf{x}} \right)(\mathbf{x}) \\ &= \int_{(0,1)^d} \phi_{\mathbf{l}, \mathbf{i}}(\tilde{\mathbf{x}}) \mathcal{L}_{\tilde{\mathbf{x}}} \left(\mathcal{P}_n (k^*(\cdot, \tilde{\mathbf{x}}))(\mathbf{x}) \right) d\tilde{\mathbf{x}} \\ &= \int_{(0,1)^d} \phi_{\mathbf{l}, \mathbf{i}}(\tilde{\mathbf{x}}) \mathcal{L}_{\tilde{\mathbf{x}}} \left(\sum_{(\mathbf{l}', \mathbf{i}'): \mathbf{c}_{\mathbf{l}', \mathbf{i}'} \in \mathcal{X}_n^{\text{TSG}}} \frac{\langle k^*(\cdot, \tilde{\mathbf{x}}), \phi_{\mathbf{l}', \mathbf{i}'} \rangle_{\mathcal{H}_k}}{\|\phi_{\mathbf{l}', \mathbf{i}'}\|_{\mathcal{H}_k}^2} \phi_{\mathbf{l}', \mathbf{i}'}(\mathbf{x}) \right) d\tilde{\mathbf{x}} \\ &= \sum_{(\mathbf{l}', \mathbf{i}'): \mathbf{c}_{\mathbf{l}', \mathbf{i}'} \in \mathcal{X}_n^{\text{TSG}}} \frac{\phi_{\mathbf{l}', \mathbf{i}'}(\mathbf{x})}{\|\phi_{\mathbf{l}', \mathbf{i}'}\|_{\mathcal{H}_k}^2} \int_{(0,1)^d} \int_{(0,1)^d} \phi_{\mathbf{l}, \mathbf{i}}(\tilde{\mathbf{x}}) (\mathcal{L}_{\tilde{\mathbf{x}}} k^*(\mathbf{x}', \tilde{\mathbf{x}})) (\mathcal{L}_{\mathbf{x}'} \phi_{\mathbf{l}', \mathbf{i}'}(\mathbf{x}')) d\tilde{\mathbf{x}} d\mathbf{x}'. \end{aligned}$$

Therefore,

$$\begin{aligned} & |\mathcal{P}_n (\langle k^*(\cdot, \cdot), \phi_{\mathbf{l}, \mathbf{i}} \rangle_{\mathcal{H}_k})(\mathbf{x})| \\ & \leq \sum_{(\mathbf{l}', \mathbf{i}'): \mathbf{c}_{\mathbf{l}', \mathbf{i}'} \in \mathcal{X}_n^{\text{TSG}}} \frac{\phi_{\mathbf{l}', \mathbf{i}'}(\mathbf{x})}{\|\phi_{\mathbf{l}', \mathbf{i}'}\|_{\mathcal{H}_k}^2} \int_{(0,1)^d} \phi_{\mathbf{l}, \mathbf{i}}(\tilde{\mathbf{x}}) d\tilde{\mathbf{x}} \cdot \sup_{\tilde{\mathbf{x}} \in (0,1)^d} \left| \int_{(0,1)^d} (\mathcal{L}_{\tilde{\mathbf{x}}} k^*(\mathbf{x}', \tilde{\mathbf{x}})) (\mathcal{L}_{\mathbf{x}'} \phi_{\mathbf{l}', \mathbf{i}'}(\mathbf{x}')) d\mathbf{x}' \right| \\ &= \int_{(0,1)^d} \phi_{\mathbf{l}, \mathbf{i}}(\tilde{\mathbf{x}}) d\tilde{\mathbf{x}} \cdot \sum_{(\mathbf{l}', \mathbf{i}'): \mathbf{c}_{\mathbf{l}', \mathbf{i}'} \in \mathcal{X}_n^{\text{TSG}}} \frac{\phi_{\mathbf{l}', \mathbf{i}'}(\mathbf{x})}{\|\phi_{\mathbf{l}', \mathbf{i}'}\|_{\mathcal{H}_k}^2} \cdot \sup_{\tilde{\mathbf{x}} \in (0,1)^d} |\langle \mathcal{L}_{\tilde{\mathbf{x}}} k^*(\cdot, \tilde{\mathbf{x}}), \phi_{\mathbf{l}', \mathbf{i}'} \rangle_{\mathcal{H}_k}| \\ & \leq \int_{(0,1)^d} \phi_{\mathbf{l}, \mathbf{i}}(\tilde{\mathbf{x}}) d\tilde{\mathbf{x}} \cdot \sum_{(\mathbf{l}', \mathbf{i}'): \mathbf{c}_{\mathbf{l}', \mathbf{i}'} \in \mathcal{X}_n^{\text{TSG}}} \frac{\phi_{\mathbf{l}', \mathbf{i}'}(\mathbf{x})}{\|\phi_{\mathbf{l}', \mathbf{i}'}\|_{\mathcal{H}_k}^2} \cdot \sup_{\tilde{\mathbf{x}} \in (0,1)^d} \|\mathcal{L}_{\tilde{\mathbf{x}}} k^*(\cdot, \tilde{\mathbf{x}})\|_{\mathcal{H}_k}, \quad (\text{EC.2.24}) \end{aligned}$$

where the last inequality follows from the Cauchy-Schwarz inequality.

By Assumption 2,

$$C_5 := \sup_{\tilde{\mathbf{x}} \in (0,1)^d} \|(\mathcal{L}_{\tilde{\mathbf{x}}} k^*(\cdot, \tilde{\mathbf{x}}))\|_{\mathcal{H}_k} = \prod_{j=1}^d \|(\mathcal{L}_{j, \tilde{x}_j} k_j^*(\cdot, \tilde{x}_j))\|_{\mathcal{H}_{k_j}} < \infty. \quad (\text{EC.2.25})$$

Moreover, applying Lemma EC.2, we have

$$\begin{aligned}
\sum_{(\mathbf{l}', \mathbf{i}'): \mathbf{c}_{\mathbf{l}', \mathbf{i}'} \in \mathcal{X}_n^{\text{TSG}}} \frac{\phi_{\mathbf{l}', \mathbf{i}'}(\mathbf{x})}{\|\phi_{\mathbf{l}', \mathbf{i}'}\|_{\mathcal{H}_k}} &\leq \sum_{|\mathbf{l}'| \geq d} \sum_{\mathbf{i}' \in \rho(\mathbf{l}')} \frac{\phi_{\mathbf{l}', \mathbf{i}'}(\mathbf{x})}{\|\phi_{\mathbf{l}', \mathbf{i}'}\|_{\mathcal{H}_k}} \\
&= \sum_{|\mathbf{l}'| \geq d} \frac{\phi_{\mathbf{l}', \mathbf{i}^*(\mathbf{l}')}(\mathbf{x})}{\|\phi_{\mathbf{l}', \mathbf{i}^*(\mathbf{l}')} \|_{\mathcal{H}_k}} \\
&\leq C_6 \sum_{|\mathbf{l}'| \geq d} 2^{-|\mathbf{l}'|/2} := C_7 < \infty,
\end{aligned} \tag{EC.2.26}$$

for some constant $C_6 > 0$, where $\mathbf{i}^*(\mathbf{l}')$ is the unique index in $\rho(\mathbf{l}')$ for which $\mathbf{x} \in \text{supp}(\phi_{\mathbf{l}', \mathbf{i}^*(\mathbf{l}')})$, and the last step follows from Lemma 3.7 in Bungartz and Griebel (2004).

Combining (EC.2.18), (EC.2.24), (EC.2.25), and (EC.2.26) yields

$$|\mathcal{P}_n(\langle k^*(\cdot, \cdot), \phi_{\mathbf{l}, \mathbf{i}} \rangle_{\mathcal{H}_k})(\mathbf{x})| \leq C_5 C_7 2^{d-|\mathbf{l}|},$$

for all $\mathbf{x} \in (0, 1)^d$. It then follows from (EC.2.23) that

$$\begin{aligned}
|h(\mathbf{x}, \mathbf{x}') - (\mathcal{P}_n h(\mathbf{x}', \cdot))(\mathbf{x})| &\leq \sum_{(\mathbf{l}, \mathbf{i}): \mathbf{l} \in \mathbb{N}^d, \mathbf{i} \in \rho(\mathbf{l}), \mathbf{c}_{\mathbf{l}, \mathbf{i}} \notin \mathcal{X}_n^{\text{TSG}}} C_5 C_7 2^{d-|\mathbf{l}|} \frac{\phi_{\mathbf{l}, \mathbf{i}}(\mathbf{x}')}{\|\phi_{\mathbf{l}, \mathbf{i}}\|_{\mathcal{H}_k}^2} \\
&\leq \sum_{|\mathbf{l}| > \tau + d - 1} \sum_{\mathbf{i} \in \rho(\mathbf{l})} C_5 C_7 2^{d-|\mathbf{l}|} \frac{\phi_{\mathbf{l}, \mathbf{i}}(\mathbf{x}')}{\|\phi_{\mathbf{l}, \mathbf{i}}\|_{\mathcal{H}_k}^2} \\
&= \sum_{|\mathbf{l}| > \tau + d - 1} C_5 C_7 2^{d-|\mathbf{l}|} \frac{\phi_{\mathbf{l}, \mathbf{i}^*(\mathbf{l})}(\mathbf{x}')}{\|\phi_{\mathbf{l}, \mathbf{i}^*(\mathbf{l})}\|_{\mathcal{H}_k}^2} \\
&\leq \sum_{|\mathbf{l}| > \tau + d - 1} C_8 2^{d-2|\mathbf{l}|} \\
&\leq C_9 n^{-2} (\log n)^{3(d-1)},
\end{aligned}$$

for some positive constants C_8 and C_9 , where $\mathbf{i}^*(\mathbf{l})$ is the unique index in $\rho(\mathbf{l})$ for which $\mathbf{x}' \in \text{supp}(\phi_{\mathbf{l}, \mathbf{i}^*(\mathbf{l})})$, and the last step follows an argument similar to (EC.2.20). Hence,

$$\sup_{\mathbf{x} \in (0, 1)^d} |h(\mathbf{x}, \mathbf{x}') - (\mathcal{P}_n h(\mathbf{x}', \cdot))(\mathbf{x})| \leq C_9 n^{-2} (\log n)^{3(d-1)}, \tag{EC.2.27}$$

for all $\mathbf{x}' \in (0, 1)^d$.

It can be shown via a calculation similar to (EC.2.13) that $\mathbb{E}[(\mathcal{P}_n \mathbf{Y}^*)(\mathbf{x}))^2] = (\mathcal{P}_n h(\mathbf{x}, \cdot))(\mathbf{x})$. Therefore, by (EC.2.27),

$$|I_2(\mathbf{x})| = |h(\mathbf{x}, \mathbf{x}) - (\mathcal{P}_n h(\cdot, \mathbf{x}))(\mathbf{x})| \leq C_9 n^{-2} (\log n)^{3(d-1)}. \tag{EC.2.28}$$

The proof is completed in light of (EC.2.12), (EC.2.21), (EC.2.28), and the fact that the constants C_i 's are independent of \mathbf{x} . \square

EC.3. Convergence Rate Analysis for Stochastic Simulation

In this section, we analyze the convergence rates for the stochastic kriging predictor with TM kernels and TSG designs. Specifically, we prove Theorem 3 and Theorem 4.

In addition to the operator \mathcal{P}_n , we define the following operator for each $\lambda > 0$,

$$(\mathcal{P}_n^\lambda f)(\cdot) := \mathbf{k}^\top(\cdot)(\mathbf{K} + \lambda \mathbf{I})^{-1} \mathbf{f}, \quad (\text{EC.3.1})$$

where $\mathbf{k}(\cdot) = (k(\mathbf{x}_1, \cdot), \dots, k(\mathbf{x}_n, \cdot))^\top$, $\mathbf{f} = (f(\mathbf{x}_1), \dots, f(\mathbf{x}_n))^\top$, and \mathbf{I} is the $n \times n$ identity matrix.

LEMMA EC.7. *Suppose the design points $\{\mathbf{x}_1, \dots, \mathbf{x}_n\}$ form a TSG $\mathcal{X}_n^{\text{TSG}}$. Let \mathcal{G}_n be the span of $\{\phi_{\mathbf{l}, \mathbf{i}} : \mathbf{c}_{\mathbf{l}, \mathbf{i}} \in \mathcal{X}_n^{\text{TSG}}\}$. Then,*

$$\sup_{\mathbf{x} \in (0,1)^d} |g(\mathbf{x})| \leq C(\log n)^d \cdot \sup_{1 \leq i \leq n} |g(\mathbf{x}_i)|,$$

for all $g \in \mathcal{G}_n$ and some constant $C > 0$ that is independent of g and n .

Proof of Lemma EC.7. Fix an arbitrary $g \in \mathcal{G}_n$ and decompose it as follows,

$$g(\mathbf{x}) = \sum_{(\mathbf{l}, \mathbf{i}) : \mathbf{c}_{\mathbf{l}, \mathbf{i}} \in \mathcal{X}_n^{\text{TSG}}} \left\langle g, \frac{\phi_{\mathbf{l}, \mathbf{i}}}{\|\phi_{\mathbf{l}, \mathbf{i}}\|_{\mathcal{H}_k}^2} \right\rangle_{\mathcal{H}_k} \phi_{\mathbf{l}, \mathbf{i}}(\mathbf{x}). \quad (\text{EC.3.2})$$

By virtue of Lemma EC.2 and (EC.1.8), we have

$$\frac{\phi_{\mathbf{l}, \mathbf{i}}(\mathbf{x})}{\|\phi_{\mathbf{l}, \mathbf{i}}\|_{\mathcal{H}_k}^2} = \prod_{j=1}^d \left(k_j(x_j, \mathbf{c}_{l_j, i_j}) + \frac{\eta_{l_j, i_j-1}}{\eta_{l_j, i_j}} k_j(x_j, \mathbf{c}_{l_j, i_j-1}) + \frac{\eta_{l_j, i_j+1}}{\eta_{l_j, i_j}} k_j(x_j, \mathbf{c}_{l_j, i_j+1}) \right), \quad (\text{EC.3.3})$$

where $\eta_{l, i}$ is given by (EC.1.9). For simplicity, we first consider $d = 1$ and suppress the dependence on j . For all (l, i) such that $\mathbf{c}_{l, i} \in \mathcal{X}_n^{\text{TSG}}$,

$$\begin{aligned} \left| \left\langle g, \frac{\phi_{l, i}}{\|\phi_{l, i}\|_{\mathcal{H}_k}^2} \right\rangle_{\mathcal{H}_k} \right| &= \left| \left\langle g, k(\mathbf{c}_{l, i}, \cdot) + \frac{\eta_{l, i-1}}{\eta_{l, i}} k(\mathbf{c}_{l, i-1}, \cdot) + \frac{\eta_{l, i+1}}{\eta_{l, i}} k(\mathbf{c}_{l, i+1}, \cdot) \right\rangle_{\mathcal{H}_k} \right| \\ &= \left| g(\mathbf{c}_{l, i}) + \frac{\eta_{l, i-1}}{\eta_{l, i}} g(\mathbf{c}_{l, i-1}) + \frac{\eta_{l, i+1}}{\eta_{l, i}} g(\mathbf{c}_{l, i+1}) \right| \end{aligned} \quad (\text{EC.3.4})$$

$$\begin{aligned} &\leq \left| 1 + \frac{\eta_{l, i-1}}{\eta_{l, i}} + \frac{\eta_{l, i+1}}{\eta_{l, i}} \right| \cdot \sup_{i-1 \leq i' \leq i+1} |g(\mathbf{c}_{l, i'})| \\ &\leq C_2 \sup_{(l, i) : \mathbf{c}_{l, i} \in \mathcal{X}_n^{\text{TSG}}} |g(\mathbf{c}_{l, i})|, \end{aligned} \quad (\text{EC.3.5})$$

for some constant $C_2 > 0$ independent of g, l, i . Here, (EC.3.4) follows from the reproducing property of the kernel k , and (EC.3.5) follows from the fact that $\eta_{l, i'}/\eta_{l, i}$ converges to $-\frac{1}{2}$, $i' = i \pm 1$ as $l \rightarrow \infty$, which can be seen from (EC.1.10).

For a general $d \geq 2$, we can apply the same argument to show that,

$$\begin{aligned} \left| \left\langle g, \frac{\phi_{\mathbf{l}, \mathbf{i}}}{\|\phi_{\mathbf{l}, \mathbf{i}}\|_{\mathcal{H}_k}^2} \right\rangle_{\mathcal{H}_k} \right| &= \left| \left\langle g, \prod_{j=1}^d \left(k_j(\mathbf{c}_{l_j, i_j}, \cdot) + \frac{\eta_{l_j, i_j-1}}{\eta_{l_j, i_j}} k_j(\mathbf{c}_{l_j, i_j-1}, \cdot) + \frac{\eta_{l_j, i_j+1}}{\eta_{l_j, i_j}} k_j(\mathbf{c}_{l_j, i_j+1}, \cdot) \right) \right\rangle_{\mathcal{H}_k} \right| \\ &\leq C_2^d \sup_{(\mathbf{l}, \mathbf{i}) : \mathbf{c}_{\mathbf{l}, \mathbf{i}} \in \mathcal{X}_n^{\text{TSG}}} |g(\mathbf{c}_{\mathbf{l}, \mathbf{i}})|, \end{aligned} \quad (\text{EC.3.6})$$

for all (\mathbf{l}, \mathbf{i}) such that $\mathbf{c}_{\mathbf{l}, \mathbf{i}} \in \mathcal{X}_n^{\text{TSG}}$. It follows from (EC.3.2) and (EC.3.6) that

$$|g(\mathbf{x})| \leq C_2^d \sup_{(\mathbf{l}, \mathbf{i}): \mathbf{c}_{\mathbf{l}, \mathbf{i}} \in \mathcal{X}_n^{\text{TSG}}} |g(\mathbf{c}_{\mathbf{l}, \mathbf{i}})| \cdot \sum_{(\mathbf{l}, \mathbf{i}): \mathbf{c}_{\mathbf{l}, \mathbf{i}} \in \mathcal{X}_n^{\text{TSG}}} \phi_{\mathbf{l}, \mathbf{i}}(\mathbf{x}). \quad (\text{EC.3.7})$$

Further, note that

$$\sum_{(\mathbf{l}, \mathbf{i}): \mathbf{c}_{\mathbf{l}, \mathbf{i}} \in \mathcal{X}_n^{\text{TSG}}} \phi_{\mathbf{l}, \mathbf{i}}(\mathbf{x}) \leq \sum_{|\mathbf{l}| \leq \tau+d} \sum_{\mathbf{i} \in \rho(\mathbf{l})} \phi_{\mathbf{l}, \mathbf{i}}(\mathbf{x}) = \sum_{|\mathbf{l}| \leq \tau+d} \phi_{\mathbf{l}, i^*(\mathbf{l})}(\mathbf{x}) \leq \sum_{|\mathbf{l}| \leq \tau+d} 1 = \sum_{\ell=d}^{\tau+d} \binom{\ell-1}{d-1}, \quad (\text{EC.3.8})$$

where $i^*(\mathbf{l})$ is the unique index in $\rho(\mathbf{l})$ for which $\mathbf{x} \in \text{supp}(\phi_{\mathbf{l}, i^*(\mathbf{l})})$, and that

$$\sum_{\ell=d}^{\tau+d} \binom{\ell-1}{d-1} \leq (\tau+1) \binom{\tau+d-1}{d-1} \asymp \tau^d \leq C_3 (\log n)^d, \quad (\text{EC.3.9})$$

for some constant $C_3 > 0$, where the asymptotic equivalence can be shown via Stirling's approximation for factorials. Hence, by (EC.3.7),

$$|g(\mathbf{x})| \leq C_2^d C_3 (\log n)^d \cdot \sup_{(\mathbf{l}, \mathbf{i}): \mathbf{c}_{\mathbf{l}, \mathbf{i}} \in \mathcal{X}_n^{\text{TSG}}} |g(\mathbf{c}_{\mathbf{l}, \mathbf{i}})|. \quad \square$$

LEMMA EC.8. *Suppose the design points $\{\mathbf{x}_1, \dots, \mathbf{x}_n\}$ form a TSG $\mathcal{X}_n^{\text{TSG}}$. Then,*

$$\|\mathcal{P}_n^\lambda f\|_\infty \leq \|f\|_\infty + \lambda^{1/2} C (\log n)^d \|f\|_{\mathcal{H}_k}, \quad (\text{EC.3.10})$$

and

$$\|\mathcal{P}_n f - \mathcal{P}_n^\lambda f\|_\infty \leq C \lambda^{1/2} (\log n)^d \|f\|_{\mathcal{H}_k}, \quad (\text{EC.3.11})$$

for all $\lambda > 0$, all $f \in \mathcal{H}_k$, and some constant $C > 0$.

Proof of Lemma EC.8. Let $g^\lambda(\cdot) := f(\cdot) - (\mathcal{P}_n^\lambda f)(\cdot)$. Note that $g^\lambda(\cdot)$ can be expressed as a linear combination of $\{k(\mathbf{x}_i, \cdot) : i = 1, \dots, n\}$, so it lies in \mathcal{F}_n , the span of $\{k(\mathbf{x}_i, \cdot) : i = 1, \dots, n\}$. Since the design points $\{\mathbf{x}_1, \dots, \mathbf{x}_n\}$ form a TSG $\mathcal{X}_n^{\text{TSG}}$, by the orthogonal expansion (EC.1.3), \mathcal{F}_n is identical to \mathcal{G}_n , the span of $\{\phi_{\mathbf{l}, \mathbf{i}} : \mathbf{c}_{\mathbf{l}, \mathbf{i}} \in \mathcal{X}_n^{\text{TSG}}\}$. Applying Lemma EC.7,

$$\|g^\lambda\|_\infty \leq C (\log n)^d \max_{1 \leq i \leq n} |g^\lambda(\mathbf{x}_i)|.$$

for some constant $C > 0$. Hence,

$$\|f - \mathcal{P}_n^\lambda f\|_\infty \leq C (\log n)^d \max_{1 \leq i \leq n} |f(\mathbf{x}_i) - (\mathcal{P}_n^\lambda f)(\mathbf{x}_i)|. \quad (\text{EC.3.12})$$

In the same vein, we can show that

$$\|\mathcal{P}_n f - \mathcal{P}_n^\lambda f\|_\infty \leq C (\log n)^d \max_{1 \leq i \leq n} |(\mathcal{P}_n f)(\mathbf{x}_i) - (\mathcal{P}_n^\lambda f)(\mathbf{x}_i)|.$$

Since $\mathcal{P}_n f$ is the kriging predictor of f with kernel k and design $\mathcal{X}_n^{\text{TSG}}$, it performs interpolation on $\{f(\mathbf{x}_i) : \mathbf{x}_i \in \mathcal{X}_n^{\text{TSG}}\}$, that is, $(\mathcal{P}_n f)(\mathbf{x}_i) = f(\mathbf{x}_i)$, for all $i = 1, \dots, n$. Hence,

$$\|\mathcal{P}_n f - \mathcal{P}_n^\lambda f\|_\infty \leq C(\log n)^d \max_{1 \leq i \leq n} |f(\mathbf{x}_i) - (\mathcal{P}_n^\lambda f)(\mathbf{x}_i)|. \quad (\text{EC.3.13})$$

The representer theorem (Schölkopf and Smola 2002, Section 4.2) implies that $\mathcal{P}_n^\lambda f$ solves the minimization problem below

$$\min_{h \in \mathcal{H}_k} \sum_{i=1}^n (h(\mathbf{x}_i) - f(\mathbf{x}_i))^2 + \lambda \|h\|_{\mathcal{H}_k}^2.$$

It then follows immediately from Proposition 3.1 in Wendland and Rieger (2005) that

$$|f(\mathbf{x}_i) - (\mathcal{P}_n^\lambda f)(\mathbf{x}_i)| \leq \lambda^{1/2} \|f\|_{\mathcal{H}_k}, \quad \forall i = 1, \dots, n. \quad (\text{EC.3.14})$$

Hence, (EC.3.10) follows from (EC.3.12) and (EC.3.14), whereas (EC.3.11) follows from (EC.3.13) and (EC.3.14). \square

EC.3.1. Proof of Theorem 3

Proof of Theorem 3. Let $\lambda := \max_{1 \leq i \leq n} \sigma^2(\mathbf{x}_i)/m_i$. It is easy to see that the MSE of the stochastic kriging predictor (2) satisfies

$$\begin{aligned} \mathbb{E}[(\hat{Y}_n(\mathbf{x}) - Y(\mathbf{x}))^2] &= k(\mathbf{x}, \mathbf{x}) - \mathbf{k}^\top(\mathbf{x})[\mathbf{K} + \boldsymbol{\Sigma}]^{-1} \mathbf{k}(\mathbf{x}) \\ &\leq k(\mathbf{x}, \mathbf{x}) - \mathbf{k}^\top(\mathbf{x})[\mathbf{K} + \lambda \mathbf{I}]^{-1} \mathbf{k}(\mathbf{x}) \\ &= \underbrace{k(\mathbf{x}, \mathbf{x}) - \mathbf{k}^\top(\mathbf{x})\mathbf{K}^{-1} \mathbf{k}(\mathbf{x})}_{J_1(\mathbf{x})} + \underbrace{\mathbf{k}^\top(\mathbf{x})\mathbf{K}^{-1} \mathbf{k}(\mathbf{x}) - \mathbf{k}^\top(\mathbf{x})[\mathbf{K} + \lambda \mathbf{I}]^{-1} \mathbf{k}(\mathbf{x})}_{J_2(\mathbf{x})}. \end{aligned} \quad (\text{EC.3.15})$$

Notice that $J_1(\mathbf{x})$ is the MSE of the kriging predictor in the absence of simulation noise. Theorem 1 asserts that

$$\sup_{\mathbf{x} \in (0,1)^d} J_1(\mathbf{x}) = \mathcal{O}(n^{-1}(\log n)^{2(d-1)}). \quad (\text{EC.3.16})$$

By the definitions of \mathcal{P}_n and \mathcal{P}_n^λ in (EC.2.10) and (EC.3.1), respectively,

$$\begin{aligned} |J_2(\mathbf{x})| &= |(\mathcal{P}_n k(\mathbf{x}, \cdot))(\mathbf{x}) - (\mathcal{P}_n^\lambda k(\mathbf{x}, \cdot))(\mathbf{x})| \\ &\leq C_1 \lambda^{1/2} (\log n)^d \|k(\mathbf{x}, \cdot)\|_{\mathcal{H}_k} \\ &= C_1 (\log n)^d \sqrt{\lambda k(\mathbf{x}, \mathbf{x})}, \end{aligned}$$

for some constant $C_1 > 0$, where the inequality follows from (EC.3.11) in Lemma EC.8. Therefore,

$$\sup_{\mathbf{x} \in (0,1)^d} |J_2(\mathbf{x})| \leq C_2 \lambda^{1/2} (\log n)^d, \quad (\text{EC.3.17})$$

where $C_2 = C_1 \sup_{\mathbf{x} \in (0,1)^d} \sqrt{k(\mathbf{x}, \mathbf{x})} < \infty$. Combining (EC.3.15), (EC.3.16), and (EC.3.17) yields

$$\sup_{\mathbf{x} \in (0,1)^d} \mathbb{E}[(\hat{Y}_n(\mathbf{x}) - Y(\mathbf{x}))^2] = \mathcal{O}\left(n^{-1}(\log n)^{2(d-1)} + (\log n)^d \max_{1 \leq i \leq n} m_i^{-1/2} \sigma(\mathbf{x}_i)\right). \quad \square$$

EC.3.2. Proof of Theorem 4

The techniques used here are analogous to those in the proofs of Theorems 2 and 3.

Proof of Theorem 4. We first write explicitly the MSE of the misspecified stochastic kriging predictor $\hat{Y}_n^{\text{mis}}(\mathbf{x})$ as follows,

$$\begin{aligned}
& \mathbb{E}[(\hat{Y}_n^{\text{mis}}(\mathbf{x}) - Y^*(\mathbf{x}))^2] \\
&= \mathbb{E}[(Y^*(\mathbf{x}))^2] + \mathbb{E}[(\mathbf{k}^\top(\mathbf{x})(\mathbf{K} + \Sigma)^{-1}\bar{Y}^*)^2] - 2\mathbb{E}[Y^*(\mathbf{x})\mathbf{k}^\top(\mathbf{x})(\mathbf{K} + \Sigma)^{-1}\bar{Y}^*] \\
&= k^*(\mathbf{x}, \mathbf{x}) + \mathbf{k}^\top(\mathbf{x})(\mathbf{K} + \Sigma)^{-1}(\mathbf{K}^* + \Sigma)(\mathbf{K} + \Sigma)^{-1}\mathbf{k}(\mathbf{x}) - 2\mathbf{k}^\top(\mathbf{x})(\mathbf{K} + \Sigma)^{-1}\mathbf{k}^*(\mathbf{x}) \\
&\leq k^*(\mathbf{x}, \mathbf{x}) + \mathbf{k}^\top(\mathbf{x})(\mathbf{K} + \lambda\mathbf{I})^{-1}(\mathbf{K}^* + \lambda\mathbf{I})(\mathbf{K} + \lambda\mathbf{I})^{-1}\mathbf{k}(\mathbf{x}) - 2\mathbf{k}^\top(\mathbf{x})(\mathbf{K} + \lambda\mathbf{I})^{-1}\mathbf{k}^*(\mathbf{x}) \\
&= M_1(\mathbf{x}) - M_2(\mathbf{x}) + M_3(\mathbf{x}), \tag{EC.3.18}
\end{aligned}$$

where \mathbf{K}^* denotes the kernel matrix associated with k^* , $\lambda := \max_{1 \leq i \leq n} \sigma^2(\mathbf{x}_i)/m_i$, and

$$\begin{aligned}
M_1(\mathbf{x}) &:= k^*(\mathbf{x}, \mathbf{x}) - \mathbf{k}^\top(\mathbf{x})(\mathbf{K} + \lambda\mathbf{I})^{-1}\mathbf{k}^*(\mathbf{x}), \\
M_2(\mathbf{x}) &:= \mathbf{k}^\top(\mathbf{x})(\mathbf{K} + \lambda\mathbf{I})^{-1}\mathbf{k}^*(\mathbf{x}) - \mathbf{k}^\top(\mathbf{x})(\mathbf{K} + \lambda\mathbf{I})^{-1}\mathbf{K}^*(\mathbf{K} + \lambda\mathbf{I})^{-1}\mathbf{k}(\mathbf{x}), \\
M_3(\mathbf{x}) &:= \lambda\mathbf{k}^\top(\mathbf{x})(\mathbf{K} + \lambda\mathbf{I})^{-2}\mathbf{k}(\mathbf{x}).
\end{aligned}$$

We express $M_1(\mathbf{x})$ in the way similar to (EC.3.15),

$$\begin{aligned}
M_1(\mathbf{x}) &= [k^*(\mathbf{x}, \mathbf{x}) - \mathbf{k}^\top(\mathbf{x})\mathbf{K}^{-1}\mathbf{k}^*(\mathbf{x})] + [\mathbf{k}^\top(\mathbf{x})\mathbf{K}^{-1}\mathbf{k}^*(\mathbf{x}) - \mathbf{k}^\top(\mathbf{x})(\mathbf{K} + \lambda\mathbf{I})^{-1}\mathbf{k}^*(\mathbf{x})] \\
&= \underbrace{k^*(\mathbf{x}, \mathbf{x}) - (\mathcal{P}_n k^*(\mathbf{x}, \cdot))(\mathbf{x})}_{M_{1,1}(\mathbf{x})} + \underbrace{(\mathcal{P}_n k^*(\cdot, \mathbf{x}))(\mathbf{x}) - (\mathcal{P}_n^\lambda k^*(\cdot, \mathbf{x}))(\mathbf{x})}_{M_{1,2}(\mathbf{x})}
\end{aligned}$$

By (EC.2.21), we immediately have

$$\sup_{\mathbf{x} \in (0,1)^d} |M_{1,1}(\mathbf{x})| \leq C_1 n^{-2} (\log n)^{3(d-1)},$$

for some constant $C_1 > 0$. Moreover, note that for all $\mathbf{x} \in (0,1)^d$, $k^*(\mathbf{x}, \cdot) \in \mathcal{H}_k$, so applying (EC.3.11) in Lemma EC.8 yields

$$\sup_{\mathbf{x} \in (0,1)^d} |M_{1,2}(\mathbf{x})| \leq C_2 \lambda^{1/2} (\log n)^d,$$

for some constant $C_2 > 0$. Hence,

$$\sup_{\mathbf{x} \in (0,1)^d} |M_1(\mathbf{x})| \leq C_1 n^{-2} (\log n)^{3(d-1)} + C_2 \lambda^{1/2} (\log n)^d. \tag{EC.3.19}$$

For $M_2(\mathbf{x})$, we adopt the approach used to analyze $I_2(\mathbf{x})$ in the proof of Theorem 2. Let $h^\lambda(\mathbf{x}, \mathbf{x}') := (\mathcal{P}_n^\lambda k^*(\cdot, \mathbf{x}'))(\mathbf{x})$. Then

$$h^\lambda(\mathbf{x}, \mathbf{x}') - (\mathcal{P}_n^\lambda h^\lambda(\mathbf{x}', \cdot))(\mathbf{x}) = \left(\mathcal{P}_n^\lambda (k^*(\cdot, \mathbf{x}') - h^\lambda(\mathbf{x}', \cdot)) \right)(\mathbf{x}). \tag{EC.3.20}$$

Applying (EC.3.10) in Lemma EC.8, there exists a constant $C_3 > 0$ such that

$$\begin{aligned} & \left\| \mathcal{P}_n^\lambda(k^*(\cdot, \mathbf{x}') - h^\lambda(\mathbf{x}', \cdot)) \right\|_\infty \\ & \leq C_3 \left(\|k^*(\cdot, \mathbf{x}') - h^\lambda(\mathbf{x}', \cdot)\|_\infty + \lambda^{1/2}(\log n)^d \|k^*(\cdot, \mathbf{x}') - h^\lambda(\mathbf{x}', \cdot)\|_{\mathcal{H}_k} \right) \\ & \leq C_3 \left(\|k^*(\cdot, \mathbf{x}') - h^\lambda(\mathbf{x}', \cdot)\|_\infty + \lambda^{1/2}(\log n)^d (\|k^*(\cdot, \mathbf{x}')\|_{\mathcal{H}_k} + \|h^\lambda(\mathbf{x}', \cdot)\|_{\mathcal{H}_k}) \right). \end{aligned} \quad (\text{EC.3.21})$$

Note that

$$\begin{aligned} \|k^*(\cdot, \mathbf{x}') - h^\lambda(\mathbf{x}', \cdot)\|_\infty &= \sup_{\mathbf{x} \in (0,1)^d} |k^*(\mathbf{x}, \mathbf{x}') - h^\lambda(\mathbf{x}', \mathbf{x})| \\ &= \sup_{\mathbf{x} \in (0,1)^d} |k^*(\mathbf{x}', \mathbf{x}) - (\mathcal{P}_n^\lambda k^*(\cdot, \mathbf{x}))(\mathbf{x}')| \\ &= \sup_{\mathbf{x} \in (0,1)^d} |M_1(\mathbf{x})| \\ &\leq C_1 n^{-2} (\log n)^{3(d-1)} + C_2 \lambda^{1/2} (\log n)^d. \end{aligned} \quad (\text{EC.3.22})$$

We now estimate $\|k^*(\cdot, \mathbf{x}')\|_{\mathcal{H}_k}$. Applying the orthogonal expansion,

$$\|k^*(\cdot, \mathbf{x}')\|_{\mathcal{H}_k}^2 = \sum_{\mathbf{l} \in \mathbb{N}^d} \sum_{\mathbf{i} \in \rho(\mathbf{l})} \frac{\langle k^*(\mathbf{x}', \cdot), \phi_{\mathbf{l}, \mathbf{i}} \rangle_{\mathcal{H}_k}^2}{\|\phi_{\mathbf{l}, \mathbf{i}}\|_{\mathcal{H}_k}^2} \leq C_4 \sum_{\mathbf{l} \in \mathbb{N}^d} \sum_{\mathbf{i} \in \rho(\mathbf{l})} \frac{2^{-2|\mathbf{l}|}}{2^{|\mathbf{l}|}} = C_4 \sum_{\mathbf{l} \in \mathbb{N}^d} \sum_{\mathbf{i} \in \rho(\mathbf{l})} 2^{-3|\mathbf{l}|},$$

where the inequality follows from (EC.1.5) and (EC.2.19). Further, note that

$$|\rho(\mathbf{l})| = \prod_{j=1}^d 2^{-l_j/2} = 2^{-|\mathbf{l}|/2}. \quad (\text{EC.3.23})$$

Hence,

$$\|k^*(\cdot, \mathbf{x}')\|_{\mathcal{H}_k}^2 \leq C_4 \sum_{\mathbf{l} \in \mathbb{N}^d} 2^{-5|\mathbf{l}|/2} := C_5 < \infty, \quad (\text{EC.3.24})$$

by Lemma 3.7 in Bungartz and Griebel (2004).

We next estimate $\|h^\lambda(\mathbf{x}', \cdot)\|_{\mathcal{H}_k}$. To this end, we rewrite $h^\lambda(\mathbf{x}', \cdot)$ as

$$h^\lambda(\mathbf{x}', \cdot) = \sum_{i=1}^n \alpha_i^\lambda(\mathbf{x}') k^*(\mathbf{x}_i, \cdot),$$

where $\alpha_i^\lambda(\mathbf{x}')$ is the i^{th} entry of $\mathbf{k}^\top(\mathbf{x}')(\mathbf{K} + \lambda \mathbf{I})^{-1}$. Applying the orthogonal expansion again,

$$\begin{aligned} \|h^\lambda(\mathbf{x}', \cdot)\|_{\mathcal{H}_k}^2 &= \sum_{\mathbf{l} \in \mathbb{N}^d} \sum_{\mathbf{i} \in \rho(\mathbf{l})} \frac{\langle h^\lambda(\mathbf{x}', \cdot), \phi_{\mathbf{l}, \mathbf{i}} \rangle_{\mathcal{H}_k}^2}{\|\phi_{\mathbf{l}, \mathbf{i}}\|_{\mathcal{H}_k}^2} \\ &= \sum_{\mathbf{l} \in \mathbb{N}^d} \sum_{\mathbf{i} \in \rho(\mathbf{l})} \frac{1}{\|\phi_{\mathbf{l}, \mathbf{i}}\|_{\mathcal{H}_k}^2} \left| \sum_{i=1}^n \alpha_i^\lambda(\mathbf{x}') \langle k^*(\mathbf{x}_i, \cdot), \phi_{\mathbf{l}, \mathbf{i}} \rangle_{\mathcal{H}_k} \right|^2 \\ &= \sum_{\mathbf{l} \in \mathbb{N}^d} \sum_{\mathbf{i} \in \rho(\mathbf{l})} \frac{1}{\|\phi_{\mathbf{l}, \mathbf{i}}\|_{\mathcal{H}_k}^2} \left| \mathcal{P}_n^\lambda \langle k^*(\mathbf{x}', \cdot), \phi_{\mathbf{l}, \mathbf{i}} \rangle_{\mathcal{H}_k} \right|^2 \\ &\leq \sum_{\mathbf{l} \in \mathbb{N}^d} \sum_{\mathbf{i} \in \rho(\mathbf{l})} \frac{1}{\|\phi_{\mathbf{l}, \mathbf{i}}\|_{\mathcal{H}_k}^2} \left\| \mathcal{P}_n^\lambda \langle k^*(\cdot, \cdot), \phi_{\mathbf{l}, \mathbf{i}} \rangle_{\mathcal{H}_k} \right\|_\infty^2. \end{aligned} \quad (\text{EC.3.25})$$

Applying (EC.3.10) in Lemma EC.8,

$$\|\mathcal{P}_n^\lambda \langle k^*(\cdot, \cdot), \phi_{1,i} \rangle_{\mathcal{H}_k}\|_\infty \leq \|\langle k^*(\cdot, \cdot), \phi_{1,i} \rangle_{\mathcal{H}_k}\|_\infty + C_6 \lambda^{1/2} (\log n)^d \|\langle k^*(\cdot, \cdot), \phi_{1,i} \rangle_{\mathcal{H}_k}\|_{\mathcal{H}_k}, \quad (\text{EC.3.26})$$

for some constant $C_6 > 0$. It follows from (EC.3.25) and (EC.3.26) that

$$\begin{aligned} & \|h^\lambda(\mathbf{x}', \cdot)\|_{\mathcal{H}_k}^2 \\ & \leq \sum_{\mathbf{l} \in \mathbb{N}^d} \sum_{\mathbf{i} \in \rho(\mathbf{l})} \frac{1}{\|\phi_{1,i}\|_{\mathcal{H}_k}^2} \left(\|\langle k^*(\cdot, \cdot), \phi_{1,i} \rangle_{\mathcal{H}_k}\|_\infty + C_6 \lambda^{1/2} (\log n)^d \|\langle k^*(\cdot, \cdot), \phi_{1,i} \rangle_{\mathcal{H}_k}\|_{\mathcal{H}_k} \right)^2 \\ & \asymp \sum_{\mathbf{l} \in \mathbb{N}^d} \sum_{\mathbf{i} \in \rho(\mathbf{l})} 2^{-|\mathbf{l}|} \left(\|\langle k^*(\cdot, \cdot), \phi_{1,i} \rangle_{\mathcal{H}_k}\|_\infty + \lambda^{1/2} (\log n)^d \|\langle k^*(\cdot, \cdot), \phi_{1,i} \rangle_{\mathcal{H}_k}\|_{\mathcal{H}_k} \right)^2. \end{aligned} \quad (\text{EC.3.27})$$

For notational simplicity, let $w(\mathbf{x}, \tilde{\mathbf{x}}) := (\mathcal{L}_{\tilde{\mathbf{x}}} k^*(\cdot, \mathbf{x}))(\tilde{\mathbf{x}})$. Then,

$$\begin{aligned} & \|\langle k^*(\cdot, \cdot), \phi_{1,i} \rangle_{\mathcal{H}_k}\|_{\mathcal{H}_k}^2 \\ & = \int_{(0,1)^d} \int_{(0,1)^d} \int_{(0,1)^d} \left(\phi_{1,i}(\mathbf{s}) (\mathcal{L}_{\mathbf{s}} k^*(\mathbf{x}, \cdot))(\mathbf{s}) \right) \left(\mathcal{L}_{\mathbf{x}} (\mathcal{L}_{\mathbf{t}} \phi_{1,i})(\mathbf{t}) k^*(\cdot, \mathbf{t}) \right)(\mathbf{x}) d\mathbf{x} d\mathbf{t} d\mathbf{s} \\ & = \int_{(0,1)^d} \int_{(0,1)^d} \int_{(0,1)^d} \left(\phi_{1,i}(\mathbf{s}) w(\mathbf{x}, \mathbf{s}) \right) (\mathcal{L}_{\mathbf{t}} \phi_{1,i})(\mathbf{t}) w(\mathbf{t}, \mathbf{x}) d\mathbf{x} d\mathbf{t} d\mathbf{s} \\ & \leq \left(\sup_{\mathbf{x} \in (0,1)^d, \mathbf{s} \in (0,1)^d} |w(\mathbf{x}, \mathbf{s})| \right) \cdot \int_{(0,1)^d} \phi_{1,i}(\mathbf{s}) d\mathbf{s} \cdot \int_{(0,1)^d} \left| \int_{(0,1)^d} (\mathcal{L}_{\mathbf{t}} \phi_{1,i})(\mathbf{t}) w(\mathbf{t}, \mathbf{x}) d\mathbf{t} \right| d\mathbf{x} \\ & = \left(\sup_{\mathbf{s} \in (0,1)^d} \|w(\cdot, \mathbf{s})\|_\infty \right) \cdot \int_{(0,1)^d} \phi_{1,i}(\mathbf{s}) d\mathbf{s} \cdot \int_{(0,1)^d} |\langle w(\cdot, \mathbf{x}), \phi_{1,i} \rangle_{\mathcal{H}_k}| d\mathbf{x} \\ & \leq \left(\sup_{\mathbf{s} \in (0,1)^d} \|w(\cdot, \mathbf{s})\|_\infty \right) \cdot \int_{(0,1)^d} \phi_{1,i}(\mathbf{s}) d\mathbf{s} \cdot \left(\sup_{\mathbf{x} \in (0,1)^d} |\langle w(\cdot, \mathbf{x}), \phi_{1,i} \rangle_{\mathcal{H}_k}| \right) \end{aligned} \quad (\text{EC.3.28})$$

Applying the Cauchy-Schwarz inequality,

$$\sup_{\mathbf{x} \in (0,1)^d} |\langle w(\cdot, \mathbf{x}), \phi_{1,i} \rangle_{\mathcal{H}_k}| \leq \|\phi_{1,i}\|_{\mathcal{H}_k} \cdot \sup_{\mathbf{x} \in (0,1)^d} \|w(\cdot, \mathbf{x})\|_{\mathcal{H}_k} = C_7 \|\phi_{1,i}\|_{\mathcal{H}_k}, \quad (\text{EC.3.29})$$

where $C_7 = \sup_{\mathbf{x} \in (0,1)^d} \|w(\cdot, \mathbf{x})\|_{\mathcal{H}_k} < \infty$ by Assumption 2.

Moreover, note that for all $f \in \mathcal{H}_k$,

$$\|f\|_\infty = \sup_{\mathbf{x} \in (0,1)^d} |\langle f, k(\cdot, x) \rangle_{\mathcal{H}_k}| \leq \|f\|_{\mathcal{H}_k} \cdot \sup_{\mathbf{x} \in (0,1)^d} \|k(\cdot, x)\|_{\mathcal{H}_k} := C_8 \|f\|_{\mathcal{H}_k}.$$

Hence,

$$\sup_{\mathbf{s} \in (0,1)^d} \|w(\cdot, \mathbf{s})\|_\infty \leq C_8 \sup_{\mathbf{s} \in (0,1)^d} \|w(\cdot, \mathbf{s})\|_{\mathcal{H}_k} = C_7 C_8. \quad (\text{EC.3.30})$$

Plugging (EC.2.18), (EC.3.29) and (EC.3.30) into (EC.3.28) leads to

$$\|\langle k^*(\cdot, \cdot), \phi_{1,i} \rangle_{\mathcal{H}_k}\|_{\mathcal{H}_k}^2 \leq C_9 2^{-|\mathbf{l}|} \|\phi_{1,i}\|_{\mathcal{H}_k} \asymp 2^{-|\mathbf{l}|/2}, \quad (\text{EC.3.31})$$

for some constant $C_9 > 0$, where the last step follows from (EC.1.5).

In addition, it follows from (EC.2.19) that

$$\left\| \langle k^*(\cdot, \cdot), \phi_{1,i} \rangle_{\mathcal{H}_k} \right\|_{\infty} \leq C_{10} 2^{-|l|}, \quad (\text{EC.3.32})$$

for some constant $C_{10} > 0$.

We now combine (EC.3.27), (EC.3.31), and (EC.3.32) to derive the following,

$$\begin{aligned} \|h^\lambda(\mathbf{x}', \cdot)\|_{\mathcal{H}_k}^2 &\leq C_{11} \sum_{\mathbf{l} \in \mathbb{N}^d} \sum_{\mathbf{i} \in \rho(\mathbf{l})} 2^{-|\mathbf{l}|} \left(2^{-|\mathbf{l}|} + \lambda^{1/2} (\log n)^d \cdot 2^{-|\mathbf{l}|/4} \right)^2 \\ &= C_{11} \sum_{\mathbf{l} \in \mathbb{N}^d} 2^{|\mathbf{l}|/2} \cdot 2^{-|\mathbf{l}|} \left(2^{-|\mathbf{l}|} + \lambda^{1/2} (\log n)^d \cdot 2^{-|\mathbf{l}|/4} \right)^2 \end{aligned} \quad (\text{EC.3.33})$$

$$\begin{aligned} &= C_{11} \sum_{\mathbf{l} \in \mathbb{N}^d} \left(2^{-5|\mathbf{l}|/2} + 2\lambda^{1/2} (\log n)^d \cdot 2^{-7|\mathbf{l}|/4} + \lambda (\log n)^{2d} \cdot 2^{-|\mathbf{l}|} \right) \\ &\leq C_{12} \left(1 + \lambda^{1/2} (\log n)^d + \lambda (\log n)^{2d} \right), \end{aligned} \quad (\text{EC.3.34})$$

for some positive constants C_{11} and C_{12} , where (EC.3.33) follows from (EC.3.23), while (EC.3.34) holds because $\sum_{\mathbf{l} \in \mathbb{N}^d} 2^{-s|\mathbf{l}|} < \infty$, for all $s > 0$ by Lemma 3.7 in Bungartz and Griebel (2004).

Therefore, plugging (EC.3.22), (EC.3.24), and (EC.3.34) into (EC.3.21) yields

$$\begin{aligned} &\sup_{\mathbf{x} \in (0,1)^d} |M_2(\mathbf{x})| \\ &= \sup_{\mathbf{x} \in (0,1)^d} |h^\lambda(\mathbf{x}, \mathbf{x}) - (\mathcal{P}_n^\lambda h^\lambda(\mathbf{x}, \cdot))(\mathbf{x})| \\ &\leq \left\| \mathcal{P}_n^\lambda (k^*(\cdot, \mathbf{x}') - h^\lambda(\mathbf{x}', \cdot)) \right\|_{\infty} \\ &\leq C_{13} \left[n^{-2} (\log n)^{3(d-1)} + \lambda^{1/2} (\log n)^d + \lambda^{1/2} (\log n)^d \left(1 + \sqrt{1 + \lambda^{1/2} (\log n)^d + \lambda (\log n)^{2d}} \right) \right] \\ &\leq C_{14} \left[n^{-2} (\log n)^{3(d-1)} + \lambda^{1/2} (\log n)^d \left(1 \vee \lambda^{1/4} (\log n)^{d/2} \vee \lambda^{1/2} (\log n)^d \right) \right], \end{aligned} \quad (\text{EC.3.35})$$

for some positive constants C_{13} and C_{14} .

The final piece of the proof is to analyze $M_3(\mathbf{x})$. Clearly,

$$M_3(\mathbf{x}) = \lambda \mathbf{k}^\top(\mathbf{x}) (\mathbf{K} + \lambda \mathbf{I})^{-2} \mathbf{k}(\mathbf{x}) \leq \lambda \mathbf{k}^\top(\mathbf{x}) \mathbf{K}^{-2} \mathbf{k}(\mathbf{x}) = \lambda \mathbf{k}^\top(\mathbf{x}) \mathbf{K}^{-1} \mathbf{I} \mathbf{K}^{-1} \mathbf{k}(\mathbf{x}). \quad (\text{EC.3.36})$$

Consider the following indicator function

$$I(\mathbf{x}, \mathbf{x}') = \begin{cases} 1, & \text{if } \mathbf{x} = \mathbf{x}', \\ 0, & \text{otherwise.} \end{cases}$$

Note that $\mathbf{k}^\top(\mathbf{x}) \mathbf{K}^{-1} \mathbf{I} \mathbf{K}^{-1} \mathbf{k}(\mathbf{x}')$ can be obtained by applying the operator \mathcal{P}_n twice to $I(\mathbf{x}, \mathbf{x}')$, first acting on the variable \mathbf{x} and then on \mathbf{x}' . This implies the following expansion,

$$\begin{aligned} &\mathbf{k}^\top(\mathbf{x}) \mathbf{K}^{-1} \mathbf{I} \mathbf{K}^{-1} \mathbf{k}(\mathbf{x}) \\ &= \sum_{(\mathbf{l}, \mathbf{i}): \mathbf{c}_{\mathbf{l}, \mathbf{i}} \in \mathcal{X}_n^{\text{TSG}}(\mathbf{l}', \mathbf{i}')} \sum_{\mathbf{c}_{\mathbf{l}', \mathbf{i}'} \in \mathcal{X}_n^{\text{TSG}}} \frac{\langle \langle I(\cdot, \cdot), \phi_{1, \mathbf{i}} \rangle_{\mathcal{H}_k}, \phi_{\mathbf{l}', \mathbf{i}'} \rangle_{\mathcal{H}_k}}{\|\phi_{\mathbf{l}', \mathbf{i}'}\|_{\mathcal{H}_k}^2 \|\phi_{1, \mathbf{i}}\|_{\mathcal{H}_k}^2} \phi_{1, \mathbf{i}}(\mathbf{x}) \phi_{\mathbf{l}', \mathbf{i}'}(\mathbf{x}) \end{aligned}$$

$$\begin{aligned}
&\leq \left(\sup_{(1,i),(l',i'): \mathbf{c}_{1,i}, \mathbf{c}_{l',i'} \in \mathcal{X}_n^{\text{TSG}}} \frac{|\langle I(\cdot, \cdot), \phi_{1,i} \rangle_{\mathcal{H}_k}, \phi_{l',i'} \rangle_{\mathcal{H}_k}|}{\|\phi_{l',i'}\|_{\mathcal{H}_k}^2 \|\phi_{1,i}\|_{\mathcal{H}_k}^2} \right) \cdot \left(\sum_{(1,i),(l',i'): \mathbf{c}_{1,i}, \mathbf{c}_{l',i'} \in \mathcal{X}_n^{\text{TSG}}} \phi_{1,i}(\mathbf{x}) \phi_{l',i'}(\mathbf{x}) \right) \\
&= \left(\sup_{(1,i),(l',i'): \mathbf{c}_{1,i}, \mathbf{c}_{l',i'} \in \mathcal{X}_n^{\text{TSG}}} \frac{|\langle I(\cdot, \cdot), \phi_{1,i} \rangle_{\mathcal{H}_k}, \phi_{l',i'} \rangle_{\mathcal{H}_k}|}{\|\phi_{l',i'}\|_{\mathcal{H}_k}^2 \|\phi_{1,i}\|_{\mathcal{H}_k}^2} \right) \cdot \left(\sum_{(1,i): \mathbf{c}_{1,i} \in \mathcal{X}_n^{\text{TSG}}} \phi_{1,i}(\mathbf{x}) \right)^2. \tag{EC.3.37}
\end{aligned}$$

With an argument similar to (EC.3.6), we can show that

$$\sup_{(1,i),(l',i'): \mathbf{c}_{1,i}, \mathbf{c}_{l',i'} \in \mathcal{X}_n^{\text{TSG}}} \frac{|\langle I(\cdot, \cdot), \phi_{1,i} \rangle_{\mathcal{H}_k}, \phi_{l',i'} \rangle_{\mathcal{H}_k}|}{\|\phi_{l',i'}\|_{\mathcal{H}_k}^2 \|\phi_{1,i}\|_{\mathcal{H}_k}^2} \leq C_{15},$$

for some constant $C_{15} > 0$ that is independent of n . Moreover, by (EC.3.8) and (EC.3.9),

$$\sum_{(1,i): \mathbf{c}_{1,i} \in \mathcal{X}_n^{\text{TSG}}} \phi_{1,i}(\mathbf{x}) \leq C_{16}(\log n)^d, \tag{EC.3.38}$$

for some constant $C_{16} > 0$. Plugging (EC.3.37) and (EC.3.38) into (EC.3.36) gives

$$\mathbf{k}^\top(\mathbf{x}) \mathbf{K}^{-1} \mathbf{T} \mathbf{K}^{-1} \mathbf{k}(\mathbf{x}) \leq C_{17}(\log n)^{2d},$$

for all $\mathbf{x} \in (0, 1)^d$, and some constant $C_{17} > 0$. Therefore,

$$\sup_{\mathbf{x} \in (0,1)^d} |M_3(\mathbf{x})| \leq C_{17} \lambda (\log n)^{2d}. \tag{EC.3.39}$$

At last, It follows from (EC.3.18), (EC.3.19), (EC.3.35), and (EC.3.39) that

$$\begin{aligned}
&\sup_{\mathbf{x} \in (0,1)^d} \mathbb{E}[(\hat{Y}_n^{\text{mis}}(\mathbf{x}) - Y^*(\mathbf{x}))^2] \\
&= \mathcal{O}\left(n^{-2}(\log n)^{3(d-1)} + \lambda^{1/2}(\log n)^d (1 \vee \lambda^{1/4}(\log n)^{d/2} \vee \lambda^{1/2}(\log n)^d)\right).
\end{aligned}$$

Note that if $\lambda(\log n)^{2d} \rightarrow 0$, then

$$1 > \lambda^{1/4}(\log n)^{d/2} > \lambda^{1/2}(\log n)^d.$$

Therefore, if $(\max_{1 \leq i \leq n} m_i^{-1/2} \sigma(\mathbf{x}_i)) = o((\log n)^{-d})$, then as $n \rightarrow \infty$,

$$\sup_{\mathbf{x} \in (0,1)^d} \mathbb{E}[(\hat{Y}_n(\mathbf{x}) - Y(\mathbf{x}))^2] = \mathcal{O}\left(n^{-2}(\log n)^{3(d-1)} + (\log n)^d \max_{1 \leq i \leq n} m_i^{-1/2} \sigma(\mathbf{x}_i)\right). \quad \square$$

EC.4. Kernel Matrix Inversion in One Dimension

In this section, we prove Proposition 1. The proof relies on explicit calculation using the following basic property of the multivariate normal distribution; see, e.g., Theorem 2.3 in Rue and Held (2005) for its proof.

LEMMA EC.9. Let $Z = (Z_1, \dots, Z_n)$ be a multivariate normal random variable with covariance matrix $\mathbf{C} \in \mathbb{R}^{n \times n}$. Then, $(\mathbf{C}^{-1})_{ii} = 1/\text{Var}[Z_i|Z_{-i}]$ for all i and $(\mathbf{C}^{-1})_{ij} = -\text{Cov}[Z_i, Z_j|Z_{-ij}]$ for all $i \neq j$, where $Z_{-i} = (Z_\ell : \ell \neq i)$ and $Z_{-ij} = (Z_\ell : \ell \notin \{i, j\})$.

Proof of Part (i) of Proposition 1. Let \mathbf{Y} be a one-dimensional GP with mean zero and kernel $k(x, x') = p(x \wedge x')q(x \vee x')$. Then, \mathbf{Y} is a Gauss-Markov process by Lemma 1, so $\{\Psi_i := \mathbf{Y}(x_i) : i = 1, \dots, n\}$ form a discrete-time Markov chain, since $x_1 < \dots < x_n$.

Consider two indices $i, j \in \{1, \dots, n\}$ with $j - i \geq 2$. Then, $i < j - 1 < j$, and thus

$$\mathbb{P}(\Psi_j \in \cdot | \Psi_i, \Psi_{-ij}) = \mathbb{P}(\Psi_j \in \cdot | \Psi_1, \dots, \Psi_i, \dots, \Psi_{j-1}, \Psi_{j+1}, \dots, \Psi_n) = \mathbb{P}(\Psi_j \in \cdot | \Psi_{j-1}, \Psi_{j+1}),$$

where the second inequality follows from the Markov property. In the same vein, we can show $\mathbb{P}(\Psi_j \in \cdot | \Psi_{-ij}) = \mathbb{P}(\Psi_j \in \cdot | \Psi_{j-1}, \Psi_{j+1})$, implying that $\mathbb{P}(\Psi_j \in \cdot | \Psi_i, \Psi_{-ij}) = \mathbb{P}(\Psi_j \in \cdot | \Psi_{-ij})$. Therefore, Ψ_j and Ψ_i are conditionally independent given Ψ_{-ij} . It follows immediately from Lemma EC.9 that

$$(\mathbf{K}^{-1})_{i,j} = -\text{Cov}[\mathbf{Y}(x_i), \mathbf{Y}(x_j) | \mathbf{Y}(x_\ell) : \ell \notin \{i, j\}] = -\text{Cov}[\Psi_i, \Psi_j | \Psi_{-ij}] = 0.$$

By symmetry, we also have $(\mathbf{K}^{-1})_{i,j} = 0$ if $i - j \geq 2$. Thus, \mathbf{K}^{-1} is a tridiagonal matrix.

By Lemma EC.9, it suffices to calculate $\text{Var}(\Psi_i | \Psi_{-i})$ and $\text{Cov}[\Psi_i, \Psi_{i+1} | \Psi_{-\{i, i+1\}}]$ in order to calculate $(\mathbf{K}^{-1})_{ii}$ and $(\mathbf{K}_{i, i+1})^{-1}$, respectively. To this end, we note that by the Markov property, $\mathbb{P}(\Psi_i \in \cdot | \Psi_{-i}) = \mathbb{P}(\Psi_i \in \cdot | \Psi_{i-1}, \Psi_{i+1})$. Moreover, $(\Psi_{i-1}, \Psi_i, \Psi_{i+1})$ has the multivariate normal distribution with mean $\mathbf{0}$ and covariance matrix with entries $\mathbf{K}_{\ell, \ell'}$ for all $\ell, \ell' = i-1, i, i+1$. Thus,

$$\text{Var}(\Psi_i | \Psi_{i-1}, \Psi_{i+1}) = \mathbf{K}_{ii} - \begin{pmatrix} \mathbf{K}_{i, i-1} & \mathbf{K}_{i, i+1} \end{pmatrix} \begin{pmatrix} \mathbf{K}_{i-1, i-1} & \mathbf{K}_{i-1, i+1} \\ \mathbf{K}_{i+1, i-1} & \mathbf{K}_{i+1, i+1} \end{pmatrix}^{-1} \begin{pmatrix} \mathbf{K}_{i, i-1} \\ \mathbf{K}_{i, i+1} \end{pmatrix}.$$

Likewise, by the Markov property, $\mathbb{P}((\Psi_i, \Psi_{i+1}) \in \cdot | \Psi_{-\{i, i+1\}}) = \mathbb{P}((\Psi_i, \Psi_{i+1}) \in \cdot | \Psi_{i-1}, \Psi_{i+2})$, so

$$\begin{aligned} & \begin{pmatrix} \text{Cov}[\Psi_i, \Psi_i | \Psi_{i-1}, \Psi_{i+2}] & \text{Cov}[\Psi_i, \Psi_{i+1} | \Psi_{i-1}, \Psi_{i+2}] \\ \text{Cov}[\Psi_{i+1}, \Psi_i | \Psi_{i-1}, \Psi_{i+2}] & \text{Cov}[\Psi_{i+1}, \Psi_{i+1} | \Psi_{i-1}, \Psi_{i+2}] \end{pmatrix} \\ &= \begin{pmatrix} \mathbf{K}_{i, i} & \mathbf{K}_{i, i+1} \\ \mathbf{K}_{i+1, i} & \mathbf{K}_{i+1, i+1} \end{pmatrix} - \begin{pmatrix} \mathbf{K}_{i, i-1} & \mathbf{K}_{i, i+2} \\ \mathbf{K}_{i+1, i-1} & \mathbf{K}_{i+1, i+2} \end{pmatrix} \begin{pmatrix} \mathbf{K}_{i-1, i-1} & \mathbf{K}_{i+2, i+2} \\ \mathbf{K}_{i-1, i+1} & \mathbf{K}_{i+2, i+1} \end{pmatrix}^{-1} \begin{pmatrix} \mathbf{K}_{i, i-1} & \mathbf{K}_{i, i+2} \\ \mathbf{K}_{i+1, i-1} & \mathbf{K}_{i+1, i+2} \end{pmatrix} \end{aligned}$$

Then, for all $i \leq j$, plugging $\mathbf{K}_{ij} = k(x_i, x_j) = p(x_i)q(x_j) = \mathbf{p}_i \mathbf{q}_j$, we can verify via direct but tedious calculation that the formula (7) holds.

Proof of Part (ii) of Proposition 1. Let $x \in [x_{i^*}, x_{i^*+1})$. For each $i = 1, \dots, d$,

$$\begin{aligned} & (\mathbf{K}^{-1} \mathbf{k}(x))_i \\ &= \sum_{j=1}^n (\mathbf{K}^{-1})_{ij} k(x, x_j) \\ &= \frac{(\mathbf{p}_{i+1} \mathbf{q}_{i-1} - \mathbf{p}_{i-1} \mathbf{q}_{i+1})k(x, x_i) - (\mathbf{p}_{i+1} \mathbf{q}_i - \mathbf{p}_i \mathbf{q}_{i+1})k(x, x_{i-1}) - (\mathbf{p}_i \mathbf{q}_{i-1} - \mathbf{p}_{i-1} \mathbf{q}_i)k(x, x_{i+1})}{(\mathbf{p}_i \mathbf{q}_{i-1} - \mathbf{p}_{i-1} \mathbf{q}_i)(\mathbf{p}_{i+1} \mathbf{q}_i - \mathbf{p}_i \mathbf{q}_{i+1})}. \end{aligned} \tag{EC.4.1}$$

If $i \leq i^* - 1$, then $x_{i-1} < x_i < x_{i+1} \leq x$, so $k(x_j, x) = \mathbf{p}_j q(x)$ for all $j = i - 1, i, i + 1$. Thus, the numerator of (EC.4.1) equals $q(x)$ multiplied by

$$(\mathbf{p}_{i+1}\mathbf{q}_{i-1} - \mathbf{p}_{i-1}\mathbf{q}_{i+1})\mathbf{p}_i - (\mathbf{p}_{i+1}\mathbf{q}_i - \mathbf{p}_i\mathbf{q}_{i+1})\mathbf{p}_{i-1} - (\mathbf{p}_i\mathbf{q}_{i-1} - \mathbf{p}_{i-1}\mathbf{q}_i)\mathbf{p}_{i+1} = 0,$$

so $(\mathbf{K}^{-1}\mathbf{k}(x))_i = 0$ for $i \leq i^* - 1$. Likewise, we may show $(\mathbf{K}^{-1}\mathbf{k}(x))_i = 0$ for $i \geq i^* + 2$, in which case $k(x_j, x) = p(x)\mathbf{q}_j$ for $j = i - 1, i, i + 1$.

If $i = i^*$, then $x_{i-1} < x_i \leq x < x_{i+1}$, so $k(x_j, x) = \mathbf{p}_j q(x)$ for $j = i - 1, i$, and $k(x_{i+1}, x) = p(x)\mathbf{q}_{i+1}$. Thus, the numerator of (EC.4.1) equals

$$\begin{aligned} & (\mathbf{p}_{i+1}\mathbf{q}_{i-1} - \mathbf{p}_{i-1}\mathbf{q}_{i+1})\mathbf{p}_{i-1}q(x) - (\mathbf{p}_{i+1}\mathbf{q}_i - \mathbf{p}_i\mathbf{q}_{i+1})\mathbf{p}_i q(x) - (\mathbf{p}_i\mathbf{q}_{i-1} - \mathbf{p}_{i-1}\mathbf{q}_i)p(x)\mathbf{q}_{i+1} \\ &= (\mathbf{p}_i\mathbf{q}_{i-1} - \mathbf{p}_{i-1}\mathbf{q}_i)(\mathbf{p}_{i+1}q(x) - p(x)\mathbf{q}_{i+1}). \end{aligned}$$

Applying (EC.4.1),

$$(\mathbf{K}^{-1}\mathbf{k}(x))_i = \frac{\mathbf{p}_{i+1}q(x) - p(x)\mathbf{q}_{i+1}}{\mathbf{p}_{i+1}\mathbf{q}_i - \mathbf{p}_i\mathbf{q}_{i+1}},$$

proving the formula (8) for $i = i^*$. The case of $i = i^* + 1$ can be verified similarly. \square

EC.5. Kernel Matrix Inversion on Truncated Sparse Grids

In this section, we prove Theorem 5. Prior to the proof, we first discuss the number of nonzero entries in the inverse of the kernel matrix on a classical SG. The following result will be used for proving part (iii) of Theorem 5.

PROPOSITION EC.4. *Let $k(\mathbf{x}, \mathbf{x}') = \prod_{j=1}^d k_j(x_j, x'_j)$ be a TM kernel that satisfies Assumption 1, $\mathbf{K} = k(\mathcal{X}_\tau^{\text{SG}}, \mathcal{X}_\tau^{\text{SG}})$, and $\mathbf{k}(\mathbf{x}) = k(\mathcal{X}_\tau^{\text{SG}}, \{\mathbf{x}\})$ for some $\mathbf{x} \in (0, 1)^d$. Then,*

$$\text{nnz}(\mathbf{K}^{-1}) = \mathcal{O}(|\mathcal{X}_\tau^{\text{SG}}|) \quad \text{and} \quad \text{nnz}(\mathbf{K}^{-1}\mathbf{k}(\mathbf{x})) = \mathcal{O}(\log(|\mathcal{X}_\tau^{\text{SG}}|)^{d-1}),$$

where $\text{nnz}(\cdot)$ denotes the number of nonzero entries of a vector or matrix.

Proof of Proposition EC.4. Since the design involved here is a classical SG, we can use Algorithm 3 to compute both \mathbf{K}^{-1} and $\mathbf{K}^{-1}\mathbf{k}(\mathbf{x})$.

We first analyze $\text{nnz}(\mathbf{K}^{-1})$. In Algorithm 3, \mathbf{K}^{-1} is initialized as a zero matrix. Then, for each iteration \mathbf{l} for which $\tau \leq |\mathbf{l}| \leq \tau + d - 1$, the recursion (21) updates the submatrix of \mathbf{K}^{-1} with indices $\{((\mathbf{l}', \mathbf{i}'), (\mathbf{l}', \mathbf{i}'')) : \mathbf{c}_{\mathbf{l}', \mathbf{i}'}, \mathbf{c}_{\mathbf{l}', \mathbf{i}''} \in \mathcal{X}_1^{\text{FG}}\}$ are updated, where $\mathcal{X}_1^{\text{FG}}$ denotes the full grid $\times_{j=1}^d \mathcal{X}_{j, l_j}$ and \mathcal{X}_{j, l_j} 's are defined in (9); moreover, this submatrix is a multiple of $\mathbf{K}_1^{-1} = (k(\mathcal{X}_1^{\text{FG}}, \mathcal{X}_1^{\text{FG}}))^{-1}$. Therefore, the number of nonzero entries of \mathbf{K}^{-1} is at most the sum of the number of nonzero entries of \mathbf{K}_1^{-1} over all the iterations, namely,

$$\text{nnz}(\mathbf{K}^{-1}) \leq \sum_{\tau \leq |\mathbf{l}| \leq \tau + d - 1} \text{nnz}(\mathbf{K}_1^{-1}) = \sum_{\tau \leq |\mathbf{l}| \leq \tau + d - 1} \prod_{j=1}^d \text{nnz}(k_j(\mathcal{X}_{j, l_j}, \mathcal{X}_{j, l_j})^{-1}), \quad (\text{EC.5.1})$$

where the equality holds because $\mathbf{K}_1 = \bigotimes_{j=1}^d k_j(\mathcal{X}_{j,l_j}, \mathcal{X}_{j,l_j})$. Further, since \mathcal{X}_{j,l_j} is a one-dimensional grid, we may apply (7) in Proposition 1 to deduce that $k_j(\mathcal{X}_{j,l_j}, \mathcal{X}_{j,l_j})^{-1}$ is a tridiagonal matrix, so

$$\text{nnz}(k_j(\mathcal{X}_{j,l_j}, \mathcal{X}_{j,l_j})^{-1}) = \mathcal{O}(|\mathcal{X}_{j,l_j}|). \quad (\text{EC.5.2})$$

Combining (EC.5.1) and (EC.5.2) yields

$$\text{nnz}(\mathbf{K}^{-1}) \leq \sum_{\tau \leq |\mathbf{l}| \leq \tau+d-1} \prod_{j=1}^d \mathcal{O}(|\mathcal{X}_{j,l_j}|) = \sum_{\tau \leq |\mathbf{l}| \leq \tau+d-1} \mathcal{O}(2^{l_j}) = \sum_{\tau \leq |\mathbf{l}| \leq \tau+d-1} \mathcal{O}(2^l).$$

Note that

$$\sum_{\tau \leq |\mathbf{l}| \leq \tau+d-1} 2^{|\mathbf{l}|} = \sum_{\ell=d \vee \tau}^{\tau+d-1} 2^\ell \binom{\ell-1}{d-1} = \sum_{\ell=0 \vee (\tau-d)}^{\tau-1} 2^{\ell+d} \binom{\ell+d-1}{d-1} \leq 2^d \cdot |\mathcal{X}_\tau^{\text{SG}}|,$$

where the inequality follows from (14). Therefore, $\text{nnz}(\mathbf{K}^{-1}) = \mathcal{O}(|\mathcal{X}_\tau^{\text{SG}}|)$.

We can apply a similar argument, albeit with the use of the recursion (22) and the formula (8) in Proposition 1, to show that $\text{nnz}(\mathbf{K}^{-1}\mathbf{k}(\mathbf{x})) = \mathcal{O}(\log(|\mathcal{X}_\tau^{\text{SG}}|)^{d-1})$. \square

Proof of Part (i) of Theorem 5. Let $\{\mathbf{Y}(\mathbf{x}) : \mathbf{x} \in (0, 1)^d\}$ be a zero mean TMGP with kernel k . Then, $(\mathbf{Y}(\mathbf{c}_{1,i}) : \mathbf{c}_{1,i} \in \mathcal{X}_n^{\text{TSG}})$ is a multivariate normal random variable with covariance matrix \mathbf{K} .

We cast \mathbf{K} into the form of a block matrix,

$$\mathbf{K} = \begin{pmatrix} |\mathcal{X}_\tau^{\text{SG}}| \text{ dim.} & \tilde{n} \text{ dim.} \\ \mathbf{A} & \mathbf{F} \\ \mathbf{F}^\top & \mathbf{G} \end{pmatrix}, \quad (\text{EC.5.3})$$

where $\mathbf{A} = k(\mathcal{X}_\tau^{\text{SG}}, \mathcal{X}_\tau^{\text{SG}})$, $\mathbf{F} = k(\mathcal{X}_\tau^{\text{SG}}, \mathcal{A}_{\tilde{n}})$, and $\mathbf{G} = k(\mathcal{A}_{\tilde{n}}, \mathcal{A}_{\tilde{n}})$. Then, the formula for inverting 2×2 block matrices asserts that

$$\mathbf{K}^{-1} = \begin{pmatrix} \mathbf{A}^{-1} + \mathbf{A}^{-1}\mathbf{F}\mathbf{D}\mathbf{F}^\top\mathbf{A}^{-1} & -\mathbf{A}^{-1}\mathbf{F}\mathbf{D} \\ -\mathbf{D}\mathbf{F}^\top\mathbf{A}^{-1} & \mathbf{D} \end{pmatrix}, \quad (\text{EC.5.4})$$

where $\mathbf{D} = (\mathbf{G} - \mathbf{F}^\top\mathbf{A}^{-1}\mathbf{F})^{-1}$.

Let $\mathbf{D}_{(\mathbf{l}', \mathbf{i}'), (\mathbf{l}'', \mathbf{i}'')}$ denote an arbitrary entry of \mathbf{D} indexed by $((\mathbf{l}', \mathbf{i}'), (\mathbf{l}'', \mathbf{i}''))$ for which $\mathbf{c}_{\mathbf{l}', \mathbf{i}'}, \mathbf{c}_{\mathbf{l}'', \mathbf{i}''} \in \mathcal{A}_{\tilde{n}}$. By Lemma EC.9,

$$\mathbf{D}_{(\mathbf{l}', \mathbf{i}'), (\mathbf{l}'', \mathbf{i}'')} = \begin{cases} 1 / \text{Var}[\mathbf{Y}(\mathbf{c}_{\mathbf{l}', \mathbf{i}'}) | \mathbf{Y}(\mathbf{x}), \mathbf{x} \in \mathcal{X}_n^{\text{TSG}} \setminus \{\mathbf{c}_{\mathbf{l}', \mathbf{i}'}\}] & \text{if } (\mathbf{l}', \mathbf{i}') = (\mathbf{l}'', \mathbf{i}''), \\ -\text{Cov}[\mathbf{Y}(\mathbf{c}_{\mathbf{l}', \mathbf{i}'}), \mathbf{Y}(\mathbf{c}_{\mathbf{l}'', \mathbf{i}''}) | \mathbf{Y}(\mathbf{x}), \mathbf{x} \in \mathcal{X}_n^{\text{TSG}} \setminus \{\mathbf{c}_{\mathbf{l}', \mathbf{i}'}, \mathbf{c}_{\mathbf{l}'', \mathbf{i}''}\}], & \text{otherwise.} \end{cases}$$

We then apply Proposition EC.2 to deduce that

$$\mathbf{D}_{(\mathbf{l}', \mathbf{i}'), (\mathbf{l}'', \mathbf{i}'')} = \begin{cases} \|\phi_{\mathbf{l}', \mathbf{i}'}\|_{\mathcal{H}_k}^2, & \text{if } (\mathbf{l}', \mathbf{i}') = (\mathbf{l}'', \mathbf{i}''), \\ 0, & \text{otherwise.} \end{cases}$$

In light of the expression (EC.1.4), it is straightforward to see that (EC.5.4) yields (24). \square

Proof of Part (ii) of Theorem 5. We analyze the three cases separately.

Case (a.) This case follows immediately from that \mathbf{D} is a diagonal matrix.

Case (b.) Fix indices $(\mathbf{l}', \mathbf{i}')$ and $(\mathbf{l}'', \mathbf{i}'')$ such that $\mathbf{c}_{\mathbf{l}', \mathbf{i}'} \in \mathcal{X}_\tau^{\text{SG}}$, $\mathbf{c}_{\mathbf{l}'', \mathbf{i}''} \in \mathcal{X}_n^{\text{TSG}}$, and $\mathbf{c}_{\mathbf{l}'', \mathbf{i}''} \notin \mathcal{R}_{\mathbf{l}', \mathbf{i}'}$. Then, $(\mathbf{K}^{-1})_{(\mathbf{l}', \mathbf{i}'), (\mathbf{l}'', \mathbf{i}'')} = -(\mathbf{A}^{-1} \mathbf{F} \mathbf{D})_{(\mathbf{l}', \mathbf{i}'), (\mathbf{l}'', \mathbf{i}'')}$, belonging to the top-right block of \mathbf{K}^{-1} in (EC.5.4). It suffices to show that

$$(\mathbf{A}^{-1} \mathbf{F})_{(\mathbf{l}', \mathbf{i}'), (\mathbf{l}'', \mathbf{i}'')} = 0, \quad (\text{EC.5.5})$$

because \mathbf{D} is diagonal, and multiplying a matrix by a diagonal matrix will retain the zero entries of the former.

Consider the indicator function $f(x) = \mathbb{I}(\mathbf{x} = \mathbf{c}_{\mathbf{l}', \mathbf{i}'}) = \prod_{j=1}^d \mathbb{I}(x_j = c_{l'_j, i'_j})$. Then,

$$(\mathbf{A}^{-1} \mathbf{F})_{(\mathbf{l}', \mathbf{i}'), (\mathbf{l}'', \mathbf{i}'')} = k(\mathbf{c}_{\mathbf{l}'', \mathbf{i}''}, \mathcal{X}_\tau^{\text{SG}}) (k(\mathcal{X}_\tau^{\text{SG}}, \mathcal{X}_\tau^{\text{SG}}))^{-1} f(\mathcal{X}_\tau^{\text{SG}}),$$

where $f(\mathcal{X}_\tau^{\text{SG}})$ denotes the vector having entries $f(\mathbf{c}_{\mathbf{l}, \mathbf{i}})$ for all $\mathbf{c}_{\mathbf{l}, \mathbf{i}} \in \mathcal{X}_\tau^{\text{SG}}$.

Note that $k(\cdot, \mathcal{X}_\tau^{\text{SG}}) (k(\mathcal{X}_\tau^{\text{SG}}, \mathcal{X}_\tau^{\text{SG}}))^{-1} f(\mathcal{X}_\tau^{\text{SG}})$ can be expressed as a linear combination of $\{k(\cdot, \mathbf{c}_{\mathbf{l}, \mathbf{i}}) : \mathbf{c}_{\mathbf{l}, \mathbf{i}} \in \mathcal{X}_\tau^{\text{SG}}\}$, so it lies in the span of $\{k(\cdot, \mathbf{c}_{\mathbf{l}, \mathbf{i}}) : \mathbf{c}_{\mathbf{l}, \mathbf{i}} \in \mathcal{X}_\tau^{\text{SG}}\}$, which is identical to the span of $\{\phi_{\mathbf{l}, \mathbf{i}} : \mathbf{c}_{\mathbf{l}, \mathbf{i}} \in \mathcal{X}_\tau^{\text{SG}}\}$ by virtue of the orthogonal expansion (EC.1.3). Therefore, it follows from (EC.3.2) and (EC.3.3) that

$$(\mathbf{A}^{-1} \mathbf{F})_{(\mathbf{l}', \mathbf{i}'), (\mathbf{l}'', \mathbf{i}'')} = \sum_{|\mathbf{l}| \leq \tau + d - 1} \sum_{\mathbf{i} \in \rho(\mathbf{l})} \beta_{\mathbf{l}, \mathbf{i}} \phi_{\mathbf{l}, \mathbf{i}}(\mathbf{c}_{\mathbf{l}'', \mathbf{i}''}), \quad (\text{EC.5.6})$$

where

$$\begin{aligned} \beta_{\mathbf{l}, \mathbf{i}} &= \left\langle f, \frac{\phi_{\mathbf{l}, \mathbf{i}}}{\|\phi_{\mathbf{l}, \mathbf{i}}\|_{\mathcal{H}_k}^2} \right\rangle_{\mathcal{H}_k} \\ &= \left\langle \mathbb{I}(\cdot = \mathbf{c}_{\mathbf{l}', \mathbf{i}'}), \prod_{j=1}^d \left(k_j(\mathbf{c}_{l_j, i_j}, \cdot) + \frac{\eta_{l_j, i_j-1}}{\eta_{l_j, i_j}} k_j(\mathbf{c}_{l_j, i_j-1}, \cdot) + \frac{\eta_{l_j, i_j+1}}{\eta_{l_j, i_j}} k_j(\mathbf{c}_{l_j, i_j+1}, \cdot) \right) \right\rangle_{\mathcal{H}_k} \\ &= \prod_{j=1}^d \left\langle \mathbb{I}(\cdot = \mathbf{c}_{l'_j, i'_j}), k_j(\mathbf{c}_{l_j, i_j}, \cdot) + \frac{\eta_{l_j, i_j-1}}{\eta_{l_j, i_j}} k_j(\mathbf{c}_{l_j, i_j-1}, \cdot) + \frac{\eta_{l_j, i_j+1}}{\eta_{l_j, i_j}} k_j(\mathbf{c}_{l_j, i_j+1}, \cdot) \right\rangle_{\mathcal{H}_{k_j}}. \end{aligned}$$

Hence, $\beta_{\mathbf{l}, \mathbf{i}} \neq 0$ only if $l_j = l'_j$ and $i_j \in \{i'_j - 1, i'_j, i'_j + 1\}$ for all $j = 1, \dots, d$. Further, note that i_j and i'_j are both odd numbers by definition, since $\mathbf{c}_{\mathbf{l}, \mathbf{i}}, \mathbf{c}_{\mathbf{l}', \mathbf{i}'} \in \mathcal{X}_\tau^{\text{SG}}$. Thus, $\beta_{\mathbf{l}, \mathbf{i}} \neq 0$ only if $(\mathbf{l}, \mathbf{i}) = (\mathbf{l}', \mathbf{i}')$. We may simplify (EC.5.6) to

$$(\mathbf{A}^{-1} \mathbf{F})_{(\mathbf{l}', \mathbf{i}'), (\mathbf{l}'', \mathbf{i}'')} = \beta_{\mathbf{l}', \mathbf{i}'} \phi_{\mathbf{l}', \mathbf{i}'}(\mathbf{c}_{\mathbf{l}'', \mathbf{i}''}). \quad (\text{EC.5.7})$$

Note that $\text{supp}(\phi_{\mathbf{l}', \mathbf{i}'}) = \mathcal{R}_{\mathbf{l}', \mathbf{i}'}$ by the definition (EC.1.2). The condition $\mathbf{c}_{\mathbf{l}'', \mathbf{i}''} \notin \mathcal{R}_{\mathbf{l}', \mathbf{i}'}$ then implies that $\phi_{\mathbf{l}', \mathbf{i}'}(\mathbf{c}_{\mathbf{l}'', \mathbf{i}'}) = 0$, proving (EC.5.5).

Case (c.) Fix indices $(\mathbf{l}', \mathbf{i}')$ and $(\mathbf{l}'', \mathbf{i}'')$ such that $\mathbf{c}_{\mathbf{l}', \mathbf{i}'}, \mathbf{c}_{\mathbf{l}'', \mathbf{i}''} \in \mathcal{X}_\tau^{\text{SG}}$,

$$\left| i'_j \cdot 2^{l'_j \vee l''_j - l'_j} - i''_j \cdot 2^{l'_j \vee l''_j - l''_j} \right| \geq 2, \quad \text{for some } j = 1, \dots, d, \quad (\text{EC.5.8})$$

and

$$\mathbf{c}_{\mathbf{l},\mathbf{i}} \notin \mathcal{R}_{\mathbf{l}',\mathbf{i}'} \cap \mathcal{R}_{\mathbf{l}'',\mathbf{i}''}, \quad \text{for all } \mathbf{c}_{\mathbf{l},\mathbf{i}} \in \mathcal{A}_{\tilde{n}}. \quad (\text{EC.5.9})$$

Then, $(\mathbf{K}^{-1})_{(\mathbf{l}',\mathbf{i}'),(\mathbf{l}'',\mathbf{i}'')}$ belongs to the top-right block of \mathbf{K}^{-1} in (EC.5.4), and it suffices to prove

$$(\mathbf{A}^{-1})_{(\mathbf{l}',\mathbf{i}'),(\mathbf{l}'',\mathbf{i}'')} = 0, \quad (\text{EC.5.10})$$

$$(\mathbf{A}^{-1}\mathbf{F}\mathbf{D}\mathbf{F}^\top\mathbf{A}^{-1})_{(\mathbf{l}',\mathbf{i}'),(\mathbf{l}'',\mathbf{i}'')} = 0. \quad (\text{EC.5.11})$$

Since \mathbf{A} is the kernel matrix defined on the classical SG $\mathcal{X}_\tau^{\text{SG}}$, its entries can be calculated via the additive recursion (21) in Algorithm 3. In particular, $(\mathbf{A}^{-1})_{(\mathbf{l}',\mathbf{i}'),(\mathbf{l}'',\mathbf{i}'')}$ is updated in each iteration \mathbf{l} such that $\tau \leq |\mathbf{l}| \leq \tau + d - 1$, if and only if both $\mathbf{c}_{\mathbf{l}',\mathbf{i}'}$ and $\mathbf{c}_{\mathbf{l}'',\mathbf{i}''}$ belong to the full grid $\mathcal{X}_1^{\text{FG}} = \bigtimes_{j=1}^d \mathcal{X}_{j,l_j}$, where \mathcal{X}_{j,l_j} 's are defined in (9). In this case, this entry of \mathbf{A}^{-1} is increased by $C \cdot ((k(\mathcal{X}_1^{\text{FG}}, \mathcal{X}_1^{\text{FG}}))^{-1})_{(\mathbf{l}',\mathbf{i}'),(\mathbf{l}'',\mathbf{i}'')}$, where $C := (-1)^{\tau+d-1-|\mathbf{l}|} \binom{d-1}{\tau+d-1-|\mathbf{l}|}$. Note that $k(\mathcal{X}_1^{\text{FG}}, \mathcal{X}_1^{\text{FG}})$ can be expressed as a Kronecker product. Hence, by Algorithm 2,

$$\begin{aligned} ((k(\mathcal{X}_1^{\text{FG}}, \mathcal{X}_1^{\text{FG}}))^{-1})_{(\mathbf{l}',\mathbf{i}'),(\mathbf{l}'',\mathbf{i}'')} &= \left(\bigotimes_{j=1}^d (k_j(\mathcal{X}_{j,l_j}, \mathcal{X}_{j,l_j}))^{-1} \right)_{(\mathbf{l}',\mathbf{i}'),(\mathbf{l}'',\mathbf{i}'')} \\ &= \prod_{j=1}^d (k_j(\mathcal{X}_{j,l_j}, \mathcal{X}_{j,l_j}))_{(l'_j, i'_j), (l''_j, i''_j)}^{-1}. \end{aligned} \quad (\text{EC.5.12})$$

Consider the j -th dimension for which the condition (EC.5.8) holds. Since $\mathbf{c}_{\mathbf{l}',\mathbf{i}'}, \mathbf{c}_{\mathbf{l}'',\mathbf{i}''} \in \mathcal{X}_1^{\text{FG}}$, we know that both $\mathbf{c}_{l'_j, i'_j}$ and $\mathbf{c}_{l''_j, i''_j}$ are design points in the one-dimensional grid \mathcal{X}_{j,l_j} , and particularly, $l'_j, l''_j \leq l_j$. Hence, $\mathbf{c}_{l'_j, i'_j}$ and $\mathbf{c}_{l''_j, i''_j}$ can be rewritten as

$$\mathbf{c}_{l'_j, i'_j} = (i'_j \cdot 2^{l_j - l'_j}) \cdot 2^{-l_j} \quad \text{and} \quad \mathbf{c}_{l''_j, i''_j} = (i''_j \cdot 2^{l_j - l''_j}) \cdot 2^{-l_j}.$$

It is then straightforward to see from (EC.5.8) that $\mathbf{c}_{l'_j, i'_j}$ and $\mathbf{c}_{l''_j, i''_j}$ are neither identical nor adjacent points in \mathcal{X}_{j,l_j} . It then follows from (7) in Proposition 1 that $(k_j(\mathcal{X}_{j,l_j}, \mathcal{X}_{j,l_j}))_{(l'_j, i'_j), (l''_j, i''_j)}^{-1} = 0$, which implies $((k(\mathcal{X}_1^{\text{FG}}, \mathcal{X}_1^{\text{FG}}))^{-1})_{(\mathbf{l}',\mathbf{i}'),(\mathbf{l}'',\mathbf{i}'')} = 0$ by (EC.5.12). Since this is true for each iteration \mathbf{l} that is involved for computing $(\mathbf{A}^{-1})_{(\mathbf{l}',\mathbf{i}'),(\mathbf{l}'',\mathbf{i}'')}$, we conclude that (EC.5.10) holds.

Let $\mathbf{B} := \mathbf{A}^{-1}\mathbf{F}$. Since \mathbf{D} is a diagonal matrix,

$$\begin{aligned} (\mathbf{A}^{-1}\mathbf{F}\mathbf{D}\mathbf{F}^\top\mathbf{A}^{-1})_{(\mathbf{l}',\mathbf{i}'),(\mathbf{l}'',\mathbf{i}'')} &= (\mathbf{B}\mathbf{D}\mathbf{B}^\top)_{(\mathbf{l}',\mathbf{i}'),(\mathbf{l}'',\mathbf{i}'')} \\ &= \sum_{(\mathbf{l},\mathbf{i}): \mathbf{c}_{\mathbf{l},\mathbf{i}} \in \mathcal{A}_{\tilde{n}}} \mathbf{B}_{(\mathbf{l}',\mathbf{i}'),(\mathbf{l},\mathbf{i})} \mathbf{D}_{(\mathbf{l},\mathbf{i}),(\mathbf{l},\mathbf{i})} \mathbf{B}_{(\mathbf{l}'',\mathbf{i}''),(\mathbf{l},\mathbf{i})} \\ &= \sum_{(\mathbf{l},\mathbf{i}): \mathbf{c}_{\mathbf{l},\mathbf{i}} \in \mathcal{A}_{\tilde{n}}} \beta_{\mathbf{l}',\mathbf{i}'} \beta_{\mathbf{l}'',\mathbf{i}''} \mathbf{D}_{(\mathbf{l},\mathbf{i}),(\mathbf{l},\mathbf{i})} \phi_{\mathbf{l}',\mathbf{i}'}(\mathbf{c}_{\mathbf{l},\mathbf{i}}) \phi_{\mathbf{l}'',\mathbf{i}''}(\mathbf{c}_{\mathbf{l},\mathbf{i}}), \end{aligned} \quad (\text{EC.5.13})$$

where the last step follows from (EC.5.7). Note that $\phi_{\mathbf{l}',\mathbf{i}'}(\mathbf{c}_{\mathbf{l},\mathbf{i}}) \phi_{\mathbf{l}'',\mathbf{i}''}(\mathbf{c}_{\mathbf{l},\mathbf{i}}) \neq 0$ if and only if $\mathbf{c}_{\mathbf{l},\mathbf{i}} \in \text{supp}(\phi_{\mathbf{l}',\mathbf{i}'}) \cap \text{supp}(\phi_{\mathbf{l}'',\mathbf{i}''}) = \mathcal{R}_{\mathbf{l}',\mathbf{i}'} \cap \mathcal{R}_{\mathbf{l}'',\mathbf{i}''}$. It then follows from the condition (EC.5.9) that each term in the summation (EC.5.13) is zero, proving (EC.5.11). \square

Proof of Part (iii) of Theorem 5. Recall that $\mathbf{A} = k(\mathcal{X}_\tau^{\text{SG}}, \mathcal{X}_\tau^{\text{SG}})$, and that each column of \mathbf{F} is $k(\mathcal{X}_\tau^{\text{SG}}, \{\mathbf{c}_{\mathbf{l}'', \mathbf{i}''}\})$ for $\mathbf{c}_{\mathbf{l}'', \mathbf{i}''} \in \mathcal{A}_{\tilde{n}} \subset \mathcal{X}_{\tau+1}^{\text{SG}} \setminus \mathcal{X}_\tau^{\text{SG}}$. It follows from Proposition EC.4 that each column of $\mathbf{A}^{-1}\mathbf{F}$, which is of the form $\mathbf{A}^{-1}k(\mathcal{X}_\tau^{\text{SG}}, \{\mathbf{c}_{\mathbf{l}'', \mathbf{i}''}\})$, has $\mathcal{O}(\log(|\mathcal{X}_\tau^{\text{SG}}|)^{d-1})$ nonzero entries. Hence, $\text{nnz}(\mathbf{A}^{-1}\mathbf{F}) = \mathcal{O}(\tilde{n} \log(|\mathcal{X}_\tau^{\text{SG}}|)^{d-1})$. Since \mathbf{D} is a diagonal matrix, we conclude that

$$\text{nnz}(\mathbf{A}^{-1}\mathbf{F}\mathbf{D}) = \text{nnz}(\mathbf{A}^{-1}\mathbf{F}) = \mathcal{O}(\tilde{n} \log(|\mathcal{X}_\tau^{\text{SG}}|)^{d-1}) = \mathcal{O}(n(\log n)^{d-1}).$$

We now consider the top-left block of \mathbf{K}^{-1} . Note that an entry of \mathbf{E}^{-1} is nonzero if either the same entry of \mathbf{A}^{-1} is nonzero or that of $\mathbf{A}^{-1}\mathbf{F}\mathbf{D}\mathbf{F}^\top\mathbf{A}^{-1}$ is nonzero. Hence,

$$\text{nnz}(\mathbf{E}) \leq \text{nnz}(\mathbf{A}^{-1}) + \text{nnz}(\mathbf{A}^{-1}\mathbf{F}\mathbf{D}\mathbf{F}^\top\mathbf{A}^{-1}). \quad (\text{EC.5.14})$$

By Proposition EC.4,

$$\text{nnz}(\mathbf{A}^{-1}) = \mathcal{O}(|\mathcal{X}_\tau^{\text{SG}}|). \quad (\text{EC.5.15})$$

On the other hand, the analysis that follows (EC.5.13) asserts that $(\mathbf{A}^{-1}\mathbf{F}\mathbf{D}\mathbf{F}^\top\mathbf{A}^{-1})_{(\mathbf{l}', \mathbf{i}'), (\mathbf{l}'', \mathbf{i}'')} = 0$ if $\mathbf{c}_{\mathbf{l}, \mathbf{i}} \notin \mathcal{R}_{\mathbf{l}', \mathbf{i}'} \cap \mathcal{R}_{\mathbf{l}'', \mathbf{i}''}$ for all $\mathbf{c}_{\mathbf{l}, \mathbf{i}} \in \mathcal{A}_{\tilde{n}}$. Therefore,

$$\begin{aligned} & \text{nnz}(\mathbf{A}^{-1}\mathbf{F}\mathbf{D}\mathbf{F}^\top\mathbf{A}^{-1}) \\ & \leq |\{((\mathbf{l}', \mathbf{i}'), (\mathbf{l}'', \mathbf{i}'')) : \mathbf{c}_{\mathbf{l}', \mathbf{i}'}, \mathbf{c}_{\mathbf{l}'', \mathbf{i}''} \in \mathcal{X}_\tau^{\text{SG}}, \mathbf{c}_{\mathbf{l}, \mathbf{i}} \in \mathcal{R}_{\mathbf{l}', \mathbf{i}'} \cap \mathcal{R}_{\mathbf{l}'', \mathbf{i}''} \text{ for some } \mathbf{c}_{\mathbf{l}, \mathbf{i}} \in \mathcal{A}_{\tilde{n}}\}| \\ & \leq \sum_{(\mathbf{l}, \mathbf{i}) : \mathbf{c}_{\mathbf{l}, \mathbf{i}} \in \mathcal{A}_{\tilde{n}}} |\{((\mathbf{l}', \mathbf{i}'), (\mathbf{l}'', \mathbf{i}'')) : \mathbf{c}_{\mathbf{l}', \mathbf{i}'}, \mathbf{c}_{\mathbf{l}'', \mathbf{i}''} \in \mathcal{X}_\tau^{\text{SG}}, \mathbf{c}_{\mathbf{l}, \mathbf{i}} \in \mathcal{R}_{\mathbf{l}', \mathbf{i}'} \cap \mathcal{R}_{\mathbf{l}'', \mathbf{i}''}\}|. \end{aligned} \quad (\text{EC.5.16})$$

Fix an arbitrary $\mathbf{c}_{\mathbf{l}, \mathbf{i}} \in \mathcal{A}_{\tilde{n}}$. For each $\mathbf{l}' \in \mathbb{N}^d$ with $|\mathbf{l}'| \leq \tau + d - 1$, there exists a unique $i^*(\mathbf{l}') \in \rho(\mathbf{l}')$ such that $\mathbf{c}_{\mathbf{l}, \mathbf{i}} \in \mathcal{R}_{\mathbf{l}', i^*(\mathbf{l}')}$, because $\{\mathcal{R}_{\mathbf{l}', \mathbf{i}'} : \mathbf{i}' \in \rho(\mathbf{l}')\}$ forms a partition of the design space $(0, 1)^d$. Hence, for each $\mathbf{l}' \in \mathcal{X}_\tau^{\text{SG}}$, the number of $\mathcal{R}_{\mathbf{l}', \mathbf{i}'}$'s that cover $\mathbf{c}_{\mathbf{l}, \mathbf{i}}$ is exactly 1. This implies that

$$|\{(\mathbf{l}', \mathbf{i}') : \mathbf{c}_{\mathbf{l}', \mathbf{i}'} \in \mathcal{X}_\tau^{\text{SG}}, \mathbf{c}_{\mathbf{l}, \mathbf{i}} \in \mathcal{R}_{\mathbf{l}', \mathbf{i}'}\}| = |\{\mathbf{l}' \in \mathbb{N}^d : |\mathbf{l}'| \leq \tau + d - 1\}| = \sum_{\ell=d}^{\tau+d-1} \binom{\ell-1}{d-1} = \mathcal{O}(\tau^d),$$

where the last step follows from a derivation similar to (EC.3.9). Thus,

$$\begin{aligned} & |\{((\mathbf{l}', \mathbf{i}'), (\mathbf{l}'', \mathbf{i}'')) : \mathbf{c}_{\mathbf{l}', \mathbf{i}'}, \mathbf{c}_{\mathbf{l}'', \mathbf{i}''} \in \mathcal{X}_\tau^{\text{SG}}, \mathbf{c}_{\mathbf{l}, \mathbf{i}} \in \mathcal{R}_{\mathbf{l}', \mathbf{i}'} \cap \mathcal{R}_{\mathbf{l}'', \mathbf{i}''}\}| \\ & = |\{(\mathbf{l}', \mathbf{i}') : \mathbf{c}_{\mathbf{l}', \mathbf{i}'} \in \mathcal{X}_\tau^{\text{SG}}, \mathbf{c}_{\mathbf{l}, \mathbf{i}} \in \mathcal{R}_{\mathbf{l}', \mathbf{i}'}\}| \times |\{(\mathbf{l}'', \mathbf{i}'') : \mathbf{c}_{\mathbf{l}'', \mathbf{i}''} \in \mathcal{X}_\tau^{\text{SG}}, \mathbf{c}_{\mathbf{l}, \mathbf{i}} \in \mathcal{R}_{\mathbf{l}'', \mathbf{i}''}\}| \\ & = \mathcal{O}(\tau^{2d}). \end{aligned} \quad (\text{EC.5.17})$$

It follows from (EC.5.16) and (EC.5.17) that

$$\text{nnz}(\mathbf{A}^{-1}\mathbf{F}\mathbf{D}\mathbf{F}^\top\mathbf{A}^{-1}) = \mathcal{O}(\tilde{n}\tau^{2d}),$$

which, in conjunction with (EC.5.14) and (EC.5.15), implies that

$$\text{nnz}(\mathbf{E}) = \mathcal{O}(|\mathcal{X}_\tau^{\text{SG}}| + \tilde{n}\tau^{2d}) = \mathcal{O}(n(\log n)^{2d}),$$

since $|\mathcal{X}_\tau^{\text{SG}}| = \mathcal{O}(n)$, $\tilde{n} = \mathcal{O}(n)$, and $\tau = \mathcal{O}(\log(n))$. Consequently, the density of \mathbf{K}^{-1} is

$$\begin{aligned} \frac{1}{n^2} (\text{nnz}(\mathbf{E}) + 2 \times \text{nnz}(\mathbf{A}^{-1}\mathbf{F}\mathbf{D}) + \text{nnz}(\mathbf{D})) &= \frac{1}{n^2} (\mathcal{O}(n(\log n)^{2d}) + \mathcal{O}(n(\log n)^{d-1}) + \mathcal{O}(n)) \\ &= \mathcal{O}(n^{-1}(\log n)^{2d}). \quad \square \end{aligned}$$

References

- Adler RJ, Taylor JE (2009) *Random Fields and Geometry* (Springer).
- Bungartz HJ, Griebel M (2004) Sparse grids. *Acta Numerica* 13:147–269.
- Ding L, Tuo R, Shahrampour S (2020) Generalization guarantees for sparse kernel approximation with entropic optimal features. *Proceedings of the 37th International Conference on Machine Learning*, 2545–2555.
- Kanagawa M, Hennig P, Sejdinovic D, Sriperumbudur BK (2018) Gaussian processes and kernel methods: A review on connections and equivalences. *arXiv: 1807.02582*.
- Rue H, Held L (2005) *Gaussian Markov Random Fields: Theory and Applications* (CRC Press).
- Schölkopf, B, Smola AJ (2002) *Learning with Kernels: Support Vector Machines, Regularization, Optimization, and Beyond* (MIT Press).
- Wendland H, Rieger C (2005) Approximate interpolation with applications to selecting smoothing parameters. *Numer. Math.* 101:729–748.